BIOGEOCHEMICAL CONTROLS ON ARSENIC CYCLING IN A HYDROCARBON PLUME

Brady Allen Ziegler

Dissertation submitted to the faculty of the Virginia Polytechnic Institute and State University in partial fulfillment of the requirements for the degree of

Doctor of Philosophy
In
Geosciences

Madeline E. Schreiber, Chair
Isabelle M. Cozzarelli
J. Donald Rimstidt
F. Marc Michel

May 4, 2018
Blacksburg, VA

Keywords: groundwater, arsenic, iron, cycling, petroleum, biodegradation

BIOGEOCHEMICAL CONTROLS ON ARSENIC CYCLING IN A HYDROCARBON PLUME

Brady Allen Ziegler

ABSTRACT (ACADEMIC)

Arsenic (As) in drinking water poses a critical threat to public health. More than 150 million people worldwide are at risk of developing diseases from unsafe concentrations of As in groundwater. Arsenic occurs naturally in rocks, soils, and sediments and generally remains associated with solid phases. However, changes in aquifer geochemistry can mobilize As into groundwater, contaminating drinking water sources.

This dissertation investigates As cycling in an aquifer contaminated by petroleum hydrocarbons near Bemidji, Minnesota, where As is mobilized into groundwater due to biodegradation of hydrocarbons coupled to reduction of ferric oxides. The first project describes how aquifer sediments act as both sources and sinks for As in groundwater, depending on the prevailing redox conditions. Results show that As is released to groundwater near the hydrocarbon source but is removed near the hydrocarbon plume's leading edge. Comparison of data from 1993 to 2016 shows that As has been redistributed in aquifer sediment as the plume has expanded over time. The second project presents a mass balance for As, which shows that despite elevated As in groundwater (up to 230 μg/L), >99.7% of As mass in the aquifer is in sediments. Calculations demonstrate that As in sediment can be 22x less than the method detection limit and still cause unsafe concentrations in groundwater, suggesting that the use of standard methods limits our ability to predict where naturally occurring As poses a threat to groundwater. In the third project, a reactive transport model simulates As cycling for 400 years. Results show that sorption of As to ferrihydrite limits As transport within 300 m of the

hydrocarbon source. Modeling predicts that over the plume's lifespan, more groundwater will be contaminated by As than benzene, the primary contaminant of concern in hydrocarbon plumes.

Combined, these studies suggest that many aquifers are vulnerable to unsafe As concentrations due to mobilization of natural As if bioavailable organic carbon is introduced. Although aquifers can attenuate As, it may take centuries for As to be fully removed from groundwater, suggesting it is prudent to account for natural contaminants like As when developing remediation strategies at petroleum spill sites.

BIOGEOCHEMICAL CONTROLS ON ARSENIC CYCLING IN A HYDROCARBON PLUME

Brady Allen Ziegler

ABSTRACT (PUBLIC)

Arsenic (As) in groundwater used for drinking water is a risk to public health. More than 150 million people worldwide are at risk of developing diseases and cancer from unsafe levels of As in groundwater. Arsenic occurs naturally in rocks, soils, and sediments. However, changes in aquifer chemistry can release As from these solid materials into groundwater, contaminating drinking water sources.

This dissertation investigates As cycling in a petroleum-contaminated aquifer near Bemidji, Minnesota, where As is released into groundwater due to the breakdown of petroleum by microorganisms under zero-oxygen conditions. The first project describes how sediments release As to, and remove As from, groundwater. Results show that As in groundwater is removed by sediments under medium-to-high-oxygen conditions. Analyses of sediment collected in 1993 showed that in the past, similar processes affecting As in groundwater were occurring closer to the petroleum release site. Over time, the zero-oxygen conditions that allow As to be released into groundwater spread, causing a more widespread As release. The second project presents a mass balance for As, which shows that despite high As in groundwater (up to 230 μg/L), >99.7% of As is associated with sediments. Calculations demonstrate that the analytical methods used to detect As in sediment are not sensitive enough to predict where natural As poses a threat to groundwater. In the third project, a numerical model shows that the presence of iron oxide minerals limit As transport in groundwater. Modeling simulations suggest that in the future, more groundwater will be contaminated by As than benzene, the primary contaminant of concern in petroleum plumes.

Combined, these studies suggest that many aquifers are vulnerable to the release of unsafe levels of As from naturally occurring sources if organic carbon is introduced. Although aquifers can naturally remove As from groundwater, it may take centuries for As to be fully removed, suggesting it is prudent to account for natural contaminants like As when developing clean-up plans at oil spill sites.

ACKNOWLEDGEMENTS

I must start by thanking my advisor, Maddy Schreiber, for the integral role she has played in helping me develop as a scientist and teacher and grow as a person over the past five years. For me, she strikes a unique balance of support and gentle yet firm prodding that makes me want to continually do and be better. Thank you to Isabelle Cozzarelli, who always helps me see the big picture to my research and helps me tackle unique and interesting projects in an interdisciplinary way. Thank you, Don Rimstidt, for passing on to me a fraction of your knowledge and helping me learn to think critically. Thank you, Marc Michel, for your interest in this project and always asking thought-provoking questions that bring the research to a higher quality.

My fellow Bemidji researchers deserve a great deal of credit for their role in this dissertation. Their diverse expertise and perspectives show that even after studying a site for 35+ years, you can still make new and important discoveries. Jeanne Jaeschke, the queen of field work, deserves more praise than I could give. One day we will make it back from the field in time for the evening wine tasting. I look forward to that day. Thank you, Jennifer McGuire, for continuing to be an integral part of my professional and personal life, and my occasional Bemidji workout partner. Thank you to Mindy Erickson, Jared Trost, Andrew Berg, and Brent Mason of the Minnesota Water Science Center, who I have had the pleasure to work with every summer since 2012. Thank you for your patience and kindness while I learned the ropes of field work. Thank you to Crystal Ng and Aubrey Dunshee for helping this duck out of water grasp the basics of modeling and Matlab. I continue to be in awe of your knowledge and skills. Thank you to my other USGS collaborators and colleagues, Barbara Bekins, Denise Akob, and Adam Mumford. Your perspectives have led to interesting projects and questions to pursue.

I am grateful to all the undergraduates with whom I have had the pleasure of working. Virginia Tech students Katie Krueger, Amy Plechacek, Spencer Klepatzki, Caleb Shockley, Chelsea Delsack, Grant Plunkett, Ricardo Fernandez, and Autumn Parker have been invaluable in processing samples. University of St. Thomas students Cassie Clark, Erica Henderson, Hannah Link, and Zach Mader have been integral in planning and executing field work.

Thank you to my office mates Sheyla Palomino Oré, who occasionally indulged my rusty Spanish, and Katie Krueger (again!) for making me laugh and taking advantage of my inability to resist chocolate covered almonds. Tiffany VanDerwerker, Zach Kiracofe, Zack Munger, Denise Levitan, Amanda VanHaitsma, Rick Jayne, and Wu Hao all provided great support in the office, lab, and group meetings. Thank you to my dear Geosciences friends Sarah Ulrich, Aly Hoeher, Allie Nagurney, Rui Serra Maia, and Hannah King for making me laugh and knowing the right time to ask to go for a walk, get a coffee, and discuss science and life. Your influence has creeped into this dissertation in ways you likely do not realize. Thank you to Katrina Korman, who has proven that cell phone batteries can withstand four-hour phone calls.

This work would not be possible without funding support from the Geological Society of America, the American Water Works Association, the Virginia Water Resources Research Center, the American Association of Petroleum Geologists, The Virginia Tech Department of Geosciences, and a collaborative venture of the U.S. Geological Survey, Enbridge Energy Limited Partnership, the Minnesota Pollution Control Agency, and Beltrami County.

I would like to thank my parents for providing words of support in the moments I felt like throwing in the towel. And last, I need to thank Johnver Atienza for picking up my slack in the

most thoughtful ways. You are a stabilizing presence: much more-so than iron oxides in a petroleum hydrocarbon plume.

Table of Contents

List of Tables

List of Figures

Chapter 2. The role of alluvial aquifer sediments in attenuating a dissolved arsenic plume

Chapter 4. A reactive transport model of arsenic cycling in a petroleum-contaminated aquifer

CHAPTER 1. INTRODUCTION

A global health concern

Arsenic (As) in groundwater used for drinking water sources is a global health concern. Chronic exposure to As greater than 10 µg/L (the U.S. EPA and European Union drinking water standard, also the World Health Organization guideline) has been associated with skin, lung and bladder cancers (Knobeloch et al., 2006; Nordstrom, 2002; Smith et al., 2002); chronic exposure to concentrations < 10 µg/L has been linked to skin hyperpigmentation and lesions (Mazumder et al., 1998; Tondel et al., 1999; Tseng, 1977), respiratory (Lee and Fraumeni Jr, 1969; Mazumder et al., 2000), cardiovascular (Chen et al., 1996; Navas-Acien et al., 2005), and neurological diseases(Prakash et al., 2016; Wasserman et al., 2014). Globally, an estimated 150 million people are at risk of developing diseases due to long-term exposure to unsafe levels of As in drinking water (Ravenscroft et al., 2009), though that number may be higher as recent reports identify additional occurrences of elevated As in groundwater (Podgorski et al., 2017).

Many regions worldwide struggle with elevated As in drinking water, with examples in Latin America (Bhattacharya et al., 2006; Bundschuh et al., 2012; Del Razo et al., 1990; Smedley et al., 2005), China (Luo et al., 1997; Ma et al., 1999; Yu et al., 2007), Africa (Smedley et al., 1996; Smedley et al., 2007), the U.S. (Ayotte et al., 2003; Erickson and Barnes, 2005; Scanlon et al., 2009; Schreiber et al., 2000; Welch and Lico, 1998), and Canada (Dummer et al., 2015; Wang and Mulligan, 2006). South and Southeast Asia are the most notable examples where As in drinking water has resulted in a public health crisis (Fendorf et al., 2010; Harvey et al., 2002; McArthur et al., 2001; Smith et al., 2000; van Geen et al., 2003). In Bangladesh alone, a 2012 estimate suggested that 43,000 Bangladeshi citizens die annually from diseases related to As in alluvial and fluviodeltaic aquifers that are the main source for drinking water in the region

(Flanagan et al., 2012). This value corresponds to 5.6% of all non-accidental deaths. The World Health Organization has called the phenomenon the "largest mass poisoning of a population in history" (Smith et al., 2000).

Sources of As in groundwater

Arsenic in groundwater can originate from anthropogenic and geogenic sources. Though less common, anthropogenic sources of As, such as treated lumber (Khan et al., 2006; Saxe et al., 2007), historic tanneries (Davis et al., 1994; Sadler et al., 1994), poultry litter (Mangalgiri et al., 2015; Oyewumi and Schreiber, 2012; Xie et al., 2015), and mine tailings (Roussel et al., 2000; Wang and Mulligan, 2009) can cause localized areas of extremely high As concentrations in groundwater. However, the vast majority of sites with elevated As concentrations in groundwater originate from geogenic sources (Smedley and Kinniburgh, 2002).

Geogenic As can exist in many oxidation states, ranging from -3 to +5. Arsenic can exist in reduced forms in AsH_3 and native As with oxidation states of -3 and 0, respectively. However, these reduced forms are not found in near-surface environments. In aquifers, As occurs in oxidized forms as oxyanions of arsenite As(III) and arsenate As(V). These oxyanions commonly associate with minerals in aquifer sediments. Arsenic concentrations range from 1-20 mg/kg in the crust (Nordstrom, 2002), with U.S. soils and sediments averaging 5.2 mg/kg (Reimann et al., 2009; Shacklett and Boerngen, 1984).

Several geochemical mechanisms have been documented as important for the mobilization of geogenic As from the aquifer matrix into groundwater. These include As desorption from aquifer minerals under changing pH (Dixit and Hering, 2003), the competition of As oxyanions with competing ions (e.g, phosphate (Gao and Mucci, 2001; Hongshao and

Stanforth, 2001; Manning and Goldberg, 1996; Sø et al., 2012), bicarbonate (Appelo et al., 2002)) for sorption sites on minerals, microbially mediated reductive desorption of As(V) (Kocar et al., 2006; Tufano et al., 2008), and As desorption during Fe-reduction (Nickson et al., 2000, McArthur et al., 2001).

To conduct accurate assessments of As-contaminated groundwater, it is critical to identify 1) the source of As, 2) the mechanism by which As is included in the aquifer solid (e.g. incorporated into mineral structure vs. adsorbed) and 3) the mechanism by which As is mobilized from the aquifer solids to groundwater, which includes characterizing aquifer geochemistry. For example, As-bearing sulfides (e.g., arsenopyrite, As-rich pyrite) are stable under reducing conditions. However, if redox conditions become oxidizing, for example by recharge, sulfide minerals can oxidatively dissolve, allowing As to be mobilized into groundwater (Schreiber et al., 2000; Walker et al., 2006). In contrast, As sorbed to ferric (Fe(III)) (hydr)-oxides (e.g., ferrihydrite, goethite, hematite, lepidocrocite) is stable under oxic conditions (Bowell, 1994; Pierce and Moore, 1982). However, under reducing conditions, the Fe-oxide can be reductively dissolved coupled with microbial oxidation (biodegradation) of organic carbon. This set of interrelated reactions can mobilize previously sorbed As into groundwater (Berg et al., 2001; Nickson et al., 1998). This mechanism is the primary way by which groundwater is contaminated by As, and it is responsible for elevated As in alluvial aquifers in Southeast Asia (McArthur et al., 2001; Nickson et al., 1998; Nordstrom, 2002), Eastern Europe (Lindberg et al., 2006; Varsányi and Kovács, 2006), northern China (Luo et al., 1997; Yu et al., 2007), Argentina (Bhattacharya et al., 2006; Smedley et al., 2005; Smedley et al., 2002), and the Midwestern U.S. (Erickson and Barnes, 2005; Root et al., 2010; Warner, 2001).

Aquifer vulnerability to As mobilization from anthropogenic organic carbon

Historically, natural sources of organic carbon (e.g., peat, sedimentary organic matter) have been documented as a trigger that releases As to groundwater. However, recent studies have highlighted that anthropogenic organic carbon can trigger As mobilization due to biodegradation coupled with Fe-reduction (Hering et al., 2009). Elevated concentrations of As in groundwater have been linked to leaky landfills (deLemos et al., 2005; Keimowitz et al., 2005), leaky underground storage tanks, sewage plumes (Amirbahman et al., 2006; Kent and Fox, 2004), and biofuel (Ziegler et al., 2015) and crude oil spills (Cozzarelli et al., 2016). These studies provide strong evidence that As may be more pervasive in groundwater than previously thought due to the high frequency of anthropogenic organic carbon releases into drinking water aquifers. For example, an estimated 514,000 leaking underground storage tanks have been historically documented to release hydrocarbons into groundwater in the U.S. (USEPA, 2013). In Minnesota, an assessment of Wellhead Protection Areas (WHPAs), the area around a public water supply well or well field, showed that 54% of WHPAs contained at least one leaky underground storage tank within its boundaries (Bekins et al., 2017). Additionally, the analysis found that more than 14,000 private water supply wells were within 340 m of a leaky underground storage tank. These findings suggest that if As is mobilized at these point sources of anthropogenic organic carbon, the population exposed to As in drinking water may be greater than previously estimated.

The abundant literature on As mobilization resulting from Fe-reduction has focused on aquifers where As is mobilized due to biodegradation of naturally occurring organic matter. A fundamental challenge in predicting where As release to groundwater from Fe-reduction may occur is that the reaction is triggered by the presence of bioavailable organic matter. Studies have shown that regions with high As concentrations in groundwater often show “patchy” dissolved As distributions where As is not detected in a well near one containing elevated As (Erickson

and Barnes, 2005; Erickson et al., 2018; Pal et al., 2002; Quicksall et al., 2008; Root et al., 2010; Rowland et al., 2007) . This patchy distribution is often attributed to heterogeneous distribution of natural bioavailable organic matter in aquifer sediments, though the timing of well sampling and sampling procedure can also have an effect on measured As (Erickson et al., 2018). A second challenge is that natural organic matter has complex and spatially variable chemical structures, thus resulting in differential biodegradation pathways and rates that can ultimately affect As mobilization into groundwater. Combined, these two factors make it difficult to design meaningful assessments of As mobilization due to biodegradation processes.

Research objectives

In this dissertation, I assess As cycling at a historic oil spill site in Bemidji, MN, where the spatial distribution and chemical composition of the oil that drives Fe reduction and As mobilization is well characterized. These conditions, in combination with the abundant historic geochemical data from more than 200 publications in the peer-reviewed literature, give us the unique opportunity to examine As cycling resulting from biodegradation of a known organic carbon source. My dissertation comprises three projects: 1) evaluation of the capacity of aquifer sediments to naturally attenuate As mobilized due to biodegradation and Fe reduction over the history of a petroleum hydrocarbon plume at the Bemidji site (Chapter 2); 2) quantification of the current distribution of As mass in groundwater and aquifer sediments in the Bemidji aquifer, highlighting the dominant control that sediments play on overall As distribution (Chapter 3); and 3) simulation of As transport in the Bemidji aquifer using a reactive transport model and assessment of long-term fate of As in the hydrocarbon plume (Chapter 4). The final chapter (Chapter 5) provides suggestions for future work on As cycling.

The role of alluvial aquifer sediments in attenuating a dissolved arsenic plume

Chapter 2 provides a quasi-mechanistic spatial analysis of As in association with Fe in aquifer sediments in the contaminated aquifer. This study uses chemical extractions of aquifer sediments collected at different locations in the aquifer to assess how the capacity of sediments to attenuate dissolved As changes over the geochemical evolution of the hydrocarbon plume. It also evaluates the attenuation capacity over a 20-year time period by comparing As and Fe distributions in modern-day sediments and sediments collected in 1993. A version of this chapter was published in the *Journal of Contaminant Hydrology*.

A mass balance approach to investigate arsenic cycling in a petroleum plume

Chapter 3 presents a quantitative two-dimensional mass balance analysis of As and Fe in the Bemidji petroleum plume. Using measured concentrations of Fe and As in groundwater and sediment along petroleum plume transect, a mass partitioning calculation was used to quantify the distribution of As and Fe. A version of this chapter was published in *Environmental Pollution.*

A reactive transport model of arsenic cycling in a petroleum-contaminated aquifer

Chapter 4 presents a reactive transport model for As at the Bemidji site that builds upon a previous model constructed by Ng et al. (2015) with addition of surface complexation to simulate As sorption and desorption to iron oxyhydroxides. The model is calibrated to the current geochemical conditions observed at the site and is used to make long-term assessments of As cycling in the contaminated aquifer. This chapter is in preparation for submission to a peer-reviewed journal.

References

Amirbahman, A., Kent, D.B., Curtis, G.P. and Davis, J.A. (2006) Kinetics of sorption and abiotic oxidation of arsenic(III) by aquifer materials. Geochimica et Cosmochimica Acta 70, 533-547.

Appelo, C., Van der Weiden, M., Tournassat, C. and Charlet, L. (2002) Surface complexation of ferrous iron and carbonate on ferrihydrite and the mobilization of arsenic. Environmental Science & Technology 36, 3096-3103.

Ayotte, J.D., Montgomery, D.L., Flanagan, S.M. and Robinson, K.W. (2003) Arsenic in groundwater in eastern New England: occurrence, controls, and human health implications. Environmental science & technology 37, 2075-2083.

Bekins, B., Jo Baedecker, M., Cozzarelli, I., P. Eganhouse, R., Crystal Ng, G.H., Trost, J., Ostertag, S., Podgorski, D. and Zito, P. (2017) The legacy of spilled oil and fuel in groundwater: source zone persistence and plume growth, Geological Society of America, Seattle, WA.

Berg, M., Tran, H.C., Nguyen, T.C., Pham, H.V., Schertenleib, R. and Giger, W. (2001) Arsenic contamination of groundwater and drinking water in Vietnam: a human health threat. Environmental science & technology 35, 2621-2626.

Bhattacharya, P., Claesson, M., Bundschuh, J., Sracek, O., Fagerberg, J., Jacks, G., Martin, R.A., Storniolo, A.d.R. and Thir, J.M. (2006) Distribution and mobility of arsenic in the Río Dulce alluvial aquifers in Santiago del Estero Province, Argentina. Science of The Total Environment 358, 97-120.

Bowell, R.J. (1994) Sorption of arsenic by iron oxides and oxyhydroxides in soils. Applied Geochemistry 9, 279-286.

Bundschuh, J., Litter, M.I., Parvez, F., Román-Ross, G., Nicolli, H.B., Jean, J.-S., Liu, C.-W., López, D., Armienta, M.A. and Guilherme, L.R. (2012) One century of arsenic exposure in Latin America: A review of history and occurrence from 14 countries. Science of the Total Environment 429, 2-35.

Chen, C.-J., Chiou, H.-Y., Chiang, M.-H., Lin, L.-J. and Tai, T.-Y. (1996) Dose-response relationship between ischemic heart disease mortality and long-term arsenic exposure. Arteriosclerosis, thrombosis, and vascular biology 16, 504-510.

Cozzarelli, I.M., Schreiber, M.E., Erickson, M.L. and Ziegler, B.A. (2016) Arsenic cycling in hydrocarbon plumes: secondary effects of natural attenuation. Groundwater 54, 35-45.

Davis, A., Kempton, J.H., Nicholson, A. and Yare, B. (1994) Groundwater transport of arsenic and chromium at a historical tannery, Woburn, Massachusetts, U.S.A. Applied Geochemistry 9, 569-582.

Del Razo, L., Arellano, M. and Cebrián, M.E. (1990) The oxidation states of arsenic in well-water from a chronic arsenicism area of northern Mexico. Environmental pollution 64, 143-153.

deLemos, J.L., Bostick, B.C., Renshaw, C.E., StÜrup, S. and Feng, X. (2005) Landfill-stimulated iron reduction and arsenic release at the Coakley Superfund Site (NH). Environmental Science & Technology 40, 67-73.

Dixit, S. and Hering, J.G. (2003) Comparison of arsenic(V) and arsenic(III) sorption onto iron oxide minerals: implications for arsenic mobility. Environmental Science & Technology 37, 4182-4189.

Dummer, T., Yu, Z., Nauta, L., Murimboh, J. and Parker, L. (2015) Geostatistical modelling of arsenic in drinking water wells and related toenail arsenic concentrations across Nova Scotia, Canada. Science of the Total Environment 505, 1248-1258.

Erickson, M.L. and Barnes, R.J. (2005) Glacial sediment causing regional-scale elevated arsenic in drinking water. Ground Water 43, 796-805.

Erickson, M.L., Malenda, H.F. and Berquist, E.C. (2018) How or when samples are collected affects measured arsenic concentration in new drinking water wells. Groundwater.

Fendorf, S., Michael, H.A. and van Geen, A. (2010) Spatial and temporal variations of groundwater arsenic in South and Southeast Asia. Science 328, 1123-1127.

Flanagan, S.V., Johnston, R.B. and Zheng, Y. (2012) Arsenic in tube well water in Bangladesh: health and economic impacts and implications for arsenic mitigation. Bulletin of the World Health Organization 90, 839-846.

Gao, Y. and Mucci, A. (2001) Acid base reactions, phosphate and arsenate complexation, and their competitive adsorption at the surface of goethite in 0.7 M NaCl solution. Geochimica et Cosmochimica Acta 65, 2361-2378.

Harvey, C.F., Swartz, C.H., Badruzzaman, A., Keon-Blute, N., Yu, W., Ali, M.A., Jay, J., Beckie, R., Niedan, V. and Brabander, D. (2002) Arsenic mobility and groundwater extraction in Bangladesh. Science 298, 1602-1606.

Hering, J.G., O'Day, P.A., Ford, R.G., He, Y.T., Bilgin, A., Reisinger, H.J. and Burris, D.R. (2009) MNA as a remedy for arsenic mobilized by anthropogenic inputs of organic carbon. Ground Water Monitoring & Remediation 29, 84-92.

Hongshao, Z. and Stanforth, R. (2001) Competitive Adsorption of Phosphate and Arsenate on Goethite. Environmental Science & Technology 35, 4753-4757.

Keimowitz, A.R., Zheng, Y., Chillrud, S.N., Mailloux, B., Jung, H.B., Stute, M. and Simpson, H.J. (2005) Arsenic redistribution between sediments and water near a highly contaminated source. Environmental Science & Technology 39, 8606-8613.

Kent, D.B. and Fox, P.M. (2004) The influence of groundwater chemistry on arsenic concentrations and speciation in a quartz sand and gravel aquifer. Geochemical Transactions 5, 1.

Khan, B.I., Jambeck, J., Solo-Gabriele, H.M., Townsend, T.G. and Cai, Y. (2006) Release of arsenic to the environment from CCA-treated wood. 2. Leaching and speciation during disposal. Environmental science & technology 40, 994-999.

Knobeloch, L.M., Zierold, K.M. and Anderson, H.A. (2006) Association of arsenic-contaminated drinking-water with prevalence of skin cancer in Wisconsin's Fox River Valley. Journal of Health, Population and Nutrition, 206-213.

Kocar, B.D., Herbel, M.J., Tufano, K.J. and Fendorf, S. (2006) Contrasting effects of dissimilatory iron(III) and arsenic(V) reduction on arsenic retention and transport. Environmental Science & Technology 40, 6715-6721.

Lee, A.M. and Fraumeni Jr, J.F. (1969) Arsenic and respiratory cancer in man: an occupational study. Journal of the National Cancer Institute 42, 1045-1052.

Lindberg, A.-L., Goessler, W., Gurzau, E., Koppova, K., Rudnai, P., Kumar, R., Fletcher, T., Leonardi, G., Slotova, K. and Gheorghiu, E. (2006) Arsenic exposure in Hungary, Romania and Slovakia. Journal of Environmental Monitoring 8, 203-208.

Luo, Z.D., Zhang, Y.M., Ma, L., Zhang, G.Y., He, X., Wilson, R., Byrd, D.M., Griffiths, J.G., Lai, S., He, L., Grumski, K. and Lamm, S.H. (1997) Chronic arsenicism and cancer in Inner Mongolia — consequences of well-water arsenic levels greater than 50 μg/l, in: Abernathy, C.O., Calderon, R.L., Chappell, W.R. (Eds.), Arsenic: Exposure and Health Effects. Springer Netherlands, Dordrecht, pp. 55-68.

Ma, H.Z., Xia, Y.J., Wu, K.G., Sun, T.Z. and Mumford, J.L. (1999) Human exposure to arsenic and health effects in Bayingnormen, Inner Mongolia, Arsenic Exposure and Health Effects III. Elsevier, pp. 127-131.

Mangalgiri, K.P., Adak, A. and Blaney, L. (2015) Organoarsenicals in poultry litter: detection, fate, and toxicity. Environment international 75, 68-80.

Manning, B.A. and Goldberg, S. (1996) Modeling competitive adsorption of arsenate with phosphate and molybdate on oxide minerals. Soil Science Society of America Journal 60, 121-131.

Mazumder, D.N.G., Haque, R., Ghosh, N., De, B.K., Santra, A., Chakraborti, D. and Smith, A.H. (2000) Arsenic in drinking water and the prevalence of respiratory effects in West Bengal, India. International journal of epidemiology 29, 1047-1052.

Mazumder, D.N.G., Haque, R., Ghosh, N., De, B.K., Santra, A., Chakraborty, D. and Smith, A.H. (1998) Arsenic levels in drinking water and the prevalence of skin lesions in West Bengal, India. International Journal of Epidemiology 27, 871-877.

McArthur, J., Ravenscroft, P., Safiulla, S. and Thirlwall, M. (2001) Arsenic in groundwater: testing pollution mechanisms for sedimentary aquifers in Bangladesh. Water Resources Research 37, 109-117.

Navas-Acien, A., Sharrett, A.R., Silbergeld, E.K., Schwartz, B.S., Nachman, K.E., Burke, T.A. and Guallar, E. (2005) Arsenic exposure and cardiovascular disease: a systematic review of the epidemiologic evidence. American journal of epidemiology 162, 1037-1049.

Nickson, R., McArthur, J., Burgess, W., Ahmed, K.M., Ravenscroft, P. and Rahmanñ, M. (1998) Arsenic poisoning of Bangladesh groundwater. Nature 395, 338-338.

Nordstrom, D.K. (2002) Worldwide occurrences of arsenic in ground water. Science 296, 2143-2145.

Oyewumi, O. and Schreiber, M.E. (2012) Release of arsenic and other trace elements from poultry litter: Insights from a field experiment on the Delmarva Peninsula, Delaware. Applied geochemistry 27, 1979-1990.

Pal, T., Mukherjee, P.K. and Sengupta, S. (2002) Nature of arsenic pollutants in groundwater of Bengal basin-A case study from Baruipur area, West Bengal, India. Current Science 82, 554-561.

Pierce, M.L. and Moore, C.B. (1982) Adsorption of arsenite and arsenate on amorphous iron hydroxide. Water Research 16, 1247-1253.

Podgorski, J.E., Eqani, S.A.M.A.S., Khanam, T., Ullah, R., Shen, H. and Berg, M. (2017) Extensive arsenic contamination in high-pH unconfined aquifers in the Indus Valley. Science advances 3, e1700935.

Prakash, C., Soni, M. and Kumar, V. (2016) Mitochondrial oxidative stress and dysfunction in arsenic neurotoxicity: A review. Journal of Applied Toxicology 36, 179-188.

Quicksall, A.N., Bostick, B.C. and Sampson, M. (2008) Linking organic matter deposition and iron mineral transformations to groundwater arsenic levels in the Mekong delta, Cambodia. Applied Geochemistry 23, 3088-3098.

Ravenscroft, P., Brammer, H. and Richards, K. (2009) Arsenic pollution: a global synthesis. John Wiley & Sons.

Reimann, C., Matschullat, J., Birke, M. and Salminen, R. (2009) Arsenic distribution in the environment: The effects of scale. Applied Geochemistry 24, 1147-1167.

Root, T.L., Gotkowitz, M.B., Bahr, J.M. and Attig, J.W. (2010) Arsenic geochemistry and hydrostratigraphy in midwestern U.S. glacial deposits. Ground Water 48, 903-912.

Roussel, C., Néel, C. and Bril, H. (2000) Minerals controlling arsenic and lead solubility in an abandoned gold mine tailings. Science of the Total Environment 263, 209-219.

Rowland, H., Pederick, R., Polya, D., Pancost, R., Van Dongen, B., Gault, A., Vaughan, D., Bryant, C., Anderson, B. and Lloyd, J. (2007) The control of organic matter on microbially mediated iron reduction and arsenic release in shallow alluvial aquifers, Cambodia. Geobiology 5, 281-292.

Sadler, R., Olszowy, H., Shaw, G., Biltoft, R. and Connell, D. (1994) Soil and water contamination by arsenic from a tannery waste. Water, Air, and Soil Pollution 78, 189-198.

Saxe, J.K., Wannamaker, E.J., Conklin, S.W., Shupe, T.F. and Beck, B.D. (2007) Evaluating landfill disposal of chromated copper arsenate (CCA) treated wood and potential effects on groundwater: evidence from Florida. Chemosphere 66, 496-504.

Scanlon, B.R., Nicot, J., Reedy, R., Kurtzman, D., Mukherjee, A. and Nordstrom, D.K. (2009) Elevated naturally occurring arsenic in a semiarid oxidizing system, Southern High Plains aquifer, Texas, USA. Applied Geochemistry 24, 2061-2071.

Schreiber, M., Simo, J. and Freiberg, P. (2000) Stratigraphic and geochemical controls on naturally occurring arsenic in groundwater, eastern Wisconsin, USA. Hydrogeology Journal 8, 161-176.

Shacklett, H.T. and Boerngen, J.G. (1984) Element concentrations in soils and other surficial materials of the conterminous United States. U.S. Geological Suevey Professional Paper 1270.

Smedley, P., Edmunds, W. and Pelig-Ba, K. (1996) Mobility of arsenic in groundwater in the Obuasi gold-mining area of Ghana: some implications for human health. Geological Society, London, Special Publications 113, 163-181.

Smedley, P. and Kinniburgh, D. (2002) A review of the source, behaviour and distribution of arsenic in natural waters. Applied Geochemistry 17, 517-568.

Smedley, P., Knudsen, J. and Maiga, D. (2007) Arsenic in groundwater from mineralised Proterozoic basement rocks of Burkina Faso. Applied Geochemistry 22, 1074-1092.

Smedley, P.L., Kinniburgh, D.G., Macdonald, D.M.J., Nicolli, H.B., Barros, A.J., Tullio, J.O., Pearce, J.M. and Alonso, M.S. (2005) Arsenic associations in sediments from the loess aquifer of La Pampa, Argentina. Applied Geochemistry 20, 989-1016.

Smedley, P.L., Nicolli, H.B., Macdonald, D.M.J., Barros, A.J. and Tullio, J.O. (2002) Hydrogeochemistry of arsenic and other inorganic constituents in groundwaters from La Pampa, Argentina. Applied Geochemistry 17, 259-284.

Smith, A.H., Lingas, E.O. and Rahman, M. (2000) Contamination of drinking-water by arsenic in Bangladesh: a public health emergency. Bulletin of the World Health Organization 78, 1093-1103.

Smith, A.H., Lopipero, P.A., Bates, M.N. and Steinmaus, C.M. (2002) Arsenic epidemiology and drinking water standards. Science 296, 2145-2146.

Sø, H.U., Postma, D., Jakobsen, R. and Larsen, F. (2012) Competitive adsorption of arsenate and phosphate onto calcite; experimental results and modeling with CCM and CD-MUSIC. Geochimica et Cosmochimica Acta 93, 1-13.

Tondel, M., Rahman, M., Magnuson, A., Chowdhury, I.A., Faruquee, M.H. and Ahmad, S.A. (1999) The relationship of arsenic levels in drinking water and the prevalence rate of skin lesions in Bangladesh. Environmental health perspectives 107, 727.

Tseng, W.-P. (1977) Effects and dose-response relationships of skin cancer and blackfoot disease with arsenic. Environmental health perspectives 19, 109.

Tufano, K.J., Reyes, C., Saltikov, C.W. and Fendorf, S. (2008) Reductive processes controlling arsenic retention: revealing the relative importance of iron and arsenic reduction. Environmental Science & Technology 42, 8283-8289.

USEPA (2013) Washington D.C. (www.epa.gov/swerust1/pubs/ustfacts.pdf).

van Geen, A., Zheng, Y., Versteeg, R., Stute, M., Horneman, A., Dhar, R., Steckler, M., Gelman, A., Small, C., Ahsan, H., Graziano, J.H., Hussain, I. and Ahmed, K.M. (2003) Spatial variability of arsenic in 6000 tube wells in a 25 km2 area of Bangladesh. Water Resources Research 39, 1140.

Varsányi, I. and Kovács, L.Ó. (2006) Arsenic, iron and organic matter in sediments and groundwater in the Pannonian Basin, Hungary. Applied Geochemistry 21, 949-963.

Walker, F.P., Schreiber, M.E. and Rimstidt, J.D. (2006) Kinetics of arsenopyrite oxidative dissolution by oxygen. Geochimica et Cosmochimica Acta 70, 1668-1676.

Wang, S. and Mulligan, C.N. (2006) Effect of natural organic matter on arsenic release from soils and sediments into groundwater. Environmental Geochemistry and Health 28, 197-214.

Wang, S. and Mulligan, C.N. (2009) Enhanced mobilization of arsenic and heavy metals from mine tailings by humic acid. Chemosphere 74, 274-279.

Warner, K.L. (2001) Arsenic in glacial drift aquifers and the implication for drinking water—Lower Illinois River Basin. Groundwater 39, 433-442.

Wasserman, G., Liu, X., LoIacono, N., Kline, J., Factor-Litvak, P., van Geen, A., Mey, J., Levy, D., Abramson, R., Schwartz, A. and Graziano, J. (2014) A cross-sectional study of well water arsenic and child IQ in Maine schoolchildren. Environmental Health 13, 1-10.

Welch, A.H. and Lico, M.S. (1998) Factors controlling As and U in shallow ground water, southern Carson Desert, Nevada. Applied Geochemistry 13, 521-539.

Xie, H., Han, D., Cheng, J., Zhou, P. and Wang, W. (2015) Fate and risk assessment of arsenic compounds in soil amended with poultry litter under aerobic and anaerobic circumstances. Water, Air, & Soil Pollution 226, 390.

Yu, G., Sun, D. and Zheng, Y. (2007) Health effects of exposure to natural arsenic in groundwater and coal in China: an overview of occurrence. Environmental health perspectives 115, 636.

Ziegler, B.A., McGuire, J.T. and Cozzarelli, I.M. (2015) Rates of As and trace-element mobilization caused by Fe reduction in mixed BTEX–ethanol experimental plumes. Environmental Science & Technology 49, 13179-13189.

CHAPTER 2. THE ROLE OF ALLUVIAL AQUIFER SEDIMENTS IN ATTENUATING A DISSOLVED ARSENIC PLUME

A version of this chapter has been published in the Journal of Contaminant Hydrology.

Abstract

In a crude-oil-contaminated sandy aquifer at the Bemidji site in northern Minnesota, biodegradation of petroleum hydrocarbons has resulted in release of naturally occurring As to groundwater under Fe-reducing conditions. This study used chemical extractions of aquifer sediments collected in 1993 and 2011–2014 to evaluate the relationship between Fe and As in different redox zones (oxic, methanogenic, Fe-reducing, anoxic-suboxic transition) of the contaminated aquifer over a twenty-year period. Results show that 1) the aquifer has the capacity to naturally attenuate the plume of dissolved As, primarily through sorption; 2) Fe and As are linearly correlated in sediment across all redox zones, and a regression analysis between Fe and As reasonably predicted As concentrations in sediment from 1993 using only Fe concentrations; 3) an As-rich "iron curtain," associated with the anoxic-suboxic transition zone, migrated 30 m downgradient between 1993 and 2013 as a result of the hydrocarbon plume evolution; and 4) silt lenses in the aquifer preferentially sequester dissolved As, though As is remobilized into groundwater from sediment after reducing conditions are established. Using results of this study coupled with historical data, we develop a conceptual model which summarizes the natural attenuation of As and Fe over time and space that can be applied to other sites that experience As mobilization due to an influx of bioavailable organic matter.

Introduction

The mobilization of naturally occurring arsenic (As) to groundwater from aquifer minerals poses a threat to human health. An estimated 130 million people worldwide are at risk for diseases related to As concentrations in drinking water exceeding the World Health Organization (WHO) and U.S. Environmental Protection Agency (USEPA) standard of 10 μg/L (Ravenscroft et al., 2009); long-term exposure to As concentrations > 10 μg/L has been linked to skin, lung, and bladder cancers (Knobeloch et al., 2006; Nordstrom, 2002; Smith et al., 2002).

A notable example of elevated As concentrations in groundwater associated with alluvial aquifers is Southeast Asia (Nordstrom, 2002), where release of naturally occurring As from alluvial and deltaic sediments to groundwater has resulted in widespread As poisoning for the past 30–40 years (Harvey et al., 2002; McArthur et al., 2004; Mukherjee et al., 2006; Ravenscroft et al., 2009). Elevated concentrations of As have also been documented in other alluvial aquifers, including regions of northern China (Luo et al., 1997; Ma et al., 1999), Hungary and Romania (Lindberg et al., 2006; Varsányi and Kovács, 2006), and Argentina (Bhattacharya et al., 2006), and in glacially derived aquifers in the Midwestern United States (Erickson and Barnes, 2005; Kelly et al., 2005; Korte, 1991; Root et al., 2010; Warner, 2001).

In alluvial aquifers, As often associates with Fe, Mn, and Al hydroxides (McArthur et al., 2001; Smedley and Kinniburgh, 2002). Arsenic association with ferric (Fe(III)) hydroxides is particularly important due to the strong sorption affinity between As and Fe(III) and the abundance of Fe(III) hydroxides in alluvial aquifer sediments (De Vitre et al., 1991; Manning and Goldberg, 1996; Pierce and Moore, 1982; Stollenwerk, 2003). When As is sorbed to Fe(III) hydroxides, and groundwater has circumneutral pH, the Fe(III) hydroxide is thermodynamically stable, and As remains associated with sediment. However, the presence of bioavailable organic

carbon (BOC) can spur microbial activity that rapidly consumes oxygen in groundwater. Following oxygen depletion, reducing geochemical conditions promote microbially mediated reduction of Fe(III) hydroxides coupled with the oxidation of organic carbon, releasing aqueous Fe(II) and previously adsorbed As to groundwater (McArthur et al., 2001; McArthur et al., 2004; Nickson et al., 1998; Nickson et al., 2000; Smedley et al., 2002).

The mobilization of As due to biodegradation of natural BOC is well-documented (see Smedley and Kinniburgh (2002) for review). Heterogeneously distributed accumulations of solid-phase natural BOC in aquifers can trigger reducing conditions that promote As mobilization (Whaley-Martin et al., 2016). However, recent work has documented that anthropogenic sources of organic matter, including petroleum hydrocarbon and biofuels plumes (Cozzarelli et al., 2016; Hering et al., 2009; Ziegler et al., 2015), sewage plumes (Amirbahman et al., 2006; Kent and Fox, 2004), and landfills (deLemos et al., 2006; Keimowitz et al., 2005) can also generate the conditions necessary to mobilize naturally occurring As from aquifer sediments.

In addition to influencing the release of As to groundwater in alluvial aquifers, redox (bio)geochemistry can also play an important role in mitigating As transport in groundwater in these systems. Geochemical conditions that promote oxidization of dissolved Fe(II) to solid Fe(III) hydroxides generates new sorption sites for As (Amirbahman et al., 2006; Giménez et al., 2007; He et al., 2010; Hering et al., 2009; Stollenwerk et al., 2007; West et al., 2012). Mechanisms that have been documented for As sequestration due to oxidation include: 1) precipitation of Fe(III) minerals, followed by re-sorption of dissolved As (Giménez et al., 2007; Hering et al., 2009; Stollenwerk, 2003); 2) co-precipitation of As in the Fe-hydroxide crystal structure (Fuller et al., 1993; Gorra et al., 2012); and 3) oxidation of arsenite (As(III)) to the less

mobile arsenate (As(V)) at circumneutral-to-acidic pH, spurring re-sorption of As(V) to sediment (Amirbahman et al., 2006; Stollenwerk et al., 2007; Zhao et al., 2011). Although oxidation is an important process for the retention of dissolved As, As can also be sequestered by other Fe-bearing aquifer minerals (e.g., siderite, ferroan calcite, magnetite) in the absence of oxygen (Guo et al., 2011; Guo et al., 2007a; Jönsson and Sherman, 2008).

Despite the abundant literature on the mobilization and transport of As in groundwater in alluvial aquifers, there is much to be learned about the mechanisms of As cycling. Evaluating how naturally occurring As is both released from, and potentially sequestered within, sediment is critical for optimizing the long-term management of As-contaminated aquifers and design of remediation systems. Two interrelated challenges arise in studying As cycling between groundwater and sediments during biodegradation of natural BOC. First, natural BOC is often heterogeneously dispersed in aquifers, and the areas where As can be mobilized are also heterogeneous, resulting in a "patchy" distribution of dissolved As (Erickson and Barnes, 2005; Pal et al., 2002; Quicksall et al., 2008; Root et al., 2010; Rowland et al., 2007). Second, the dispersed nature of natural BOC often creates intermittent periods of reducing conditions during water-table fluctuations or recharge events that promote As mobilization into groundwater and oxic-suboxic conditions that favor As retention by aquifer sediments (McArthur et al., 2004). Combined, these two factors make it difficult to monitor time series changes in As concentrations in aquifer sediments, and thus, to evaluate larger patterns of As cycling, including ability of the aquifer to attenuate As.

This study investigates the role of aquifer sediments in attenuating As in groundwater under long-term reducing conditions. This study is focused on a crude-oil spill site near Bemidji, MN, where biodegradation of petroleum hydrocarbons coupled with Fe-reduction has resulted in

the mobilization of naturally occurring As from aquifer sediments into groundwater, creating a plume of dissolved As (Cozzarelli et al., 2016). Hydrocarbons have been in place at the site for more than three decades (the spill occurred in 1979), and estimates suggest that the hydrocarbons will be present in the aquifer for another ~ 75 years (Revesz et al., 1995), though Bekins et al. (2005) cautioned that biodegradation rates quantified early in life of the plume might not accurately reflect future biodegradation rates due to depletion of electron acceptors, and thus, the life span of the plume might be longer than original estimates. Given the well-documented history of this site, we have a unique opportunity to examine the complex interactions of As with Fe in the aquifer sediment under more controlled conditions due to the breadth of literature characterizing the Bemidji aquifer and geochemical reactions occurring in the plume than is typical for most As-contaminated aquifers. The presence of BOC has also created redox zones (methanogenic, Fe reducing, oxic) in the aquifer that have changed over time, which also allows the opportunity to evaluate how As mobilization from sediments to groundwater changes as redox conditions evolve. In this study, we analyzed chemical and physical characteristics of sediment cores collected from the oil-spill site and used modern and historical groundwater chemistry data to 1) examine interactions of As and Fe in aquifer sediments in different redox zones of the modern plume, and 2) compare As-Fe patterns in sediment from the modern plume to those in 1993. We use the results to develop a conceptual model that describes the distribution of Fe and As over space and time in an aquifer with an ample source of organic carbon.

Methods

Study site

In 1979, a crude oil pipeline ruptured near Bemidji, MN and sprayed 10,700 barrels of crude oil onto glacial outwash deposits (Pfannkuch, 1979). After clean-up efforts, 2600 barrels of oil

remained in the subsurface floating on the water table, causing hydrocarbons to dissolve into groundwater, creating a dissolved hydrocarbon plume (Figure 2.1). The Bemidji spill site is a U.S. Geological Survey (USGS)-sponsored National Crude Oil Spill Research Site. At the site, the hydrocarbon plume is naturally attenuated by biodegradation coupled mainly with Fe reduction, with a heterogeneous methanogenic zone near the oil body (Bekins et al., 2005; Bekins et al., 2001; Cozzarelli et al., 2001).

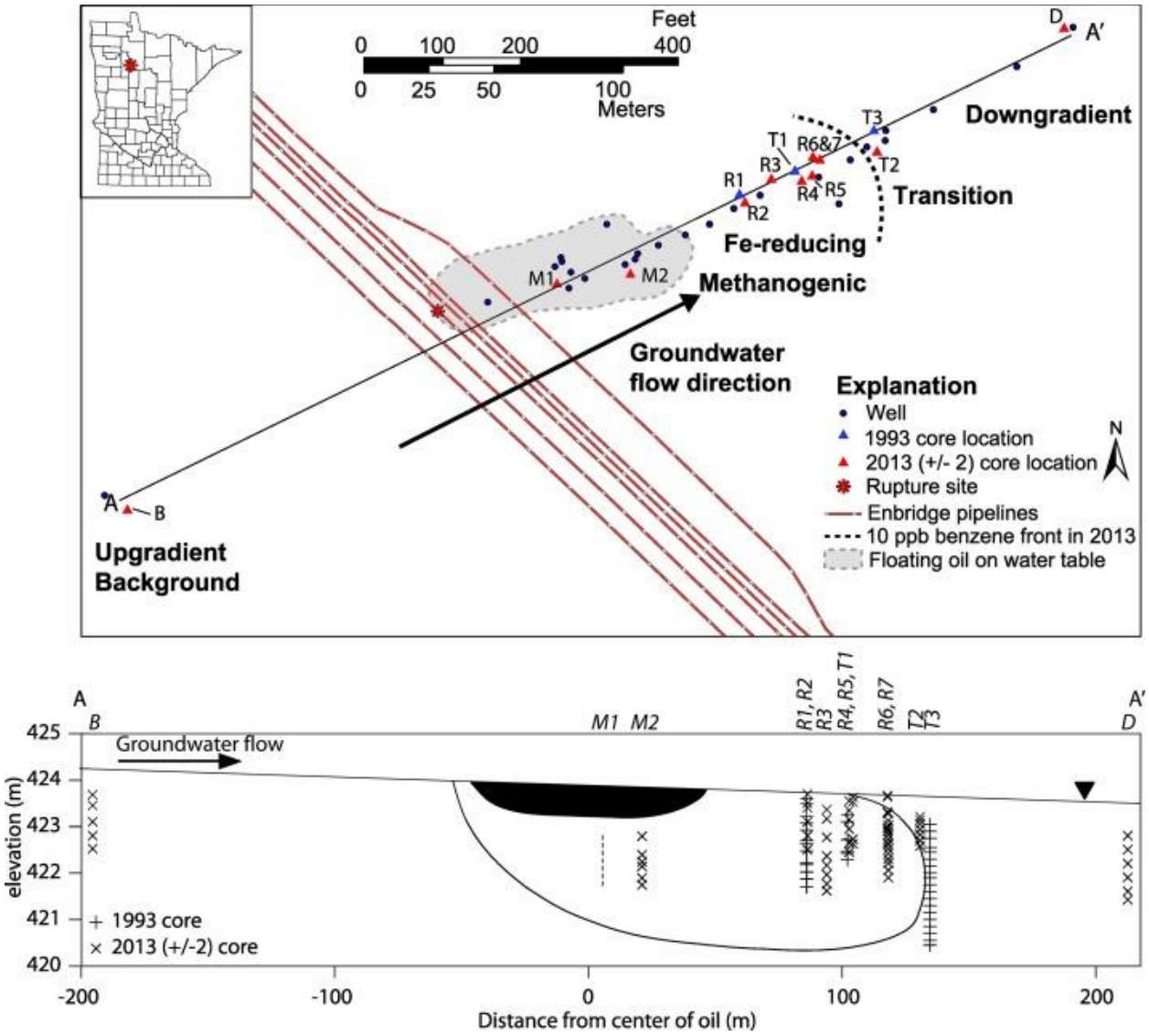

Figure 2.1. Map of the Bemidji oil spill site and locations of different cores (R1, T1, and T3 were collected in 1993; the remaining 11 cores were collected in 2011–14) along the plume transect.

See Table A.2 for core details. Vertical sampling elevations from each core are shown in cross section. The filled shape reflects the oil pool and the solid line reflects the extent of the Fe-reducing zone (Fe > 1 mg/L) in the plume. Sample elevations were not recorded for core M1, and it is represented as a dashed line in cross section. B = background, M = methanogenic zone, R = Fe-reducing zone, T = transition zone, and D = downgradient. Figure modified from Cozzarelli et al. (2016).

The aquifer is comprised mainly of gravel, sand, and silt originating from crystalline and carbonate source rocks deposited by glacial activity (Bennett et al., 1993). Uncontaminated sediments have roughly 1% Fe content with complex Fe mineralogy, including silicates (epidote, clinochlore, and muscovite), oxides and hydroxides (goethite, hematite, magnetite, and a ferrihydrite-like phase), and to a lesser degree, carbonates (ferroan calcite) (Zachara et al., 2004). Groundwater in the plume has a typical pH range of ~ 6.5 to 7.5, with pH near the oil body being on the lower end of the range. Concentrations of other common potential electron acceptors (e.g., nitrate and sulfate) are low or non-detectable in groundwater. Bicarbonate is elevated in contaminated groundwater due to biodegradation reactions.

Cozzarelli et al. (2016) recently reported findings of elevated concentrations of As (> 230 μg/L) in groundwater in the anoxic plume at Bemidji. Using groundwater chemistry from wells inside and outside of the plume, along with chemical digestions of uncontaminated sediments, Cozzarelli et al. (2016) showed that As was mobilized into groundwater due to the biodegradation of dissolved hydrocarbons coupled with Fe-reduction. The plume of As co-occurs with the anoxic plume where there are also elevated concentrations of benzene and dissolved Fe. The highest As concentrations (100–230 μg/L) were detected in groundwater near the oil body, largely defined as a methanogenic zone based on geochemical and microbiological data (Bekins et al., 2001; Cozzarelli et al., 2001). Elevated As (10–100 μg/L) is also detected in Fe-reducing groundwater, defined by dissolved Fe > 1 mg/L (Cozzarelli et al., 2016). Concentrations of Fe

and As in groundwater gradually decrease with distance from the oil body in the plume, and eventually are below detection in the "transition" zone at the leading edge of the plume where anoxic groundwater from the plume mixes with regionally oxic groundwater. Upgradient and downgradient from the plume where groundwater is oxic, As concentrations in groundwater are below detection (< 1 μg/L). Together, these data support the hypothesis that microbially mediated Fe-reduction within the plume is responsible for As release, and that As re-associates with aquifer sediments when groundwater chemistry becomes more oxic downgradient from the plume.

Sediment collection

Eleven sediment cores were collected from 2011 to 2014 to evaluate near-total and HCl-extractable concentrations of As and Fe in aquifer sediments in different redox zones along the plume transect (see Figure 2.1). Cores were collected upgradient from the contaminated site to establish baseline conditions, in the methanogenic, Fe-reducing, and anoxic/oxic transition zones to evaluate the distribution of As and Fe in sediment within the hydrocarbon plume, and downgradient from the plume to investigate Fe and As in sediment beyond the plume's leading edge. Archived samples collected from cores in 1993 (described in (Tuccillo, 1998; Tuccillo et al., 1999)) were also obtained for this study. These samples had been stored in a freezer since the 1990's.

Cores were collected by drilling with a hollow-stem auger to approximately 0.6 m below the water table. A piston core barrel was then pounded into sediment 2.1 m beneath the augers. A CO2 freeze shoe froze the bottom 10 cm of cores in-situ to ensure redox integrity of the subsurface (Murphy and Herkelrath, 1996). Upon removal, cores were covered in plastic wrap and immediately capped. Cores were visually inspected for changes in sediment coloration and

grain size and were then cut into sub-sections based on notable changes. Core sub-sections were wrapped in foil, sealed in vacuum-sealed bags, and frozen on site until they were shipped with dry ice to the U.S. Geological Survey in Reston, VA.

Chemical extractions and analyses

Three types of chemical extractions were performed in parallel to extract As associated with specific Fe phases from aquifer sediments: a phosphate extraction to estimate sorbed As, a 0.5 M HCl extraction to estimate As associated (sorbed or co-precipitated) with HCl-extractable Fe(III) minerals, and microwave-assisted nitric acid extraction to estimate a near-total concentration of As in sediments (Table 2.1). Cores collected in 1993 and 2011–2012 were originally collected for other research projects at Bemidji and were not preserved under oxygen-free conditions; thus they were only analyzed for near-total As and Fe and sorbed As for this study. Cores collected in 2013–2014 were preserved under anoxic conditions and were analyzed for As associated with HCl-extractable Fe(III).

Table 2.1 Parallel chemical extractions for As in aquifer sediments

extractant	method	target phase	references
phosphate	1 M NaH_2PO_4, pH 5-5.5, rotated 24 h, 25 C, x2 + water wash	sorbed As	(Keon et al., 2001; Welch and Lico, 1998)
HCl	0.5 M HCl, pH < 2, shaken 24 in dark, 25 C, x1, anoxic; Fe speciation using Ferrozine method	sorbed As or As co-precipitated with amorphous/ poorly crystalline Fe(III)/dissolvable Fe(II)	(Heron et al., 1994; Huerta-Diaz and Morse, 1992; Keon et al., 2001; Tuccillo et al., 1999)
Microwave assisted HNO_3	Concentrated HNO_3, microwaved 5 min., 175 °C, x1	near total As (non-silicates)	EPA method 3051A

In the laboratory, sediments were thawed and opened in a Coy anaerobic chamber (gas mix of 95% N2, 5% H2; actual H2 in chamber is 1%). Sorbed As was evaluated by the phosphate method outlined in Keon et al. (2001) (Table 2.1). Prior to this extraction, wet homogenized sediment (0.4 g) from target core intervals was placed in 50-mL centrifuge tubes and was first reacted with 1 M MgCl2 for 4 h in the dark on an end-over-end rotator to remove ion exchangeable As. Then, after rinsing and decanting with nanopure deionized water (DI), sediments were reacted with 40 mL of 1 M NaH2PO4 in the dark on an end-over-end rotator with pH adjusted to 5–5.5 for 24 h. The step was repeated followed by a nanopure DI rinse. The bulk extract was filtered through a 0.2-μm filter, and analyzed for As using inductively coupled plasma-mass spectrometry (ICP-MS; detection limit = 0.5 μg/L).

Operationally defined concentrations of Fe(II) and Fe(III) from amorphous and poorly crystalline Fe phases along with associated As were determined using the 0.5 M HCl method (Heron et al., 1994; Huerta-Diaz and Morse, 1992; Keon et al., 2001; Poulton and Canfield, 2005; Tuccillo et al., 1999). Sediment (2–3 g) from target core intervals was placed into 60-mL amber serum vials and reacted with 20 mL of 0.5 M HCl. Grains > 2 mm were removed with forceps prior to weighing. Vials were capped, crimped, wrapped in foil, and agitated on a shaker table for 24 h. Extracts were then filtered through 0.2-μm filters and analyzed for Fe(II) and total Fe using the Ferrozine method (Gibbs, 1979) (detection limit = 0.24 mg/L). Fe(III) was determined by the difference between total Fe and Fe(II). Extracts from the 0.5 M HCl digestions were also analyzed for As using ICP coupled with optical emission spectrometry (ICP-OES) with a detection limit of 10 μg/L.

Near-total Fe and As concentrations were determined by reacting sediment (0.5 g) with trace metal grade concentrated nitric acid (10 mL) using microwave-assisted digestion (EPA

Method 3051a). Extracts were diluted 1:10, filtered (0.2 μm), and analyzed for Fe and As using ICP-OES. Digestion of National Institute of Standards and Technology standard reference material 2587 showed 80–100% recovery for As.

Particle size analysis and hydraulic conductivity estimation

Particle size analyses were performed on sediments collected in 2013 only, as there was not enough sediment mass of the archived 1993 samples to perform an accurate particle size analysis. However, based on visual inspection, samples with finer grained sediments in 1993 corresponded to similar grain sizes from samples of equivalent elevation collected in 2013.

Bulk sediment from target core intervals from 2013 was dried for 48 h at 40 °C. Dried sediment was ground by mortar and pestle; ~ 40 g were placed in a stack of five sieves with pore diameters of 2 mm, 500 μm, 250 μm, 150 μm, and 75 μm. A pan was used to collect particles < 75 μm. Sieves were shaken for 5 min.

The hydraulic conductivity (K) for 2013 samples was estimated using two empirical methods, the Hazen method (Hazen, 1911) (Eq. 2.1) and the Kozeny-Carman method (Carman, 1937; Carman, 1956; Kozeny, 1927) (Eq. 2.2)):

$$K = \frac{g}{v} \times 6 \times 10^{-4}[1 + 10(n - 0.26)]d_{10}^2 \quad \text{(Eq. 2.1)}$$

$$K = \frac{g}{v} \times 8.3 \times 10^{-3} \left[\frac{n^3}{(1-n)^2}\right] d_{10}^2 \quad \text{(Eq. 2.2)}$$

where K is hydraulic conductivity, g is the acceleration due to gravity, v is kinematic viscosity of water, n is porosity, and d_{10} is the grain diameter (in mm) for which 10% of the sample is finer, based on the particle size analysis curve. Porosity (n) is estimated using the empirical relationship (Eq. 2.3) defined by Vukovic and Soro (1992):

$$n = 0.255(1 + 0.83^{U}) \quad \text{(Eq. 2.3)}$$

where U is the coefficient of grain uniformity (Eq. 2.4):

$$U = \frac{d_{60}}{d_{10}} \quad \text{(Eq. 2.4)}$$

where d_{60} is the grain diameter (in mm) for which 60% of the sample is finer than based on the particle size analysis curve.

Results

Near total sediment Fe and As

Near total concentrations of sediment samples from each target interval in cores show a linear relationship (R2 = 0.703) between As and Fe (Figure 2.2A); concentrations generally group based on sampling locations in the aquifer with similar redox geochemistry, though concentrations in the Fe-reducing zone span a broad range.

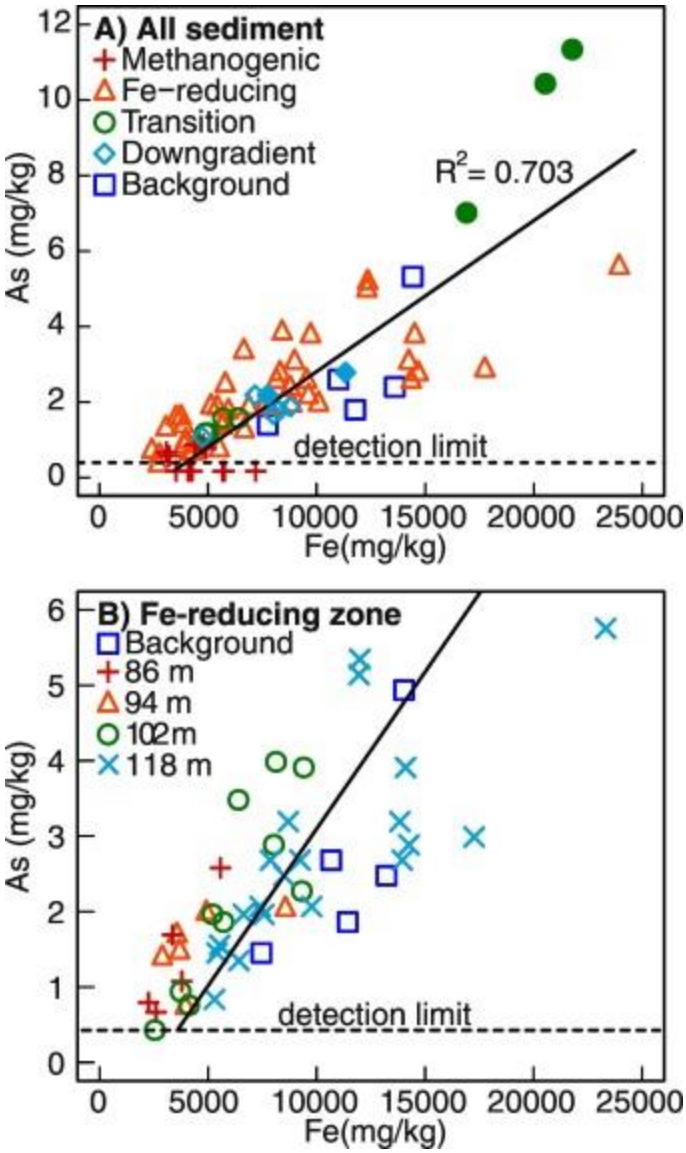

Figure 2.2. A) Near total concentrations of Fe (mg/kg) and As (mg/kg) in sediment in different redox zones of the Bemidji plume. Filled symbols in the transition and downgradient zones indicate silty sediments. B) Near total concentrations of Fe (mg/kg) and As (mg/kg) in Fe-reducing sediment only. Background samples were included for reference. The line in B is the same equation as the regression line in A. Sediments were collected in 2013 ± 2 years. See Figure 2.1 for location of sediment cores.

In background sediments where the redox conditions are oxic and reflect the prevailing geochemistry of uncontaminated sections of the aquifer (see Figure 2.1 for location), Fe concentrations range from 7750 mg/kg to 14,420 mg/kg, and As ranges from 1.4 to 4.8 mg/kg (Figure 2.2A; Table A.2). Methanogenic sediments near the oil body show 61–66% loss of Fe

compared to background and almost total removal of As. Arsenic concentrations in several sediment samples from the methanogenic zone were below detection (< 0.4 mg/kg) (Figure 2.2A), while low concentrations of Fe were prevalent.

Near-total Fe and As concentrations are highly variable in sediment in the Fe-reducing zone, with As ranging from 0.4 to 5.8 mg/kg, and Fe ranging from 2470 mg/kg to 23,850 mg/kg (Figure 2.2A; Table A.2). Some of the heterogeneity in concentrations can be explained by the sediments' distance from the oil body along the plume transect. Cores in the Fe-reducing zone were collected from four locations along the plume transect, at 86 m, 94 m, 102–104 m, and 118 m downgradient from the oil body (Figure 2.2B). Sediment in cores from 86 m and 94 m downgradient from the oil have been under Fe-reducing conditions for longer periods of time than sediments at 102 m and 118 m downgradient. As a result, the two cores nearer the oil body show an overall depletion in Fe and As relative to background, whereas Fe and As concentrations are more heterogeneous in the 102 and 118 m cores. Interestingly, some sediments at these two locations are enriched with As and/or Fe relative to background sediments, although sediments from 102 m are more depleted of Fe and As than 118 m sediments.

Cores collected from the anoxic-suboxic transition (i.e., transition zone) were composed of two distinct sediment layers. The upper layer (423.38–422.83 m AMSL; in top four samples of core T2) contained medium-to-coarse grained sand and gravel with brownish-red coloration, similar to the regional sediment throughout the aquifer observed by Zachara et al. (2004). This layer had a hydraulic conductivity (10^{-2} to 10^{-1} cm/s) reflective of medium-to-coarse grained sand (Table A.1). The bottom layer (422.83–422.58 m AMSL; bottom three samples in core T2) had lower hydraulic conductivity (10^{-3} to 10^{-4} cm/s) with a greater fraction of silt (15–20% of

bulk sediment) and was tannish-brown in color. Arsenic and Fe concentrations differ between the sand and silty layers in the transition zone core T2. In the silty zone, As ranges from 7.0 to 11.3 mg/kg, greater than the mean As concentration of 2.6 mg/kg in background sediment. In contrast, As concentrations in the sandy layer were lower, ranging from 1.2 to 1.6 mg/kg (Table A.2).

Fe and As concentrations in sediment from the core downgradient from the plume were roughly similar to background levels. The downgradient core also had a silt-rich layer, which had a mean As concentration of 2.3 mg/kg. Because the background core did not have a silt layer for comparison, we use the value of 2.3 mg/kg from the downgradient core as a proxy for the background silt layer.

Sorbed As on sediment

Comparison of the As concentrations extracted with phosphate to those from the near total extraction suggests that most (53 to 80%) of the As associated with sediments is sorbed to mineral surfaces (Figure 2.3; Table A.2). In background sediments, a mean of 69% of the near total As was sorbed. Sediment from two locations in the Fe-reducing zone (102 m and 117.7–118 m) had higher mean percentages of sorbed As than background: 73% and 78%. In the transition zone, although the near total As concentrations were higher, there was an overall decrease in the percentage of sorbed As (mean 53%). Beyond the plume, the percentage of sorbed As was also relatively low (mean 58%). In both the transition and downgradient zones, silty sediments had lower sorbed As than sandy sediments from the same core. Despite the lower percentage in these two zones, the sorbed As fraction still composes > 50% of the near total fraction.

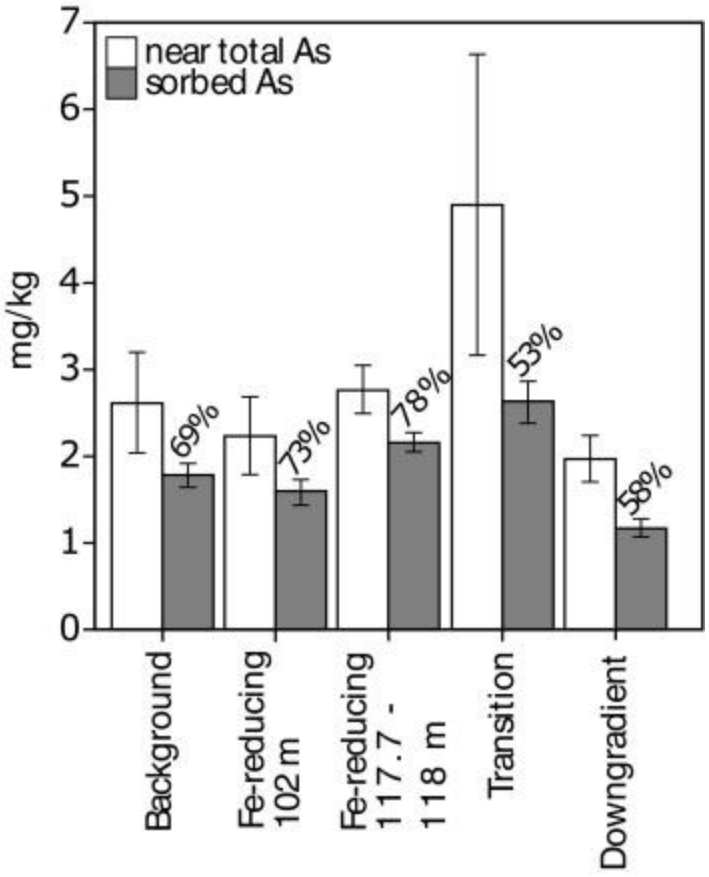

Figure 2.3. Mean concentrations of As (mg/kg) from microwave-assisted HNO3 (near total; white) and phosphate (sorbed; gray) digestions of sediments collected from cores from different redox zones. Error bars reflect the standard error from the mean for samples from each zone. Percentages reflect the sorbed fraction of As as a percent of the near total fraction.

Arsenic associated with HCl-extractable Fe

HCl extractions were used to evaluate the fraction of As associated with HCl-extractable Fe(III). This As fraction serves as a proxy for the amount of As that can be mobilized during Fe(III)-reduction. Overall, Fe and As in sediment from this extraction are positively correlated (Figure A.1), although the relationship is not as strong as Fe and As from the near-total extractions. In background sediments, the mean concentration of HCl-extractable total Fe (sum of Fe(II) and Fe(III) from HCl extractions) is 1485 mg/kg, with most (94%) existing as Fe(III) (Figure 2.4). Concentrations of As associated with HCl-extractable Fe are low in background sediments, averaging 0.35 mg/kg, about 13% of near total As in background.

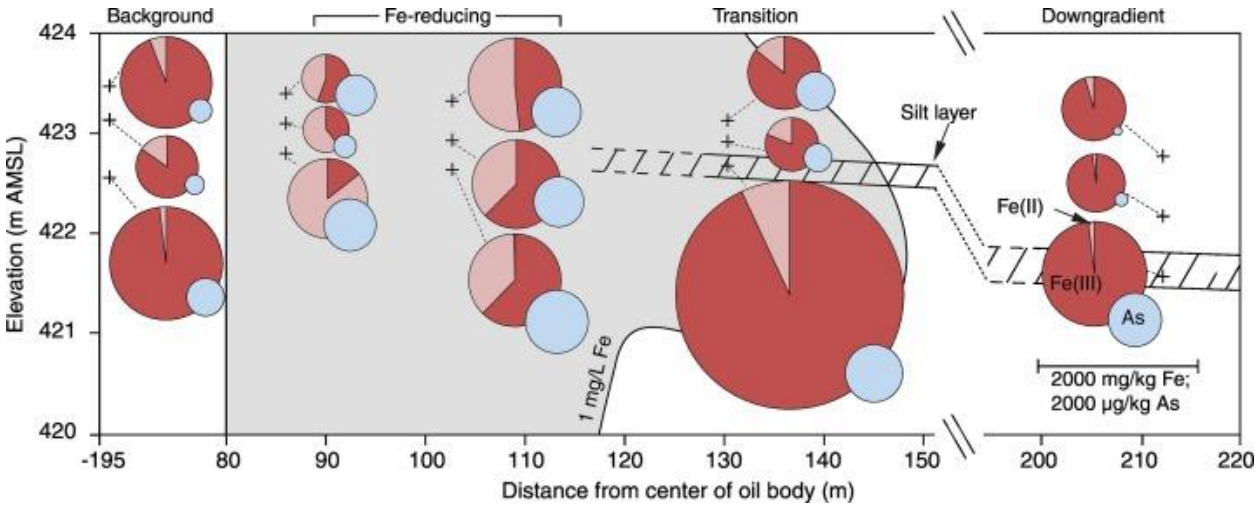

Figure 2.4. Sized pie charts (see legend in figure) of select sediment samples from Table A.2 showing concentrations of HCl-extractable Fe (red; mg/kg) and As (blue; µg/kg) associated with HCl-extractable Fe in different geochemical zones of the plume. Fe(III) and Fe(II) concentrations are shown in the darker and lighter shades, respectively. Sediment sampling locations are indicated by +. The shaded region reflects where Fe concentrations in groundwater are > 1 mg/L. Note breaks in the x-axis.

Sediments collected in the Fe-reducing zone, which is shown on Figure 2.4 as the shaded region within the 1 mg/L dissolved Fe contour, show evidence of substantial Fe-reduction. At 86 m, notable Fe mass has been lost from sediments due to reductive dissolution of Fe(III) minerals. Additionally, Fe(II) comprises most of the HCl-extractable Fe at 86 m, another indication of the extensive Fe-reduction. At 102 m, concentrations of sediment Fe(II) increase in comparison with background (Figure 2.4; Table A.2). However, the total mass of Fe in the Fe-reducing zone is roughly conserved in sediment of the reducing zone. Despite the reduction of Fe(III) at 86 and 102 m, concentrations of As associated with the HCl-extractable Fe are elevated in comparison to the background (Figure 2.4).

In the transition zone, several sediment samples were highly enriched with Fe and As relative to background, and in contrast to the upgradient Fe-reducing zone, Fe was mostly present as Fe(III). Silty sediments (see bottom sample in transition zone in Figure 2.4) contained

especially elevated concentrations of Fe and As, having 3.5 times greater Fe than background, and overall more As than in the sandy sediments in the same zone.

Downgradient from the plume, sediments have similar Fe(II):Fe(III) and As signatures to background. A silty interval at the bottom of the downgradient core had higher concentrations of As compared to sandy sediments from the same core.

Temporal patterns of As and Fe in aquifer sediments

Sediment cores collected in 1993 (cores R1, T1, T3; see Figure 2.1 for location) were originally digested for different Fe phases, but not for As. Although there was not enough remaining archived sediment from 1993 samples to conduct particle size analyses, visual inspection of sediments with a grain size card (USDA Soil Survey Manual, 1993) showed that 1993 sediments had similar grain sizes as 2013 samples from the same target elevation.

A comparison of near total digestions of sediment collected in 1993 with those in 2011–2014 show changes in As concentrations at three locations along the plume transect: 86 m, 102 m, and 132 m downgradient from the oil body (Figure 2.5; Table A.2).

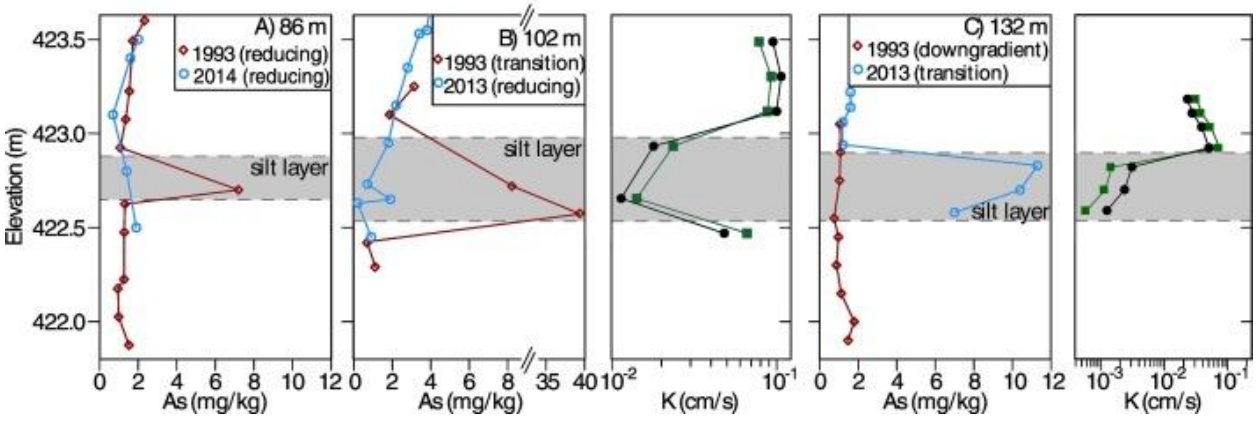

Figure 2.5. Depth profiles for near-total As concentrations in sediment from 1993 (red diamonds) and 2013–14 (blue circles) at A) 86 m, B) 102 m, and C) 132 m downgradient from the center of the oil body. The dashed gray zone indicates low K silt layers (see Table A.1). Values for hydraulic conductivity were calculated using the Hazen (black circles) and Kozeny-Carman (green squares) methods based on sediment samples from 2013. See Figure 2.1 for sampling locations.

At 86 m, Fe reducing conditions were prevalent in 1993 (Tuccillo et al., 1999) and in 2011–2014 (Cozzarelli et al., 2016). Overall, As concentrations in the 1993 sediment core (R1) were low (< 2 mg/kg) with the exception of one sample with elevated As in a silt zone (7.2 mg/kg) (Figure 2.5A). In the 2014 core (R2) at the same location, the As concentration in the same silt layer was considerably lower (1.4 mg/kg).

The 102 m location was in the transition zone in 1993 (Tuccillo et al., 1999) and in the Fe-reducing zone in 2013 (Cozzarelli et al., 2016). At this location, sandy sediments had low As (< 3 mg/kg) in both 1993 (T1) and 2013 (R4). However, the silt layer had elevated As (40.6 mg/kg) in 1993, > 15 × greater than the silt baseline As (2.3 mg/kg). In comparison, sediments collected in the silt zone in 2013 showed low concentrations of As (< 2 mg/kg) (Figure 2.5B).

The 132 m location was oxic in 1993 (Tuccillo et al., 1999); it was downgradient from the dissolved hydrocarbon plume at the time. Therefore, the As concentrations in sediments collected from this location reflect background conditions. Arsenic concentrations were homogeneous with depth in the core and were low, averaging about 1 mg/kg. In 2013, this location was in the transition zone (Cozzarelli et al., 2016). Elevated As was detected in a silty layer (Figure 2.5C), in which As concentrations were as high as 11.3 mg/kg.

Predicting As concentrations based on Fe data

The relationship between the near-total Fe and As in 2011–2014 sediments (Figure 2.2) shows that despite sediments being located in different redox zones in the plume, a linear relationship exists between Fe and As, with Fe concentrations serving as a strong predictor variable for As concentrations in sediment. Using the measured Fe and As concentrations in sediment collected in 1993 as an independent dataset, we assessed whether the regression equation from 2011 to

2014 data could accurately predict As concentrations in 1993 sediments based on only Fe concentrations. To test the relationship (Figure 2.6), measured concentrations of Fe from 1993 sediment were put into the 2011–2014 regression equation as the independent variable, and As concentrations were predicted as the dependent variable. Predicted arsenic concentrations were then compared to measured As concentrations to evaluate how accurately the regression based on current trends could predict As concentrations in different physical space in the aquifer, as well as from a different time.

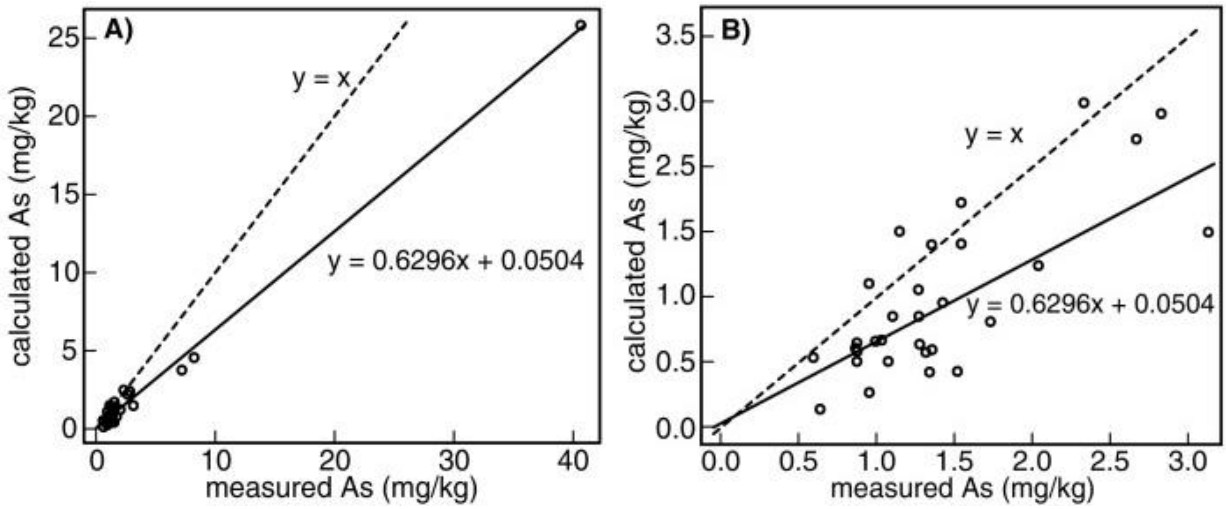

Figure 2.6. Plots of measured near-total As concentrations in sediment from 1993 compared to As concentrations calculated from the regression between Fe and As in 2011–2014 sediments (see Figure 2.2). The dashed line has a slope of one. The solid line is the best fit line through the data. A) All sediment from 1993. B) An inset of A to better show resolution at lower concentrations.

Results from the regression equation based on the Fe and As relationship from 2011 to 2014 (Figure 2.6) shows that the equation reasonably predicts As concentrations in 1993 sediments within 63% of the true concentration. One sample had extremely high As (40 mg/kg), and exhibited a strong weight in the regression analysis. To examine the effect of this sample on the regression equation, we ran a separate regression excluding the 40 mg/kg sample; the slope of measured vs. calculated As values (m = 0.58) was similar to the original regression. Other

measured parameters, including particle size, Fe(II):Fe(III), distance from the oil body center, depth in the aquifer, etc. were evaluated using a multiple linear regression to assess if more data improved the accuracy of the equation. However, these other parameters were not deemed statistically significant ($\alpha = 0.05$) in predicting As concentrations.

The regression equation indicates that the relationship between modern Fe and As slightly underpredicts the 1993 As concentrations. However, the equation reasonably predicts As concentrations in sediments in different times (1993 vs. 2011–2014) and space in sediments under different redox conditions. In fact, the 1993 dataset spanned three orders of magnitude (< 0.4 to > 40 mg/kg), and for each sample, the equation calculated the As concentration accurately within at least half an order of magnitude of the true value.

Discussion

Arsenic in Bemidji aquifer sediment

The linear correlation of near-total As and Fe in sediment (Figure 2.2) shows that As and Fe are associated in aquifer sediments. Although the extractions are not mineral specific, it can be inferred based on our dataset and previous studies that As associates with Fe(III) oxides and hydroxides. Although As also can be associated with Fe-sulfides (Berg et al., 2001; Schreiber et al., 2000; Smedley and Kinniburgh, 2002; Welch et al., 2000), previous mineralogical investigations of sediments at the Bemidji site have not detected Fe sulfides because sulfate concentrations in groundwater are low, and thus sulfate-reduction and formation of sulfides are unlikely. In contrast, abundant Fe oxides and hydroxides, including goethite, hematite, magnetite, and suspected ferrihydrite have been observed (Baedecker et al., 1993; Ng et al., 2014; Zachara et al., 2004). Based on groundwater saturation indices, the precipitation of Fe-carbonates (e.g., siderite, ferroan calcite) has been hypothesized as an important sink for Fe in

the contaminant plume (Baedecker et al., 1992; Baedecker et al., 1993; Ng et al., 2014), although their identification has proved elusive. The presence of Fe-carbonates may have implications for As mobility, as they have been documented to sorb As (Guo et al., 2011; Guo et al., 2007a; Guo et al., 2007b; Jönsson and Sherman, 2008). Arsenic associated with Fe-carbonates would be stable under anoxic conditions as Fe in siderite and ferroan calcite is in the reduced Fe(II) state, and thus not available as an electron acceptor during biodegradation reactions. However, the ability of siderite ($FeCO_3$) to sorb As is questionable under chemical conditions observed in the plume. A study of the surface chemistry of siderite reported a point of net zero charge at pH 5.3 ± 0.1 (Charlet et al., 1990). The pH in groundwater in the Bemidji plume generally ranges from 6.5 to 8; under these conditions, the overall surface charge of siderite would be negative, and thus, has lower ability to adsorb negatively charged As oxyanions. Siderite would likely be an important sorbent under lower pH (< 5.3) conditions.

Sorbed Fe(II) has also been hypothesized as an important Fe(II) sink in the Bemidji plume (Kohler et al., 2015; Ng et al., 2014; Tuccillo et al., 1999; Zachara et al., 2004). Recent reactive transport modeling suggests that 91% of Fe(II) in the bulk aquifer sediment is sorbed (Ng et al., 2015). The effect of sorbed Fe(II) on As retention is complex. For example, laboratory experiments have shown that Fe(II) can form ternary complexes with ferrihydrite and As, removing As from solution (Appelo et al., 2002). However, the introduction of bicarbonate competed with As for sorption on the ternary complex, and As retained by the complex was exchanged by bicarbonate (Appelo et al., 2002), suggesting that Fe(II) ternary complexes might not be viable long-term sinks for As in groundwater with elevated bicarbonate, such as in the Bemidji aquifer, where hydrocarbon biodegradation has resulted in elevated bicarbonate concentrations in the plume (Bennett et al., 1993).

Results from phosphate extractions suggest that As is mostly sorbed (69%) to sediments. Because not all As was extracted from phosphate digestions, some As is retained by other unknown mechanisms, possibly as co-precipitates with other detrital minerals. Nevertheless, the sorbed fraction of As is of greatest concern from a transport standpoint, as it is more easily mobilized than both As co-precipitates and more crystalline phases of As. Additionally, as poorly crystalline phases age, surface area decreases, thus decreasing the sorptive capacity, possibly resulting in As release (Stucki et al., 1988). Cozzarelli et al. (2016) estimated that the release of < 1% of sediment As can account for the observed As concentrations in groundwater. The amount of sorbed As in Bemidji sediment well exceeds 1% of the near total concentration. Given that the Fe-reducing conditions in the plume favor the release of sorbed As from Fe(III) oxides and hydroxides, the mobilization of As from other mineral phases is likely minor in comparison to the sorbed fraction.

The 0.5 M HCl extraction has commonly been used as a proxy for amorphous or poorly crystalline Fe(III) oxides that are reducible by microorganisms (Heron et al., 1994; Lovley and Phillips, 1986; Poulton and Canfield, 2005; Tuccillo et al., 1999). Arsenic extracted using this digestion is assumed to be associated with the HCl extractable Fe(III) (Keon et al., 2001) and is considered to be easily mobilized under Fe-reducing conditions. Based on comparisons of the 0.5 M HCl extractions to the near total As concentrations, only a small percentage (~ 5–30%) of sediment As is extractable by 0.5 M HCl and can be easily mobilized under Fe-reducing conditions. However, phosphate extractions showed that there is more sorbed As (60–80% of near total) than the amount of As that can be extracted by HCl (5–30%), thus indicating that there is another mechanism other than sorption to amorphous or poorly crystalline Fe(III) oxides that controls As in sediment. Due to the strong positive correlation between Fe and As and the

result that most of the As is sorbed, it is reasonable to assume that As not associated with these amorphous/poorly crystalline Fe(III) oxides is sorbed to more crystalline Fe-oxides or other Fe-minerals. This assumption is supported by the work of Tuccillo et al. (1999), which showed significant concentrations of crystalline Fe oxides that could not be extracted using 0.5 M HCl. Similarly, Zachara et al. (2004) identified goethite and hematite as intergranular precipitates in Fe-reducing sediment, suggesting these crystalline phases were more resistant to microbial reduction than amorphous Fe-hydroxides, which were depleted in contaminated sediment. However, extractions from Tuccillo et al. (1999) did observe slight decreases in crystalline Fe concentrations in the most contaminated areas of the plume, suggesting that microbes were able to reduce crystalline Fe(III) after depletion of more amorphous Fe(III), a phenomenon also observed in studies outside of Bemidji (Roden and Zachara, 1996). Data from this study in methanogenic sediments near the oil body show that As and Fe can be depleted to below detection limit concentrations, indicating that given enough time under reducing conditions (i.e., near the oil body), more recalcitrant crystalline Fe(III) phases can be reduced.

Redistribution of As due to biodegradation

A natural source of As associated with Fe(III) oxides exists in sediments in the Bemidji aquifer. Stable under regional oxic conditions, As does not pose a threat to groundwater quality. However, biodegradation of hydrocarbons coupled with Fe(III) reduction promotes the mobilization of As, causing a redistribution of As mass along the flow path in both groundwater and sediment. Downgradient from the oil body at the Bemidji site, four geochemical zones (methanogenic, Fe-reducing, anoxic-suboxic transition, and downgradient) show different As distributions due to biodegradation.

Methanogenic zone

Sediments from methanogenic cores are depleted with respect to As and Fe in comparison with background sediment. In several samples, As concentrations were even below the detection limit of 0.4 mg/kg. The removal of As and Fe results from the long-term reducing conditions in this section of the aquifer; it is adjacent to the oil body which is the source for hydrocarbons that drive biodegradation (Baedecker et al., 2011). Prior to the onset of methanogenesis, biodegradation in this zone was coupled with reduction of Fe(III) in sediments, resulting in loss (although not complete) of Fe(III) (Ng et al., 2015) and likely As from sediment. A comparison of the Fe and As concentrations in sediment and groundwater (Cozzarelli et al., 2016) show that although sediment Fe and As are depleted in the methanogenic zone, elevated Fe and As concentrations are still present in groundwater in this zone. Bekins et al. (1999) observed this phenomenon with respect to Fe and attributed it to heterogeneity in the methanogenic zone, where pockets of Fe(III) reduction are still active. However, comparison of As concentrations in groundwater near the oil in 2010 to more recent data collected in 2015 show decreases over time. We interpret this decline to continual reduction of the remaining pockets of Fe(III), resulting in flushing of As from both sediment and groundwater from the methanogenic zone.

Fe-reducing zone

The Fe-reducing zone is the primary region of As release from aquifer sediments to groundwater (Cozzarelli et al., 2016). Whereas long-term biodegradation results in depletion of near total As and Fe from Fe-reducing sediment close to the methanogenic zone, the 0.5 M HCl extractable As concentrations are highest in this zone (Figure 2.4), showing that Fe-reducing sediments retain As despite the reducing geochemical conditions. These data suggest that after mobilization into groundwater, As re-associates with Fe oxides and hydroxides, causing As enrichment in the HCl-extractable fraction. Combined, these results suggest that the release of As to groundwater does

not result from a single desorption reaction followed by transport in groundwater. Rather, As transport appears to be influenced by cycles of desorption and re-sorption, whereby the residence time of As in groundwater at any given time may be relatively short. Thus, sediments in the Fe-reducing zone act as both sources and sinks for dissolved As as long as Fe(III) sorption sites are available, resulting in heterogeneous distribution of As in the longitudinal dimension of the Fe-reducing zone (Figure 2.2; Figure A.1).

Anoxic-suboxic transition zone

In 2013, the leading edge of the anoxic plume was approximately ~ 132 m downgradient from the oil body (Cozzarelli et al., 2016). Within this transition zone, groundwater is suboxic, dissolved Fe and As concentrations are low (Fe < 2 mg/L; As < 2 μg/L), and saturation indices (calculated using The Geochemist's Workbench (Rockware Inc., Golden, CO) using groundwater chemistry data) suggest the precipitation of Fe(III) oxides and hydroxides. Fe and As concentrations in sandy sediment in this zone are similar to background, but these concentrations are elevated in a silt layer (Figs. 2 and 5). This phenomenon could be due to the greater surface area of the fine-grained sediment, thus resulting in a greater sorption capacity for As. The fine-grained sediments may also preferentially oxidize dissolved Fe(II), promoting the precipitation of Fe(III) oxides and hydroxides followed by sorption of dissolved As (Giménez et al., 2007; Hering et al., 2009; Stollenwerk, 2003). Alternatively, minerals in fine-grained sediments may also promote the oxidation of As(III) to As(V), which has been shown to enhance sorption of As to aquifer minerals (Amirbahman et al., 2006; Lin and Puls, 2000; Stollenwerk et al., 2007; Zhao et al., 2011).

Tuccillo et al. (1999) hypothesized that oxidation and precipitation of Fe(III) hydroxides at the plume's leading edge would inhibit the transport of solutes beyond the transition zone due

to the high sorption capacity of precipitated Fe(III). In an effect termed as the "iron curtain," Fe(III) acts as a barrier for migrating contaminants in the plume. The iron curtain effect has been documented to sequester oxyanions such as phosphate (Chambers and Odum, 1990; Datta et al., 2009), arsenate, and arsenite (Bone et al., 2006; Datta et al., 2009) in systems where anoxic groundwater discharges into oxic river waters. This effect is also observed in the Bemidji plume with respect to As, with As accumulating in transition zone sediments where dissolved Fe(II) is oxidized and precipitated as Fe(III) (Figure 2.4), and As is below detection in groundwater beyond the transition zone.

Downgradient zone

Downgradient sediments (200 m from the oil body) have similar Fe and As signatures as background sediments. The majority of As is sorbed, and > 95% of Fe is Fe(III), suggesting that the biogeochemical cycling has thus far not influenced the Fe and As signatures in sediment outside of the dissolved hydrocarbon plume.

Role of fine-grained sediments

Much of the temporal changes observed in sediment As concentrations between the 1993 and 2011–2014 core samples occurred in the silty layer. We acknowledge that this trend is supported by a limited dataset, and even though each sample with especially high As was always found in a silt layer, we do not aim to imply that all silt lenses in the aquifer are enriched in As. With that caveat, the silty layer of the transition zone in 1993 (102 m) had high concentrations of As (40.6 mg/kg; note that background silt As concentration is 2.3 mg/kg). In contrast, As in the sandy sediment in the 1993 transition zone at 102 m was generally < 2 mg/kg, suggesting that silty sediments at the 1993 transition zone accumulated As. A similar pattern was observed at the transition zone in 2013, where sandy sediments had low levels of As (1–2 mg/kg), and the silt

zone had 5–6 times more As than background. We were able to discount that the anomalously high As in these layers was a signature from original deposition by comparing these sediments to sediment collected in 1993 from the same section of the aquifer. In 1993, silty sediments from this section of the aquifer did not have elevated As concentrations like in 2013 (Figure 2.5C), and thus the high As is not a signature of original deposition.

Comparison of 1993 with 2013 data suggests that As sequestered in "old" transition zones is re-mobilized to groundwater as the Fe-reducing zone expands over time. In 1993, the silt layer in the transition zone had As concentrations > 40 mg/kg. However, by 2013 As concentrations in the same layer were only 2 mg/kg. The decrease in As indicates that even though the silt layers sequester As in appreciable amounts, As is not permanently sequestered, but rather is re-mobilized as groundwater becomes more reducing during plume expansion.

Long-term cycling of As

The combined processes of biodegradation and expansion of the anoxic plume have redistributed Fe and As along the plume transect over the approximate twenty-year period from 1993 to 2011–2014. Results from this study suggest that over the long-term, even under extensive Fe-reducing conditions, As and Fe remain strongly coupled in sediment, both under modern (2011–2014) and past (1993) geochemical conditions. Cozzarelli et al. (2016) showed that As and Fe were also strongly correlated in groundwater within the modern-day plume ($R2 = 0.82$). Based on the linear relationship between Fe and As in sediment, we show that Fe concentrations alone were adequately able to predict past As concentrations in the aquifer well within an order of magnitude, regardless of time, space, or geochemical conditions. This is beneficial in that Fe is a commonly measured parameter at sites impacted by organic contaminants because it is an important electron acceptor in biodegradation reactions. Arsenic in groundwater at organic

contaminated sites has not been historically documented until recently, and as a result, As has not been considered a contaminant of concern at these sites. Quantifying the Fe-As relationship can also be useful for reactive transport models, to allow for prediction of future distribution of As in groundwater at organic-contaminated sites with similar As mobilization mechanisms.

Based on historical data collected at the Bemidji site (Figure 2.7), a consistent pattern is observed in the Fe distribution in the hydrocarbon plume, which has implications for As. Early in the plume's history (1987), dissolved hydrocarbons were contained within 50 m of the oil body, with a small Fe-reducing zone in comparison to the modern day (Figure 2.7A, D).

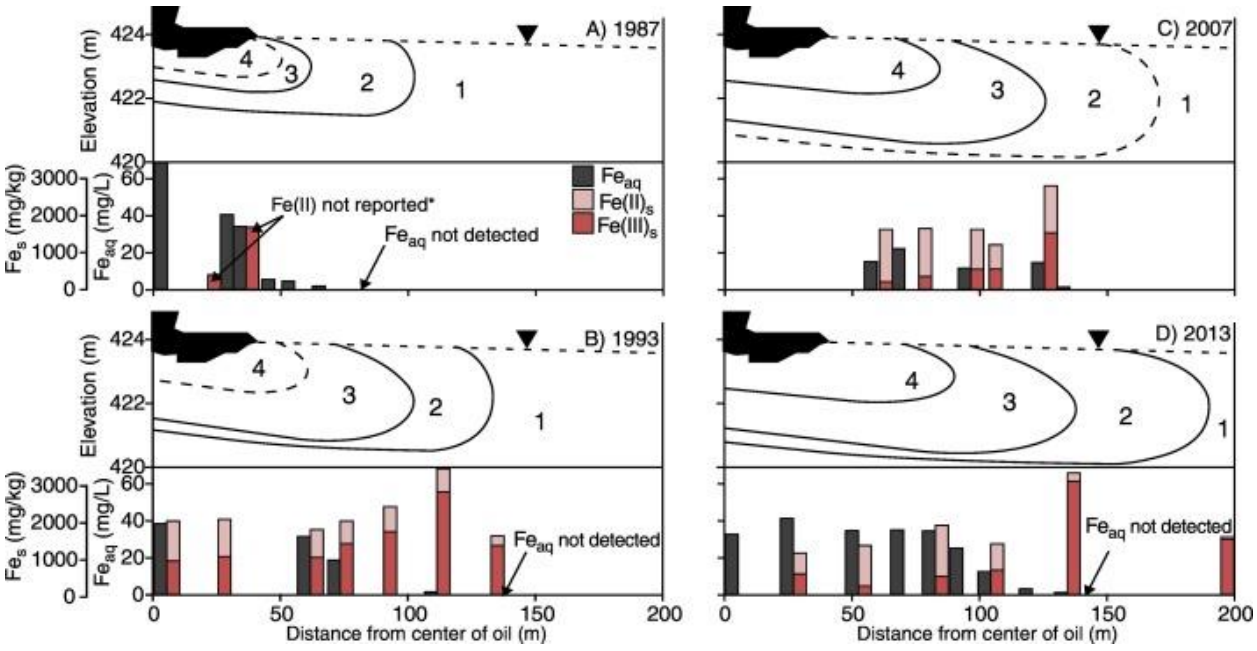

Figure 2.7. Historical data showing the distribution of Fe in groundwater and aquifer sediments in different redox zones (1 = oxic, 2 = transition, 3 = Fe-reducing, 4 = methanogenic) in A) 1987 (Baedecker et al., 1993; Bennett et al., 1993; Cozzarelli et al., 1994; Lovley et al., 1989), B) 1993 (Tuccillo, 1998; Tuccillo et al., 1999), C) 2007 (Amos et al., 2012; Amos et al., 2011), and D) 2013 (Cozzarelli et al., 2016; this study). Gray bars show Fe data in groundwater (Feaq). Red bars show Fe in sediment (Fes), with Fe(III) reported as the darker shade and Fe(II) as the lighter shade. Lines are dashed where approximated.

In 1993, as the plume expanded, the Fe reducing zone grew to encompass a much larger volume as shown by detection of dissolved Fe and elevated concentrations of Fe(II) in sediment (Figure

2.7B), and a transition zone identified by Tuccillo et al. (1999) showed enriched Fe at this anoxic-oxic transition. In 2007, the Fe-reducing zone continued to expand, reaching ~ 125 m downgradient (Figure 2.7C). By 2013, the Fe reducing zone had reached 130 m (Figure 2.7D).

We developed a conceptual model that describes these relationships at any point downgradient from the oil body, and illustrates the implications for As distribution (Figure 2.8). Prior to the breakthrough of the dissolved hydrocarbon plume, groundwater and sediment geochemistry in the aquifer reflect background conditions; dissolved oxygen (DO) is high, As is associated with Fe(III) oxides in sediment, and As and Fe are not detected in groundwater.

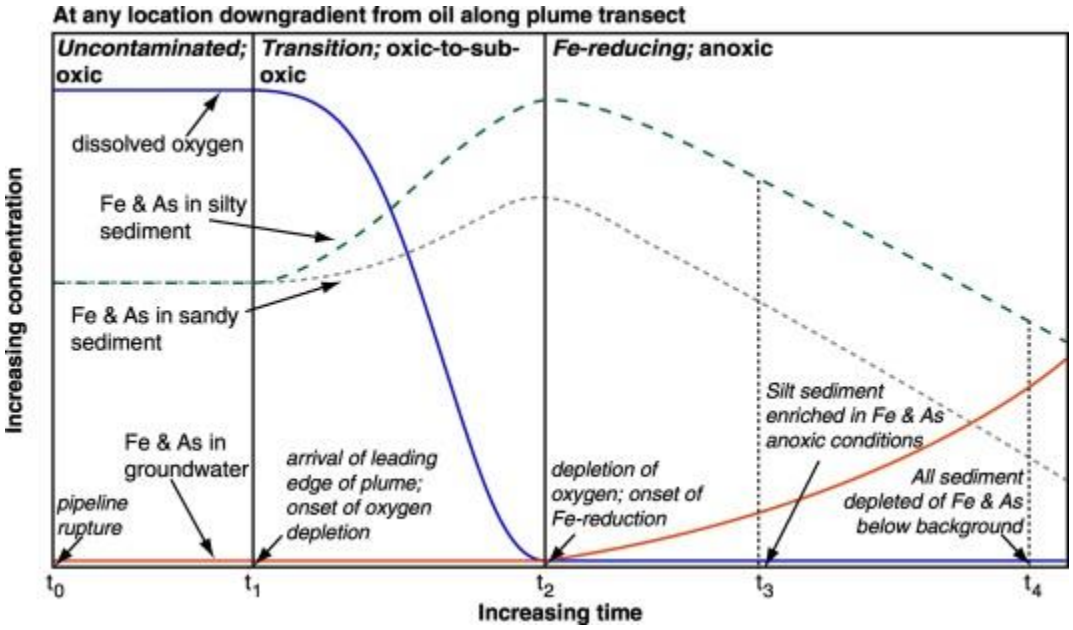

Figure 2.8 Conceptual model of the behavior of dissolved oxygen (blue), As and Fe in sand (gray, dashed) and silt (green, dashed), and groundwater (orange) cycling over time at any location downgradient from the oil body along the plume transect. t_0 reflects the pipeline rupture, t_1 reflects the arrival of the leading edge of the plume, t_2 reflects the onset of Fe-reduction, and t_3 and t_4 reflect sampling time points after the onset of Fe-reduction. The scaling of the x-axis does not accurately reflect real time, but rather shows a time series sequence of events at any location downgradient from the oil, where the length of time in each stage can vary.

After the initial breakthrough of the hydrocarbon plume, DO concentrations decrease in groundwater due to aerobic biodegradation of organics. Meanwhile, reducing conditions in

groundwater upgradient transport dissolved Fe and As to this oxygenated front, where Fe is removed via oxidation due to the presence of DO. Oxidation of Fe(II) accordingly creates sorption sites to remove As from groundwater. Based on data from this study, As and Fe accumulate at higher concentrations in silty sediment than sandy sediment in the transition zone.

After DO is depleted, anoxic conditions are established, and Fe-reduction becomes the main electron accepting process for anaerobic biodegradation. As a result, Fe(III) is reductively dissolved, releasing As into groundwater, resulting in depleted Fe and As in sediment and elevated Fe and As in groundwater. However, for some time after reducing conditions have been established, sediment, especially silt, will be elevated in Fe and As relative to background due to enrichment during the previous "transition" zone phase (see t_3 in Figure 2.8). However, given enough time under Fe-reducing conditions, both sand and silt sediments become depleted of Fe and As below background levels. Based on the current dataset and observed trend between 1993 and 2011–2014, the advancement of As in groundwater and sediment will continue to progress downgradient until the hydrocarbon plume stabilizes and begins to shrink.

Conclusions and implications

This study shows that Fe and As are linearly correlated in aquifer sediments over a range of three orders of magnitude (0.4–40 mg/kg As). The linear relationship holds true regardless of time (i.e., the same correlation was observed in contaminated sediments in 1993 and 2011–2014) and redox conditions; the relationship was valid in Fe-reducing, anoxic-suboxic transition, and uncontaminated oxic sediment. The strong sorption affinity of As for Fe(III) oxides is the main mechanism responsible for the Fe-As relationship. As a result, As cycling between groundwater and sediment in the contaminated aquifer closely mimics Fe, and the distribution of Fe in sediment serves as a useful proxy for As.

A spatial distribution of Fe and As in the aquifer shows that the leading edge of the plume (transition zone) temporarily sequesters Fe and As from groundwater by accumulating in sediment. Silt zones in particular have a high capacity to sequester As due to greater mineral surface area.

Results of this study show that Fe and As accumulate in the anoxic-suboxic transition zone, which acts as an “iron curtain”. Arsenic is not detected in groundwater downgradient from the transition zone curtain. However, As sorbed to sediment in this zone is not permanently sequestered and can be remobilized in groundwater. An assessment of the historical Fe data in sediment at Bemidji shows that the curtain is not stationary, but progresses downgradient as the contaminant plume evolves. Although the curtain has a large capacity to remove As from groundwater via sorption, the curtain itself is bioavailable under Fe-reducing conditions. As shown in this study, Fe(III) in the observed curtain from 1993 was reductively dissolved, and As was desorbed. We infer that Fe and As were then transported downgradient in groundwater to suboxic conditions and re-oxidized to form a new curtain. This set of reactions continues to occur in a cyclical pattern, making downgradient groundwater continually vulnerable to As contamination until the dissolved hydrocarbon plume stabilizes and retreats. The conceptual model is designed to serve as a guideline for assessing potential Fe and As cycling in other aquifers contaminated by organic carbon.

Acknowledgements

We thank Jeanne Jaeschke for her help collecting and analyzing samples and the team of scientists at the USGS Minnesota Water Science Center, including Jared Trost for field site coordination and support, Melinda Erickson for discussions about the study design, and Andrew Berg, Brent Mason, and John Greene for core collection. We also thank Barbara Bekins for

helpful discussions about biodegradation and Fe reduction, Chelsea Delsack and Katie Krueger for laboratory assistance, and Athena Tilley for ICP analyses.

This project was supported by the USGS Toxic Substances Hydrology Program and the National Research Program. Additional funding was provided by a collaborative venture of the USGS, Enbridge Energy Limited Partnership, the Minnesota Pollution Control Agency, and Beltrami County, MN. Any use of trade, product, or firm names in this publication is for descriptive purposes only and does not imply endorsement by the U.S. Government. A data-release product companion to this journal article (Ziegler et al., 2017) contains all the data and metadata associated with this article and can be found at http://dx.doi.org/10.5066/F7K35RWK.

References

Amirbahman, A., Kent, D.B., Curtis, G.P., Davis, J.A., 2006. Kinetics of sorption and abiotic oxidation of arsenic(III) by aquifer materials. Geochim. Cosmochim. Acta 70, 533–547.

Amos, R.T., Bekins, B.A., Delin, G.N., Cozzarelli, I.M., Blowes, D.W., Kirshtein, J.D., 2011. Methane oxidation in a crude oil contaminated aquifer: delineation of aerobic reactions at the plume fringes. J. Contam. Hydrol. 125, 13–25.

Amos, R.T., Bekins, B.A., Cozzarelli, I.M., Voytek, M.A., Kirshtein, J.D., Jones, E.J.P., Blowes, D.W., 2012. Evidence for iron-mediated anaerobic methane oxidation in a crude oil-contaminated aquifer. Geobiology 10, 506–517.

Appelo, C., Van der Weiden, M., Tournassat, C., Charlet, L., 2002. Surface complexation of ferrous iron and carbonate on ferrihydrite and the mobilization of arsenic. Environ. Sci. Technol. 36, 3096–3103.

Baedecker, M.J., Cozzarelli, I.M., Evans, J.R., Hearn, P.P., 1992. Authigenic mineral formation in aquifer rich in organic material. In: Kharaka, Y.K., Maest, A.S. (Eds.), Water-Rock Interaction-7. AA Balkeme, Rotterdam, pp. 257–261.

Baedecker, M.J., Cozzarelli, I.M., Eganhouse, R.P., Siegel, D.E., Bennett, P.C., 1993. Crude oil in a shallow sand and gravel aquifer-III. Biogeochemical reactions and mass balance modeling in anoxic groundwater. Appl. Geochem. 8, 569–586.

Baedecker, M.J., Eganhouse, R.P., Bekins, B.A., Delin, G.N., 2011. Loss of volatile hydrocarbons from an LNAPL oil source. J. Contam. Hydrol. 126, 140–152.

Bekins, B.A., Godsy, E.M., Warren, E., 1999. Distribution of microbial physiologic types in an aquifer contaminated by crude oil. Microb. Ecol. 37, 263–275.

Bekins, B.A., Cozzarelli, I.M., Godsy, E.M., Warren, E., Essaid, H., I. and Tuccillo, M.E., 2001. Progression of natural attenuation processes at a crude oil spill site: II. Controls on spatial distribution of microbial populations. J. Contam. Hydrol. 53, 387–406.

Bekins, B.A., Cozzarelli, I.M., Curtis, G.P., 2005. A simple method of calculating growth rates of petroleum hydrocarbon plumes. Ground Water 43, 817–826.

Bennett, P.C., Siegel, D.E., Baedecker, M.J., Hult, M.F., 1993. Crude oil in a shallow sand and gravel aquifer-I. Hydrogeology and inorganic chemistry. Appl. Geochem. 8, 529–549.

Berg, M., Tran, H.C., Nguyen, T.C., Pham, H.V., Schertenleib, R., Giger, W., 2001. Arsenic contamination of groundwater and drinking water in Vietnam: a human health threat. Environ. Sci. Technol. 35, 2621–2626.

Bhattacharya, P., Claesson, M., Bundschuh, J., Sracek, O., Fagerberg, J., Jacks, G., Martin, R.A., Storniolo, A.d.R. and Thir, J.M., 2006. Distribution and mobility of arsenic in the Rio Dulce alluvial aquifers in Santiago del Estero Province. Argentina Sci. Total Environ. 358, 97–120.

Bone, S.E., Gonneea, M.E., Charette, M.A., 2006. Geochemical cycling of arsenic in a coastal aquifer. Environ. Sci. Technol. 40, 3273–3278.

Carman, P.C., 1937. Fluid flow through granular beds. Transactions-Institution of Chemical Engineers 15, 150–166.

Carman, P.C., 1956. Flow of Gases through Porous Media. Academic Press.

Chambers, R.M., Odum, W.E., 1990. Porewater oxidation, dissolved phosphate and the iron curtain. Biogeochemistry 10, 37–52.

Charlet, L., Wersin, P., Stumm, W., 1990. Surface charge of MnCO3 and FeCO3. Geochim. Cosmochim. Acta 54, 2329–2336.

Cozzarelli, I.M., Baedecker, M.J., Eganhouse, R.P., Goerlitz, D.F., 1994. The geochemical evolution of low-molecular-weight organic acids derived from the degradation of petroleum contaminants in groundwater. Geochim. Cosmochim. Acta 58, 863–877.

Cozzarelli, I.M., Bekins, B.A., Baedecker, M.J., Aiken, G.M., Eganhouse, R.P., Tuccillo, M.E., 2001. Progression of natural attenuation processes at a crude-oil spill site: I. Geochemical evolution of the plume. J. Contam. Hydrol. 53, 369–385.

Cozzarelli, I.M., Schreiber, M.E., Erickson, M.L., Ziegler, B.A., 2016. Arsenic cycling in hydrocarbon plumes: secondary effects of natural attenuation. Ground Water 54, 35–45.

Datta, S., Mailloux, B., Jung, H.-B., Hoque, M., Stute, M., Ahmed, K., Zheng, Y., 2009. Redox trapping of arsenic during groundwater discharge in sediments from the Meghna riverbank in Bangladesh. Proc. Natl. Acad. Sci. 106, 16930–16935.

De Vitre, R., Belzile, N., Tessier, A., 1991. Speciation and adsorption of arsenic on diagenetic iron oxyhydroxides. Limnol. Oceanogr. 36, 1480–1485.

Erickson, M.L., Barnes, R.J., 2005. Glacial sediment causing regional-scale elevated arsenic in drinking water. Ground Water 43, 796–805.

Fuller, C.C., Davis, J.A., Waychunas, G.A., 1993. Surface chemistry of ferrihydrite: Part 2. Kinetics of arsenate adsorption and coprecipitation. Geochim. Cosmochim. Acta 57, 2271–2282.

Gibbs, M.M., 1979. A simple method for the rapid determination of iron in natural waters. Water Res. 13, 295–297.

Giménez, J., Martínez, M., de Pablo, J., Rovira, M., Duro, L., 2007. Arsenic sorption onto natural hematite, magnetite, and goethite. J. Hazard. Mater. 141, 575–580.

Gorra, R., Webster, G., Martin, M., Celi, L., Mapelli, F., Weightman, A., 2012. Dynamic microbial community associated with iron–arsenic co-precipitation products from a groundwater storage system in Bangladesh. Microb. Ecol. 64, 171–186.

Guo, H., Stüben, D., Berner, Z., 2007a. Adsorption of arsenic (III) and arsenic (V) from groundwater using natural siderite as the adsorbent. J. Colloid Interface Sci. 315, 47–53.

Guo, H., Stüben, D., Berner, Z., 2007b. Removal of arsenic from aqueous solution by natural siderite and hematite. Appl. Geochem. 22, 1039–1051.

Guo, H., Li, Y., Zhao, K., Ren, Y., Wei, C., 2011. Removal of arsenite from water bysynthetic siderite: behaviors and mechanisms. J. Hazard. Mater. 186, 1847–1854.

Harvey, C.F., Swartz, C.H., Badruzzaman, A., Keon-Blute, N., Yu, W., Ali, M.A., Jay, J., Beckie, R., Niedan, V., Brabander, D., 2002. Arsenic mobility and groundwater extraction in Bangladesh. Science 298, 1602–1606.

Hazen, A., 1911. Discussion: dams on sand foundations. Transactions 73.

He, Y.T., Fitzmaurice, A.G., Bilgin, A., Choi, S., O'Day, P., Horst, J., Harrington, J., James Reisinger, H., Burris, D.R., Hering, J.G., 2010. Geochemical processes controlling arsenic mobility in groundwater: a case study of arsenic mobilization and natural attenuation. Appl. Geochem. 25, 69–80.

Hering, J.G., O'Day, P.A., Ford, R.G., He, Y.T., Bilgin, A., Reisinger, H.J., Burris, D.R., 2009. MNA as a remedy for arsenic mobilized by anthropogenic inputs of organic carbon. Ground Water Monit. Remediat. 29, 84–92.

Heron, G., Crouzet, C., Bourg, A.C., Christensen, T.H., 1994. Speciation of Fe (II) and Fe (III) in contaminated aquifer sediments using chemical extraction techniques. Environ. Sci. Technol. 28, 1698–1705.

Huerta-Diaz, M.A., Morse, J.W., 1992. Pyritization of trace metals in anoxic marine sediments. Geochim. Cosmochim. Acta 56, 2681–2702.

Jönsson, J., Sherman, D.M., 2008. Sorption of As(III) and As(V) to siderite, green rust (fougerite) and magnetite: implications for arsenic release in anoxic groundwaters. Chem. Geol. 255, 173–181.

Keimowitz, A.R., Simpson, H.J., Stute, M., Datta, S., Chillrud, S.N., Ross, J., Tsang, M., 2005. Naturally occurring arsenic: mobilization at a landfill in Maine and implications for remediation. Appl. Geochem. 20, 1985–2002.

Kelly, W.R., Holm, T.R., Wilson, S.D., Roadcap, G.S., 2005. Arsenic in glacial aquifers: sources and geochemical controls. Groundwater 43, 500–510.

Kent, D.B., Fox, P.M., 2004. The influence of groundwater chemistry on arsenic concentrations and speciation in a quartz sand and gravel aquifer. Geochem. Trans. 5, 1–12.

Keon, N.E., Swartz, C.H., Brabander, D.J., Harvey, C., Hemond, H.F., 2001. Validation of an arsenic sequential extraction method for evaluating mobility in sediments. Environ. Sci. Technol. 35, 2778–2784.

Knobeloch, L.M., Zierold, K.M., Anderson, H.A., 2006. Association of arsenic-contaminated drinking-water with prevalence of skin cancer in Wisconsin's Fox River Valley. J. Health Popul. Nutr. 206–213.

Kohler, M., Kent, D.B., Bekins, B.A., Cozzarelli, I.M., Ng, C.G.H., 2015. Identifying and Quantifying Chemical Forms of Sediment-Bound Ferrous Iron. American Geophysical Union Fall Meeting, San Francisco, CA.

Korte, N., 1991. Naturally occurring arsenic in groundwaters of the Midwestern United States. Environ. Geol. Water Sci. 18, 137–141.

Kozeny, J., 1927. Über kapillare leitung des wassers im boden:(aufstieg, versickerung und anwendung auf die bewässerung). Hölder-Pichler-Tempsky.

deLemos, J.L., Bostick, B.C., Renshaw, C.E., Stürup, S., Feng, X., 2006. Landfill-stimulated iron reduction and arsenic release at the coakley superfund site (NH). Environ. Sci. Technol. 40, 67–73.

Lin, Z., Puls, R., 2000. Adsorption, desorption and oxidation of arsenic affected by clay minerals and aging process. Environ. Geol. 39, 753–759.

Lindberg, A.-L., Goessler, W., Gurzau, E., Koppova, K., Rudnai, P., Kumar, R., Fletcher, T., Leonardi, G., Slotova, K., Gheorghiu, E., 2006. Arsenic exposure in Hungary, Romania and Slovakia. J. Environ. Monit. 8, 203–208.

Lovley, D.R., Phillips, E.J., 1986. Organic matter mineralization with reduction of ferric iron in anaerobic sediments. Appl. Environ. Microbiol. 51, 683–689.

Lovley, D.R., Baedecker, M.J., Lonergan, D.J., Cozzarelli, I.M., Phillips, E.J.P., Siegel, D.I., 1989. Oxidation of aromatic contaminants coupled to microbial iron reduction. Nature 339, 297–300.

Luo, Z., Zhang, Y., Ma, L., Zhang, G., He, X., Wilson, R., Byrd, D., Griffiths, J., Lai, S., He, L., 1997. Chronic Arsenicism and Cancer in Inner Mongolia—Consequences of Wellwater Arsenic Levels Greater Than 50 μg/l, Arsenic. Springer. 55–68.

Ma, H.Z., Xia, Y.J., Wu, K.G., Sun, T.Z., Mumford, J.L., 1999. Human exposure to arsenic and health effects in Bayingnormen, Inner Mongolia. In: Chappell, W.R., Abernathy, C.O., Calderon, R. (Eds.), Arsenic Exposure and Health Effects. Elsevier, Amsterdam, pp. 127–131.

Manning, B.A., Goldberg, S., 1996. Modeling competitive adsorption of arsenate with phosphate and molybdate on oxide minerals. Soil Sci. Soc. Am. J. 60, 121–131.

McArthur, J., Ravenscroft, P., Safiulla, S., Thirlwall, M., 2001. Arsenic in groundwater: testing pollution mechanisms for sedimentary aquifers in Bangladesh. Water Resour. Res. 37, 109–117.

McArthur, J.M., Banerjee, D.M., Hudson-Edwards, K.A., Mishra, R., Purohit, R., Ravenscroft, P., Cronin, A., Howarth, R.J., Chatterjee, A., Talukder, T., Lowry, D., Houghton, S., Chadha, D.K., 2004. Natural organic matter in sedimentary basins and its relation to arsenic in anoxic ground water: the example of West Bengal and its worldwide implications. Appl. Geochem. 19, 1255–1293.

Mukherjee, A., Sengupta, M.K., Hossain, M.A., Ahamed, S., Das, B., Nayak, B., Lodh, D., Rahman, M.M., Chakraborti, D., 2006. Arsenic contamination in groundwater: a global perspective with emphasis on the Asian scenario. J. Health Popul. Nutr. 142–163.

Murphy, F., Herkelrath, W., 1996. A sample-freezing drive shoe for a wire line piston core sampler. Groundwater Monit. Remediat. 16, 86–90.

Ng, G.-H.C., Bekins, B.A., Cozzarelli, I.M., Baedecker, M.J., Bennett, P.C., Amos, R.T., 2014. A mass balance approach to investigating geochemical controls on secondary water quality impacts at a crude oil spill site near Bemidji, MN. J. Contam. Hydrol. 164, 1–15.

Ng, G.-H.C., Bekins, B.A., Cozzarelli, I.M., Baedecker, M.J., Bennett, P.C., Amos, R.T., Herkelrath, W.N., 2015. Reactive transport modeling of geochemical controls on secondary water quality impacts at a crude oil spill site near Bemidji, MN. Water Resour. Res. 51, 4156–4183.

Nickson, R., McArthur, J., Burgess, W., Ahmed, K.M., Ravenscroft, P., Rahmanñ, M., 1998. Arsenic poisoning of Bangladesh groundwater. Nature 395, 338.

Nickson, R., McArthur, J., Ravenscroft, P., Burgess, W., Ahmed, K., 2000. Mechanism of arsenic release to groundwater, Bangladesh and West Bengal. Appl. Geochem. 15, 403–413.

Nordstrom, D.K., 2002. Worldwide occurrences of arsenic in ground water. Science 296, 2143–2145.

Pal, T., Mukherjee, P.K., Sengupta, S., 2002. Nature of arsenic pollutants in groundwater of Bengal basin-a case study from Baruipur area, West Bengal, India. Curr. Sci. 82, 554–561.

Pfannkuch, H., 1979. Interim Report and Recommendations on Monitoring Program for Site MP 926.5. Lakehead Pipe Line Company, Inc.

Pierce, M.L., Moore, C.B., 1982. Adsorption of arsenite and arsenate on amorphous iron hydroxide. Water Res. 16, 1247–1253.

Poulton, S.W., Canfield, D.E., 2005. Development of a sequential extraction procedure for iron: Implications for iron partitioning in continentally derived particulates. Chem. Geol. 214, 209–221.

Quicksall, A.N., Bostick, B.C., Sampson, M., 2008. Linking organic matter deposition and iron mineral transformations to groundwater arsenic levels in the Mekong delta, Cambodia. Appl. Geochem. 23, 3088–3098.

Ravenscroft, P., Brammer, H., Richards, K., 2009. Arsenic Pollution: A Global Synthesis. John Wiley & Sons.

Revesz, K., Coplen, T.B., Baedecker, M.J., Glynn, P.D., Hult, M., 1995. Methane production and consumption monitored by stable H and C isotope ratios at a crude oil spill site, Bemidji, Minnesota. Appl. Geochem. 10, 505–516.

Roden, E.E., Zachara, J.M., 1996. Microbial reduction of crystalline iron (III) oxides: Influence of oxide surface area and potential for cell growth. Environ. Sci. Technol. 30, 1618–1628.

Root, T.L., Gotkowitz, M.B., Bahr, J.M., Attig, J.W., 2010. Arsenic geochemistry and hydrostratigraphy in midwestern U.S. glacial deposits. Ground Water 48, 903–912.

Rowland, H., Pederick, R., Polya, D., Pancost, R., Van Dongen, B., Gault, A., Vaughan, D., Bryant, C., Anderson, B., Lloyd, J., 2007. The control of organic matter on microbially mediated iron reduction and arsenic release in shallow alluvial aquifers, Cambodia. Geobiology 5, 281–292.

Schreiber, M., Simo, J., Freiberg, P., 2000. Stratigraphic and geochemical controls on naturally occurring arsenic in groundwater, eastern Wisconsin, USA. Hydrogeol. J. 8, 161–176.

Smedley, P., Kinniburgh, D., 2002. A review of the source, behaviour and distribution of arsenic in natural waters. Appl. Geochem. 17, 517–568.

Smedley, P.L., Nicolli, H.B., Macdonald, D.M.J., Barros, A.J., Tullio, J.O., 2002. Hydrogeochemistry of arsenic and other inorganic constituents in groundwaters from La Pampa, Argentina. Appl. Geochem. 17, 259–284.

Smith, A.H., Lopipero, P.A., Bates, M.N., Steinmaus, C.M., 2002. Arsenic epidemiology and drinking water standards. Science 296, 2145–2146.

Stollenwerk, K.G., 2003. Geochemical Processes Controlling Transport of Arsenic in Groundwater: A Review of Adsorption. Arsenic in Ground Water. Springer. 67–100.

Stollenwerk, K.G., Breit, G.N., Welch, A.H., Yount, J.C., Whitney, J.W., Foster, A.L., Uddin, M.N., Majumder, R.K., Ahmed, N., 2007. Arsenic attenuation by oxidized aquifer sediments in Bangladesh. Sci. Total Environ. 379, 133–150.

Stucki, J.W., Goodman, B.A., Schwertmann, U., 1988. Iron in Soils and Clay Minerals. Springer Science & Business Media.

Tuccillo, M.E., 1998. Processes and Effects of Iron Reduction in Anoxic Surficial Aquifers. Ph.D. dissertation Department of Environmental Sciences, University of Virginia, Charlottesville, VA.

Tuccillo, M.E., Cozzarelli, I.M., Herman, J.S., 1999. Iron reduction in the sediments of a hydrocarbon-contaminated aquifer. Appl. Geochem. 14, 655–667.

USDA, 1993. Examination and description of soil profiles. In: Soil Survey Manual.

Varsányi, I., Kovács, L.Ó., 2006. Arsenic, iron and organic matter in sediments and groundwater in the Pannonian Basin, Hungary. Appl. Geochem. 21, 949–963.

Vukovic, M., Soro, A., 1992. Determination of Hydraulic Conductivity of Porous Media from Grain-Size Composition. Water Resources Publications, Littleton, CO.

Warner, K.L., 2001. Arsenic in glacial drift aquifers and the implication for drinking water—Lower Illinois River Basin. Ground Water 39, 433–442.

Welch, A.H., Lico, M.S., 1998. Factors controlling As and U in shallow ground water, southern Carson Desert, Nevada. Appl. Geochem. 13, 521–539.

Welch, A.H., Westjohn, D., Helsel, D.R., Wanty, R.B., 2000. Arsenic in ground water of the United States: occurrence and geochemistry. Ground Water 38, 589–604.

West, N., Schreiber, M., Gotkowitz, M., 2012. Arsenic release from chlorine-promoted alteration of a sulfide cement horizon: evidence from batch studies on the St. Peter Sandstone, Wisconsin, USA. Appl. Geochem. 27, 2215–2224.

Whaley-Martin, K.J., Mailloux, B.J., Van Geen, A., Bostick, B.C., Silvern, R.F., Kim, C., Ahmed, K., Choudhury, I., Slater, G.F., 2016. Stimulation of microbially mediated arsenic release in Bangladesh aquifers by young carbon indicated by radiocarbon analysis of sedimentary bacterial lipids. Environ. Sci. Technol. 50, 7353–7363.

Zachara, J.M., Kukkadapu, R.K., Gassman, P.L., Dohnalkova, A., Fredrickson, J.K., Anderson, T., 2004. Biogeochemical transformation of Fe minerals in a petroleumcontaminated aquifer. Geochim. Cosmochim. Acta 68, 1791–1805.

Zhao, Z., Jia, Y., Xu, L., Zhao, S., 2011. Adsorption and heterogeneous oxidation of As (III) on ferrihydrite. Water Res. 45, 6496–6504.

Ziegler, B.A., McGuire, J.T., Cozzarelli, I.M., 2015. Rates of As and trace-element mobilization caused by Fe reduction in mixed BTEX–ethanol experimental plumes. Environ. Sci. Technol. 49, 13179–13189.

Ziegler, B.A., Schreiber, M.E., Cozzarelli, I.M., 2017. Chemical extraction results of aquifer sediments for concentrations of iron and arsenic in different redox zones at the crude-oil spill site near Bemidji, Minnesota. U.S. Geol. Surv. data release: https://doi.org/10.5066/F7K35RWK.

CHAPTER 3. THE ROLE OF ALLUVIAL AQUIFER SEDIMENTS IN ATTENUATING A DISSOLVED ARSENIC PLUME

A version of this chapter has been published in Environmental Pollution.

Abstract

Natural attenuation of organic contaminants in groundwater can give rise to a series of complex biogeochemical reactions that release secondary contaminants to groundwater. In a crude oil contaminated aquifer, biodegradation of petroleum hydrocarbons is coupled with the reduction of ferric iron (Fe(III)) hydroxides in aquifer sediments. As a result, naturally occurring arsenic (As) adsorbed to Fe(III) hydroxides in the aquifer sediment is mobilized from sediment into groundwater. However, Fe(III) in sediment of other zones of the aquifer has the capacity to attenuate dissolved As via resorption. In order to better evaluate how long-term biodegradation coupled with Fe-reduction and As mobilization can redistribute As mass in contaminated aquifer, we quantified mass partitioning of Fe and As in the aquifer based on field observation data. Results show that Fe and As are spatially correlated in both groundwater and aquifer sediments. Mass partitioning calculations demonstrate that 99.9% of Fe and 99.5% of As are associated with aquifer sediment. The sediments act as both sources and sinks for As, depending on the redox conditions in the aquifer. Calculations reveal that at least 78% of the original As in sediment near the oil has been mobilized into groundwater over the 35-year lifespan of the plume. However, the calculations also show that only a small percentage of As (~0.5%) remains in groundwater, due to resorption onto sediment. At the leading edge of the plume, where groundwater is suboxic, sediments sequester Fe and As, causing As to accumulate to concentrations 5.6 times greater than background concentrations. Current As sinks can serve as future sources of As as the plume evolves over time. The mass balance approach used in this study can be applied to As cycling in other aquifers where groundwater As results from biodegradation of an organic carbon point source coupled with Fe reduction.

Introduction

Monitored natural attenuation is commonly employed as a remediation strategy in aquifers impacted by organic contaminants (National Research Council, 2000). Several natural processes, including adsorption (Brusseau et al., 1989; Eganhouse et al., 1993; Chaplin et al., 2002; Cozzarelli et al., 2010; Eganhouse et al., 2001), and biodegradation (Borden and Bedient, 1986; Cerniglia, 1993; Cozzarelli et al., 1990) limit the large-scale transport of organic contaminants. Although these processes can attenuate the organic contaminants, the reactions can create secondary water quality impacts that can also diminish groundwater quality. Examples include depletion of dissolved oxygen (DO) (Baedecker et al., 1993; Rees, 1980), microbial reduction and mobilization of iron (Fe) and manganese (Mn) (Baedecker et al., 1993; Jones et al., 1984; Lovley et al., 1989), increased concentrations of methane (Baedecker et al., 1993; Dojka et al., 1998), and changes in pH (Bennett et al., 1993). One of the most important secondary effects in terms of potential human health impacts is the mobilization of arsenic (As), a toxic trace element that naturally exists in aquifer sediments.

Arsenic is a human toxin and carcinogen that poses a threat to human health via ingestion. The World Health Organization has set a drinking water standard of 10 μg/L for As in drinking water. Above this threshold, chronic exposure to As in drinking water has been linked to skin, lung, and bladder cancers (Knobeloch et al., 2006; Nordstrom, 2002; Smith et al., 2000). Most As in groundwater is derived from geogenic sources, though anthropogenic activity can cause changing conditions that allows As to be mobile in groundwater (Smedley and Kinniburgh, 2002). Worldwide, an estimated 150 million people have been exposed to unsafe levels of As in drinking water (Ravenscroft et al., 2009).

In oxic, unconsolidated aquifers, naturally occurring As is commonly associated with Fe(III) oxyhydroxide minerals due to a strong sorption affinity (McArthur et al., 2001; Smedley and Kinniburgh, 2002). However, the presence of bioavailable organic carbon can trigger microbial depletion of DO and subsequent reduction of alternate electron acceptors, including solid phase Fe(III) minerals. Reductive dissolution of Fe(III) oxyhydroxides can result in the mobilization of previously sorbed As to groundwater (Cozzarelli et al., 2016; McArthur et al., 2001; Nordstrom, 2002; Ravenscroft et al., 2009; Smedley, 2003). Additionally, oxidation of organic carbon can be coupled with reduction of naturally occurring As(V) to As(III), which can also promote As mobilization (Tufano et al., 2008). The presence of sulfur can further complicate As cycling by the formation of aqueous thioarsenic complexes (Stucker et al., 2014) and As-bearing sulfide minerals (Harper and Kingham, 1992; Kirk et al., 2004).

Arsenic release under Fe(III)-reducing conditions can be caused by both natural and anthropogenic sources of organic carbon. For example, biodegradation of natural organic carbon in fluviodeltaic aquifers in Southeast Asia is associated with widespread As levels exceeding 10 μg/L, exposing more than 110 million people in the region to unsafe drinking water (Ravenscroft et al., 2009). Although natural organic matter can trigger Fe reduction and As release, human activity can exacerbate the reactions by adding new sources of natural organic matter to the aquifer or changing the hydrogeologic systems. For example, in Bangladesh, natural organic matter in the aquifer can cause Fe-reduction and As release (Polizzotto et al., 2008), but additional organic matter originating from constructed ponds used for groundwater irrigation of rice fields can cause further Fe reduction and As release (Neumann et al., 2010). Neumann et al. (2014) showed that sedimentary organic matter was stable and not bioavailable to microbes until recharge was introduced, dissolving the sediment-associated organic matter. On smaller scales,

As can also be mobilized in aquifers contaminated by anthropogenic organic carbon such as from petroleum and biofuel spills (Cozzarelli et al., 2016; Hering et al., 2009; Ziegler et al., 2015), sewage (Amirbahman et al., 2006; Kent and Fox, 2004; Whaley-Martin et al., 2017), and landfills (deLemos et al., 2005; Keimowitz et al., 2005).

Because As in groundwater is toxic at low concentrations, understanding how As is released from geogenic sources, i.e. how the mass is partitioned between solid and aqueous phases in aquifers, is critical for predicting potential As contamination. However, quantifying As mass distribution in aquifers is challenging because of the complexity of biogeochemical processes that influence its cycling, including: pH-dependent protonation reactions; pH-dependent adsorption reactions (Dixit and Hering, 2003; Pierce and Moore, 1982; Raven et al., 1998); microbially mediated redox reactions involving both Fe and As (Kocar et al., 2006; McArthur et al., 2001; Nordstrom, 2002; Ravenscroft et al., 2009; Tufano et al., 2008); and dissolution and precipitation reactions of As-bearing minerals (Schreiber et al., 2000; Walker et al., 2006). In addition, sediment type can influence reactive transport of As. For example, fine-grained sediment can sorb As in more appreciable amounts than coarse sediment. Thus fine-grained sediments can potentially release As to groundwater for a longer time at a constant rate compared to coarser sediment because the initial sediment As concentration is higher (Ziegler et al., 2017a).

Additional complications for making quantitative assessments of As mass exchanges between sediment and groundwater include the often extreme spatial heterogeneity, bioavailability and biodegradation kinetics of the carbon source that drives As mobilization. For example, in the fluviodeltaic aquifers in Southeast Asia, spatially heterogeneous organic matter can cause dissolved As concentrations in some wells to increase, remain constant for a period, or

decrease over time (McArthur et al., 2004). In the Midwestern U.S., heterogeneous and stratigraphically discontinuous glacial sediments with varying amounts of organic matter also has led to challenging predictions of As in aquifers (Erickson and Barnes, 2005; Root et al., 2010). This challenge can be simplified at an oil spill site, where there is better understanding of the organic matter and its quantity, spatial distribution, and bioavailability. Compared to natural organic carbon, a defined anthropogenic organic carbon source, such as a hydrocarbon plume, provides the opportunity to study how a plentiful and highly bioavailable carbon source influences Fe reduction and As mobilization, resulting in changes in the mass distribution of naturally occurring As in aquifers over time.

This study quantitatively describes the partitioning of As and Fe between groundwater and aquifer sediment within a hydrocarbon plume at an oil spill site near Bemidji, Minnesota. Biodegradation of petroleum hydrocarbons has created a plume of dissolved As that is naturally attenuated by an Fe(III)-rich "curtain" at the sub-oxic leading edge of the plume (Ziegler et al., 2017a). However, historical data suggest that As attenuated by the Fe curtain is not permanently sequestered, but later can be remobilized if reducing conditions are established due to plume expansion over time (Ziegler et al., 2017a). The goal of this study is to quantify how long-term continuous Fe-reducing conditions resulting from hydrocarbon biodegradation trigger As cycling and redistribute As mass in the aquifer. Improved methods for quantifying As mass redistribution are vital to assessing long-term aquifer vulnerability to As contamination. Using this approach can help in developing necessary mitigation strategies as evolving geochemical conditions may promote future mobilization or sequestration of As, which is not commonly monitored at organic-contaminated sites.

Study site

In 1979, a crude oil pipeline ruptured near Bemidji, MN, releasing 10,700 barrels of crude oil to a shallow unconfined aquifer (Pfannkuch, 1979). Clean-up efforts were able to remediate much of the oil, but about 25% of the spilled oil infiltrated into the subsurface where it settled on the water table, creating a plume of dissolved hydrocarbons in groundwater. In 1983, the spill site became a U.S. Geological Survey (USGS) sponsored research site through the Toxics Substances Hydrology Program. The site has been intensively studied and monitored for more than 35 years to describe natural attenuation of petroleum hydrocarbons (Bekins et al., 2001, 2005; Cozzarelli et al., 2001; Essaid et al., 2011). The vast historic database containing information on biodegradation and other natural attenuation processes makes it an ideal site to investigate less understood, secondary processes that occur at oil-contaminated sites.

The shallow alluvial aquifer is highly heterogeneous, comprised mostly of silt, sand, and gravel derived from crystalline and carbonate sources and deposited by glacial outwash (Bennett et al., 1993). Groundwater velocity estimates range from 0.05 m/d in the silty layers to 0.5 m/d in the coarse sediments (Bennett et al., 1993). A tracer test estimate yielded an average linear velocity of 0.06 m/d (Essaid et al., 2003). Several studies have provided detailed descriptions of the hydrogeology and geochemical evolution of the hydrocarbon plume at the Bemidji site (Baedecker et al., 1993; Bekins et al., 2001; Bennett et al., 1993; Cozzarelli et al., 2001). A detailed study of aquifer mineralogy at the site showed that uncontaminated sediments have a total Fe content of ~1% with complex Fe mineralogy (Zachara et al., 2004). In background sediments, Fe(III) is associated with silicates (epidote, clinochlore, muscovite) and authigenic Fe(III) oxides including goethite, hematite, and magnetite; a ferrihydrite-like phase was also detected in the finer-grained fraction of uncontaminated sediments. Fe(II) was also observed in the form of clinochlore along with a ferroan calcite grain cement in carbonate lithic fragments

(Zachara et al., 2004). Methanogenesis and Fe-reduction are the two main electron accepting processes in the anoxic plume; Fe-reduction has resulted in large fractions of Fe(II) in reduced sediment (Cozzarelli et al., 1994; Lovley et al., 1989; Tuccillo et al., 1999). As the hydrocarbon plume has expanded downgradient, the signature of reduced Fe(II) in sediment can be traced further downgradient (Ng et al., 2014; Ziegler et al., 2017a). Although the Fe system has been well-studied at Bemidji, until recently, As has not been analyzed either in sediment or in groundwater.

Cozzarelli et al. (2016) first showed that As was present in groundwater of the Bemidji hydrocarbon plume. Analyses of wells sampled along the center-line transect of the contaminant plume showed a plume of dissolved As, with concentrations as high as 230 μg/L. The plume of As is imprinted on a plume of depleted DO, which also correlates with elevated concentrations of benzene and Fe(II) in groundwater. Arsenic concentrations in groundwater are highest in the methanogenic zone near the oil body, where sediments have been stripped of Fe and As (Ziegler et al., 2017a). Dissolved As and Fe concentrations are also elevated in the Fe-reducing zone of the plume and are observed to gradually decrease along the groundwater flowpath. At the leading edge of the plume, termed the transition zone, the anoxic groundwater with dissolved Fe and As encounters the regional oxic-to-sub-oxic groundwater and sediments, causing oxidation of dissolved Fe(II) and precipitation of Fe(III) followed by resorption of dissolved As, resulting in accumulation of As and Fe in aquifer sediments in discrete zones (Ziegler et al., 2017a). Further downgradient, groundwater is sub-oxic to oxic; dissolved As and Fe are not detected.

Using new and previously published groundwater and sediment data from the Bemidji site (Figure 3.1), this study calculates the spatial distribution of As mass in aquifer sediments and groundwater along the center-line transect of the hydrocarbon plume. Using background values

from uncontaminated sediments, we compare mass balance calculations for Fe and As to assess how long-term biodegradation has redistributed Fe and As masses between sediment and groundwater.

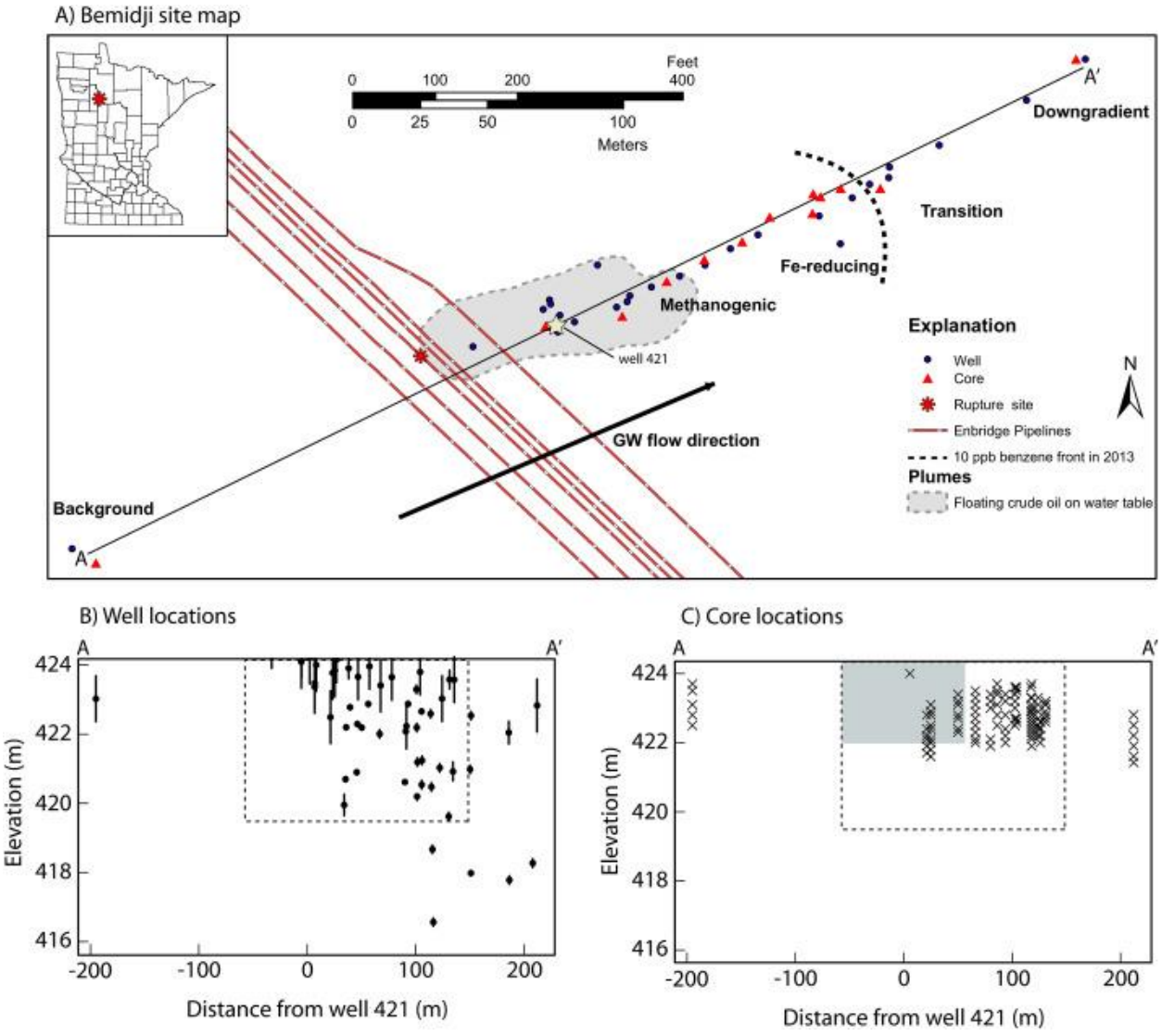

Figure 3.1. A) Map of the Bemidji oil spill site showing locations of cores and wells sampled for this study (easting 342,785, northing 5,271,040, UTM zone 15N North American Datum 1983). B) Cross section view of wells sampled. Circles indicate the center of the screen, and lines indicate the full screen length. The dashed rectangle indicates the domain used for mass balance calculations. C) Cross section view of sediment sampling locations. The gray rectangle inside the domain is where As in sediment was below detection (<0.44 mg/kg). For the mass balance, cells inside the gray rectangle were assigned As values equivalent to the detection limit. Well 421 is used as the zero reference point for plume transects located approximately at the center of the oil body, as has been done in previous Bemidji studies.

Methods

Groundwater sample collection and analysis

Groundwater samples were collected annually from 2010 to 2015 along the center-line transect of the plume (Figure 3.1). Wells that did not contain free product (oil) were sampled using a submersible Keck pump. In 2010 and 2015, groundwater samples were also collected from wells screened beneath or adjacent to the oil body that contained oil using a Teflon bailer. The bailer was lowered below the vertical thickness of the oil in the well casing to collect groundwater. Once retrieved, we allowed ten minutes of gravity separation of oil and water as an additional precaution to prevent sampling free oil product. Groundwater samples were filtered through either a Nuclepore membrane or Millipore Sterivex filter with 0.2 μm pore size into acid washed high density polyethylene bottles. Samples were preserved to pH < 2 using concentrated (70%) trace metal grade nitric acid. Any detectable Fe and As that passed through the filter was assumed to be dissolved. Samples were stored and shipped on wet ice and refrigerated in the laboratory until analyzed.

Acidified samples were analyzed for total dissolved Fe using a Perkin Elmer Optima 4300 Inductively Coupled Plasma Optical Emission Spectrometer 176 (ICP-OES; Perkin Elmer Instruments, Shelton, Connecticut) with a detection limit of 0.10 mg/L. Though reported values for Fe in groundwater are for total dissolved Fe, comparisons with Ferrozine analyses (Gibbs, 1979) conducted in the field show that total dissolved Fe largely reflects the concentration of dissolved Fe(II) (Table B.2). Samples were also analyzed for dissolved As using Perkin Elmer ELAN 9000 Inductively Coupled Plasma Mass Spectrometry (ICP-MS; Perkin Elmer Instruments), with a detection limit of 0.1 μg/L. Arsenic speciation of groundwater samples is not reported here; speciation data are presented in Cozzarelli et al. (2016).

Sediment collection, digestion, and analysis

Sediment cores were collected annually from 2011 to 2016 along the center-line transect of the dissolved hydrocarbon plume to evaluate As and Fe distribution in sediment (Figure 3.1C). Two cores were collected to establish background Fe and As in sediment: one core was collected from upgradient of the contaminated aquifer and another core was collected far downgradient of the hydrocarbon plume. Other cores were collected within or at the leading edge of the hydrocarbon plume.

Cores were collected by drilling with a hollow-stem auger to approximately 0.3 m below the water table, which ranges from eight to eleven m below land surface. Then a 2.1 m piston core barrel was pounded beneath the augers. Liquid CO2 was used to freeze the bottom ten centimeters to maintain redox integrity of the subsurface (Cozzarelli et al., 2016; Murphy and Herkelrath, 1996). After removal from the sub-surface, the core ends were covered in plastic wrap and capped. Cores were logged for physical description and then cut into smaller sub-sections, which were then also covered in plastic wrap, capped, wrapped in foil, sealed in vacuum-sealed bags, and frozen on site. Cores were shipped with dry ice to either the U.S. Geological Survey in Reston, VA, or Virginia Tech, Blacksburg, VA.

In the laboratory, sediment samples were removed from core sub-sections in an anaerobic chamber. Samples were split, with the second split set aside in the anaerobic chamber for total Fe analysis. Using sediment from the first split, a laboratory extraction of aquifer sediments using 0.5 M HCl (Bekins et al., 2001; Gibbs, 1979; Heron et al., 1994; Poulton and Canfield, 2005; Tuccillo et al., 1999) was used to quantify operationally defined concentrations of Fe(II) and Fe(III) from amorphous and poorly crystalline Fe phases. In an anaerobic chamber, 2–3 g of sediment were placed in a 60 mL amber vial and reacted with 20 mL of 0.5 M HCl. Vials were

capped, crimped wrapped in foil, and agitated for 24 h. After 24 h, extracts were filtered through filters with 0.2 μm pore size and analyzed for Fe(II) and total Fe using the Ferrozine method (detection limit of 0.24 mg/L). Fe(III) was determined from the difference between total Fe and Fe(II).

Sediment from the second split was dried in an oven for 24 h at 40 °C. Samples were ground lightly with mortar and pestle to break up clumps, and grain sizes >2 mm were manually removed. Samples were then digested using trace metal grade nitric acid using microwave-assisted digestion (EPA Method 3051a). Extracts were diluted 1:10 with deionized water (DI) and analyzed for As and Fe using inductively coupled plasma-atomic emission spectroscopy (ICP-AES) (detection limits of 10 and 6 μg/L, respectively). National Institute of Standards and Technology (NIST) standard reference material 2587, trace elements in soil, showed 80–100% recovery of As using this method. Arsenic and Fe were not detected in acid blanks. Detection limits for As and Fe in sediment were 0.44 and 0.24 mg/kg, respectively.

Statistical test for outliers

Outliers in background sediments were analyzed using Eq. 3.1, Grubbs' test for outliers (Grubbs, 1950):

$$G = \frac{\max_{i=1,\ldots,N} |C_i - \bar{C}|}{s} \qquad \text{(Eq. 3.1)}$$

where G is the Grubbs' test statistic, C_i is the concentration for the sample of interest, $\bar{C}$ is mean sample concentration, and s is the sample standard deviation.

Mass balance design

Much of the mass balance design for this study follows the methods of Ng et al. (2014) who conducted mass balance calculations for Fe, C and DO at the Bemidji site. The mass balance

calculations conducted in this study for Fe and As assumed that partitioning of the masses only occurred between sediment and groundwater (no partitioning to gas phase or vegetation) and that mass for Fe and As is conserved within the domain boundaries. With these assumptions, we used Eq. 3.2 to evaluate if mass is conserved in the domain before the spill and in the current (2013) aquifer:

$$mass_{gw,before} + mass_{sed,before} = mass_{gw,2013} + mass_{sed,2013} \quad \text{(Eq. 3.2)}$$

where $mass_{gw,}$ before and $mass_{sed}$, before are the masses of Fe or As in groundwater and sediment of the model domain before the spill occurred, respectively, and massgw,2013 and masssed,2013 are the masses of Fe or As in groundwater and sediment within the domain boundaries in 2013 ± two years, respectively.

All Fe and As data from sediment and groundwater were assigned to a cross-sectional domain grid along the center-line transect of the plume with a cell dimension of 0.5 m (vertical) by 1.5 m (horizontal). The total domain was 420 m (horizontal) by 8 m (vertical), which represents 200 m upgradient and 220 m downgradient from well 421, which denotes the center of the oil body floating on the water table and has historically been used as a reference measuring point at the Bemidji site, and 416 to 424 m in elevation. The domain dimensions used to calculate the masses for Fe and As were assigned to encapsulate the As plume and account for known sediment chemistry data for Fe and As reported in Cozzarelli et al. (2016) and Ziegler et al. (2017a). It is assumed that if the entire As plume is contained within the domain boundaries, groundwater transport of As outside the domain boundaries does not occur, thus all As cycling is contained within the boundary dimensions. These dimensions are a rectangle ranging from −60 to 150 m from well 421, and 419.5 m–424 m in elevation (Figure 3.1).

Because well depth intervals are sometimes larger than the vertical dimension length of domain grid cells, and the spacings between wells are sometimes smaller than the horizontal dimension of grid cells (i.e., wells closer together than 1.5 m), we compared two methods to assign observed groundwater As and Fe concentrations to individual grid cells: 1) apply the dissolved As or Fe mass to the cell corresponding to the center of the well screen, or 2) apply the dissolved As or Fe mass to all cells covered by the length of the well screen. If a grid cell was intercepted by more than one well with differing measurements of a dissolved constituent, the average of the measurements was assigned to the cell.

Sediment data were sparse below and adjacent to the oil body (see gray rectangle in Figure 3.1C). To account for the lack of data in this region, we used the approach of Ng et al. (2014) and assumed that conditions in the rectangle were most similar to the most reducing areas of the aquifer that were sampled, corresponding to low Fe and As in sediment and high Fe and As in groundwater. For groundwater, we conducted a series of calculations assigning to the upper and lower upgradient corners of the rectangle values equal to the 90th percentile of measured Fe and As concentrations. To test the sensitivity of the calculations to this approach, we also applied the 50th and 0th percentile to the upgradient corners of the rectangle (Table B.1). For sediment, the mean of Fe concentrations in the most reducing zone of the plume (5–25 m from well 421) were applied to the rectangle corners. For As, the value used was the detection limit (0.44 mg/kg), as all sediment in the 5–25 m section downgradient from well 421 was below detection with respect to As.

Measured Fe and As concentrations in sediment (mg/kg) were converted to mass measurements using the density of quartz (2.65 g/cm3), because the aquifer matrix is predominantly quartz. After applying the measured dissolved and solid-phase concentrations

(g/m3) to the domain grid, concentrations were kriged over the entire domain using Surfer 11 (Golden Software, Golden, Colorado). Where As was below the detection limit near the oil body (see gray rectangle in Figure 3.1), cells were manually assigned values equivalent to the detection limit. Then dissolved and solid-phase concentrations within the plume zone were integrated over the plume area (m2) to calculate the mass within the plume area (g/m), in units of mass per meter of aquifer thickness, where aquifer thickness is the dimension perpendicular to groundwater flow.

Results

Background values for Fe and As in sediment

Measured values for Fe and As in sediments collected outside the plume boundaries are reported in Table 3.1. The downgradient core was considered suitable for calculating background Fe and as that section of the aquifer is still oxic-to-sub-oxic and is far beyond the leading edge of the dissolved Fe and As front (212 m downgradient from well 421).

Table 3.1 Background sediment chemistry

Core location	Elevation (m AMSL)	As (mg/kg)	Fe[a] (mg/kg)	Fe(III)[b] (mg/kg)	Fe(II)[b] (mg/kg)	% Fe(II)[b]
upgradient	423.69	**4.8[c]**	**14400[c]**	2220	78	3.5
upgradient	423.46	2.6	11000	1260	75	6
upgradient	423.11	1.4	7750	775	138	17.8
upgradient	422.81	2.4	13600	1100	130	11.8
upgradient	422.53	1.8	11800	1610	29.7	1.8
downgradient	422.81	1.9	8800	900	39.8	4.4
downgradient	422.51	1.7	8000	1730	<7.0	<0.4
downgradient	422.21	2.2	7190	840	16.4	2.0
downgradient	421.91	1.1	4780	620	18.1	2.9
downgradient	421.61	1.8	8280	1490	26.1	1.7
downgradient	421.43	2.8	11300	810	7.2	0.9
Summary statistics						
mean		2.2	9720	1210	51.1	4.8
standard deviation		1.0	2930	500	47.7	5.4

25th percentile	1.6	7740	880	24.2	1.2
75th percentile	2.0	8160	1091	64.8	6.2
mean (excluding outlier)	2.0	9250	1110	48.4	5.0
standard deviation (excluding outlier)	0.5	2620	390	49.4	5.6
25th percentile (excluding outlier)	1.6	7490	852	20.2	1.2
75th percentile (excluding outlier)	2.3	1100	1377	87.7	8.8

[a] Near-total Fe determined from microwave-assisted concentrated HNO_3extractions.
[b] Fe(III) and Fe(II) determined from 0.5 M HCl extractions.
[c] Bold indicates outlier rejected by Grubbs' test.

The highest elevation sample in the upgradient core had abnormally high concentrations of As (4.8 mg/kg) and Fe (14,400 mg/kg) relative to other samples (Table 3.1). Grubbs' test identified this sample as an outlier ($p = 0.0037$). Thus, this sample was omitted when calculating background values for As and Fe in sediment.

Fe-reducing conditions in the aquifer

To establish the extent of Fe-reduction in the aquifer, the percent Fe(II) from the HCl extraction was kriged across the domain (Figure 3.2). Relative to background conditions, which had an average of 4.8% Fe(II), the area beneath and adjacent to the oil body has significantly higher Fe(II), ranging from 75 to 95% of the total HCl extractable Fe, showing that this area has undergone extensive Fe-reduction. At the sub-oxic leading edge of the dissolved hydrocarbon plume, ~135 m downgradient from well 421, there is only a small fraction of Fe(II), similar to background conditions.

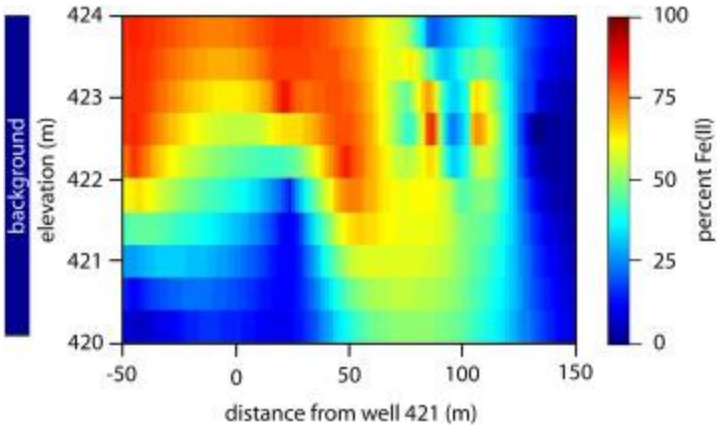

Figure 3.2. Kriged sediment concentrations of percent HCl-extractable Fe(II) within the domain under current (2013 ± 2 years) conditions. 90th percentile values were applied to the upgradient corners of the rectangle shown in Figure 3.1. The bar to the left of the plot shows the background Fe(II) percentage.

Spatial distribution of Fe and As mass in groundwater and sediment

The mass calculations assume that prior to the oil spill, As and Fe concentrations were below detection in groundwater, and all As and Fe mass was associated in sediment, as discussed in Cozzarelli et al. (2016). The mean background sediment concentrations, excluding the outlier, for Fe (9250 mg/kg) and As (2.0 mg/kg) in sediment (see Table 3.1) were applied homogeneously across the domain to calculate a domain total for Fe and As of 15,280 kg/m and 3.3 kg/m, respectively. Using the 25th and 75th percentiles based on the distribution of concentrations in background sediment, a range of uncertainty in the domain totals were calculated as 12,360 to 18,200 kg/m for Fe and 2.6 to 3.7 kg/m for As.

35 years after the spill. The kriged sediment Fe and As concentrations across the domain show substantial redistribution of As and Fe mass in the aquifer that has resulted from hydrocarbon biodegradation over the 35 year lifespan of the plume (Figure 3.3). Beneath and adjacent to the oil body, Fe and As are depleted from sediment well below the background values. For As, concentrations in this zone are below detection. There are zones of highly enriched Fe and As at

the downgradient side of the domain (~130 m), which corresponds to the leading edge for the plumes of dissolved Fe and As (Cozzarelli et al., 2016). Though As and Fe concentrations in sediment are heterogeneous within this downgradient region (As mean and standard deviation are 4.9 mg/kg and 4.6 mg/kg, respectively; Fe mean and standard deviation are 11,590 and 7720, respectively (Ziegler et al., 2017a)), it is clear that this section of the aquifer has concentrated masses of Fe and As compared to background sediments (As mean and standard deviation are 2.0 mg/kg and 0.5 mg/kg, respectively; Fe mean and standard deviation are 9250 and 2650, respectively (Table 3.1)).

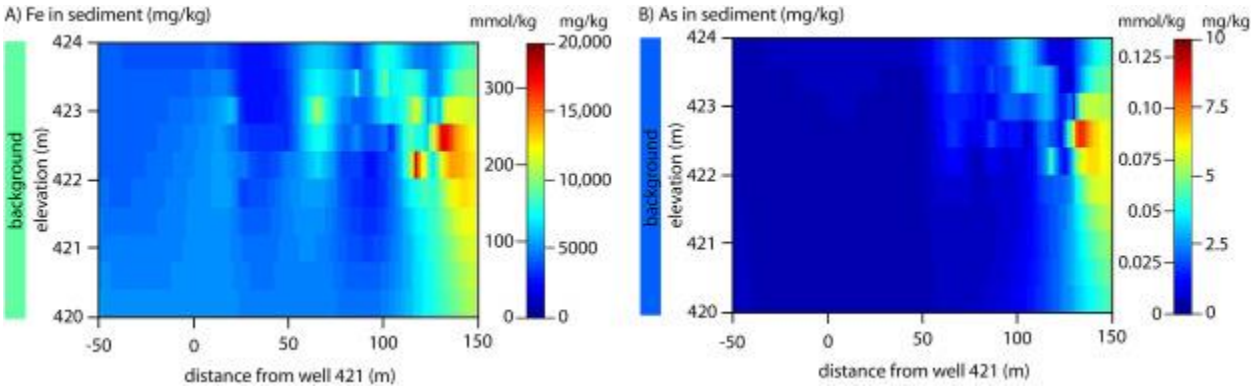

Figure 3.3. Kriged sediment concentrations (mg/kg) of A) Fe and B) As in the domain based on current (2013 ± 2 years) conditions (see Figure 3.1). The bars to the left of the plots show the background concentration.

Arsenic and Fe masses in groundwater were calculated using multiple scenarios to assess the sensitivity of our assumptions on our estimated masses (see Table B.1 in the Appendix B). A comparison of kriged groundwater concentrations using full screen simulations to the center of screen simulations shows that the two approaches yield similar results (Figs. 4 and 5). The full screen approach shows the deeper penetration of high concentrations of As and Fe near well 421 owing to the longer screen lengths for wells near the oil body (Figure 3.1). Further downgradient,

there is little difference between the two approaches as the screen lengths are shorter and do not usually intercept grid cells other than the cell at the screen center.

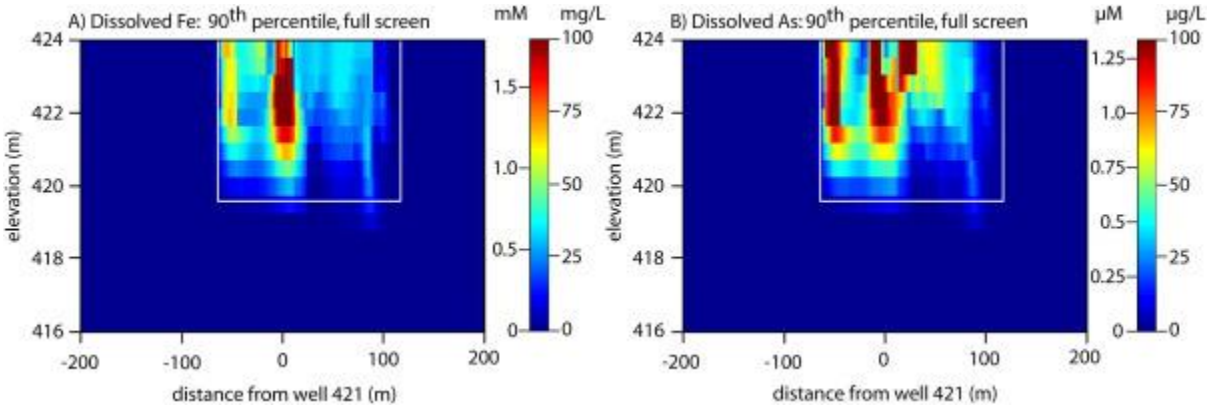

Figure 3.4. Kriged dissolved A) Fe and B) As concentrations applying the 90th percentiles at the upper and lower corners of the left boundary of the domain. Measured concentrations were applied to the full length of the screen. The white rectangle denotes the domain boundary.

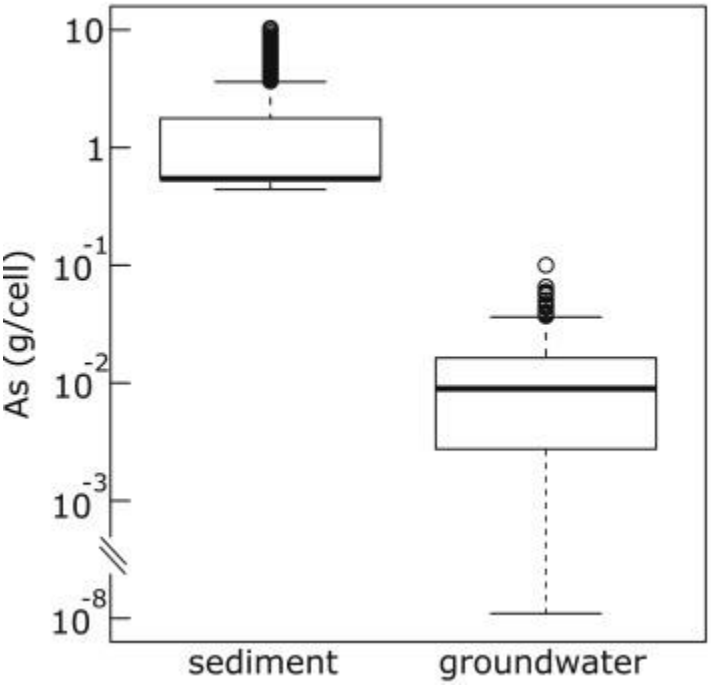

Figure 3.5. Boxplot comparing the As mass distribution between sediment and groundwater for all cells in the domain. Scenario 1 (90th percentile; full screen length) was used for groundwater masses. Note log scale and axis break.

Assigning a range of percentiles (90^{th}, 50^{th}, 0^{th}) for dissolved As and Fe below the oil body where we could not sample groundwater artificially creates “hot spots” of As that do not connect to the rest of the main center of dissolved As mass. This is caused by a well 6.5 m upgradient of well 421 having a dissolved As concentration of only 11.1 μg/L. This value, in effect, separates the two masses of high As with the kriging function. This effect is most pronounced in the 90th percentile simulations and is notable in the 50th percentile scenarios. When values of zero are applied to the left domain corners, this effect is removed.

Regardless of the assumptions used, mass calculations reveal that the bulk of dissolved As and Fe mass is concentrated beneath and adjacent to the oil body near well 421. Concentrations decrease along the flow path and with depth, until they are below detection outside of the domain.

The different assumptions used to krige the As and Fe concentrations in groundwater yield visually different distributions of As mass (i.e., see Figures B.1 and B.2). However, comparisons of the integrated plume mass for each approach show little difference in the total As and Fe masses in the dissolved phase. For both As and Fe, scenario 1 (see Table B.1) results in the greatest mass in the dissolved phase, with dissolved As and Fe mass totals of 0.0112 kg/m and 8.77 kg/m, respectively (Table B.3). Scenario 6 provides the lowest dissolved mass for As and Fe with 0.00825 kg/m and 6.94 kg/m, respectively. The lowest calculated dissolved mass for As was 74% of the highest. For Fe, the lowest calculated mass was 79% of the highest. These results show that although there is a wide range between the 90th and 0th percentile, the calculated mass is relatively insensitive to this range when calculating the total dissolved mass. Furthermore, results show that regardless of the scenario used, the total mass of Fe and As in

groundwater is <1% for As and <0.1% for Fe (0.25–0.34% for As, 0.045–0.057% for Fe) relative to the calculated domain total (Table B.3).

Arsenic and Fe mass balance

Mass balance calculations of the cross-sectional domain for Fe and As are presented in Table 3.2. Initial concentrations for As and Fe were average background sediment concentration data, and uncertainty ranges were provided as the 25th and 75th percentiles. As mentioned above, we assumed that dissolved As and Fe were zero before the spill (based on background groundwater chemistry), although we realize that actual concentrations are non-zero. To test the sensitivity of the mass calculations to this assumption, we calculated the mass of As in groundwater before the spill with the assumption that each cell in the domain had a uniform dissolved As concentration of the detection limit (1 μg/L), the maximum likely value. If so, the total dissolved mass would be ~0.1% of the domain total. Thus, we assume that the contribution of dissolved As to the total As mass before the spill is negligible and can be ignored for calculating the domain dissolved mass total.

Table 3.2 Mass balance results

Fe mass balance	mass kg/m (uncertainty[a])	percent of domain total
Prior to oil spill		
groundwater	0	0
sediment	15280 (12360, 18200)	100
total	15280 (12360, 18200)	100
Current (35 years after spill)		
groundwater	6.94-8.77	0.05-0.06
sediment	9244	60.5
total	9251-9253	60.6

As mass balance		
Prior to oil spill		
groundwater	0	0
sediment	3.3 (2.6, 3.7)	100
total	3.3 (2.6, 3.7)	100
Current (35 years after spill)		
groundwater	0.00825-0.0112	0.25-0.34
sediment	2.0	60.6
total	2.009-2.01	60.9-61.0

[a]Uncertainty presented as 25th and 75th percentiles

Using the kriged values from our sampling campaigns 35 years after the spill, we calculated the integrated domain totals for As and Fe in sediment and groundwater. For both As and Fe, aquifer sediments comprise the vast majority of the mass detected in this study (Table 3.2). Of the calculated domain totals, only 0.05–0.06% of the Fe mass and 0.25–0.36% of the As mass is contained in groundwater. However, comparison of the current mass estimates to the pre-spill estimates show that ~40% of the estimated prior Fe and As mass is not accounted for in the current-day estimate. Even when using the pre-spill domain totals for Fe and As calculated using the 25th percentile values of background concentrations, 22% of the masses is still unaccounted for.

Because dissolved concentrations of As account for such a small percentage of the total mass (Table B.3), it is unlikely that the unaccounted mass from in the mass balance calculations can be attributed to groundwater. Thus, we suspect that the "missing" mass is likely in sediment that was not sampled in the cores collected for this study. For example, we were unable to collect cores deeper in the aquifer (Figure 3.1), and thus were not able to capture the vertical transition

between the lower boundary of the plume where anoxic groundwater can mix with lower, regionally sub-oxic groundwater.

Even though As was elevated in groundwater near the oil, these high dissolved concentrations contribute less to the As mass than the sediment values for the same cell. To demonstrate this, we compared the As mass distributed between groundwater and sediment for two cells: the cell with the highest dissolved As concentration (230 μg/L) and the cell with the highest sediment As concentration (11.1 mg/kg). The cell with highest dissolved As had a sediment concentration of 0.2 mg/kg, reflecting a 90% loss of As mass from the background sediment value of 2.0 mg/kg. Despite the cell having the highest observed dissolved As and near complete removal of sediment As, more than 78% of the As mass in the cell is associated with sediment. Mass distribution calculations for the cell with the highest sediment As showed that sediment mass exceeded dissolved mass by more than eight orders of magnitude. A comparison of As mass distributed between sediment and groundwater for all cells in the domain showed that, on average, sediment contained two orders of magnitude more As mass than groundwater, and no cell had groundwater As mass that exceed the lowest sediment mass value (Figure 3.5).

Discussion

Spatial distribution of As and Fe mass in the Bemidji hydrocarbon plume

This study provides new observations and quantitative analysis that further elucidate findings from previous work showing a zone of highly elevated concentrations of As and Fe in groundwater (Figure 3.4 for scenario 1; see Figures B.1 and B.2 for scenarios 2 through 6 in Appendix B) near the oil body in the Bemidji plume (Cozzarelli et al., 2016); As concentrations in groundwater in this zone are more than 20x the U.S. EPA and WHO drinking water standard of 10 μg/L; select samples analyzed and reported by Cozzarelli et al. (2016) showed that 79–90%

of As in groundwater along the plume transect was As(III). This zone also has depleted As and Fe in sediment (Figure 3.3). In all sediment samples collected within this zone, As was below detection (<0.44 mg/kg), suggesting that a minimum of 78% of the original As mass in sediment (2.0 mg/kg) has been mobilized due to biodegradation of petroleum coupled with Fe-reduction and As mobilization over the 35-year lifetime of the plume.

At the leading edge of the plume, As and Fe concentrations are low in groundwater (Figs. 4 and 5) due to the mixing of the plume with regional oxic-to-sub-oxic groundwater (Cozzarelli et al., 2016), which promotes oxidation of Fe(II) and precipitation of Fe(III), followed by resorption of dissolved As to freshly formed Fe(III); this is evident from the enriched Fe (mostly as Fe(III)) and As in sediment at the plume's leading edge (Figure 3.3). In these sediments, As and Fe concentrations exceed background values by a factor of 5. Combined, the kriged results from groundwater and sediment show a clear removal of As and Fe from sediment near the oil body and deposition in sediment at the plume's leading edge.

Missing Fe and As mass

Comparison of the Fe and As masses calculated before the oil spill with those calculated based on current conditions (2013) shows that we were unable to account for all of the mass of Fe and As estimated in the pre-spill aquifer. We present two possible explanations for the imbalances. One explanation is that the background values used to calculate the total masses within the domain were too high, resulting in an overestimate of the As and Fe mass within the system. We believe this is likely not the case, as the background values had a reasonable sample size for estimating mean concentrations, and standard deviations were reasonably small relative to the mean for natural samples. We also calculated domain totals with the 25th and 75th percentiles based on the distribution of the background samples. Even using the domain totals calculated

using the 25th percentile, 75% and 77% of As and Fe mass, respectively, was not accounted for in the 2013 estimates, respectively. The second, and more likely, scenario is that there is spatial heterogeneity in the transition zone, with zones of elevated As and Fe in sediment that were not sampled in this study. Although we were successful in capturing the As and Fe accumulating in sediment at the leading edge of the plume, it is possible that there were other As and Fe "hot spots" in sediments that we did not sample. For example, Tuccillo (1998) showed that there were vertical intervals in the aquifer that had elevated Fe(III) that corresponded to the lower boundary of the plume, suggesting that the mixing interface between the anoxic plume and the regional oxic-to-sub-oxic groundwater created a vertical transition in which dissolved Fe(II) was oxidized and precipitated as Fe(III) hydroxides. Similarly, the upper boundary of the plume likely experiences some oxidation from recharging groundwater delivering DO to the water table (Datry et al., 2004). This trend was observed in water table wells in the reducing zone, where DO concentrations were higher (250 μg/L) in years with greater recharge and higher water table, compared years with less recharge and lower water table, where DO was <10 μg/L.

Further support of oxidation near the water table was observed by the uppermost (highest elevation) sediment samples in many of our reducing zone cores showing substantial oxidation as was evident by visual inspection and the presence of elevated concentrations of Fe(III) and As (Ziegler et al., 2017a). However, because core collection for this study began 0.3 m below the water table and cores were a maximum of 2.1 m in length, we did not capture these vertical transitions at the water table and at the lower boundary of the plume, likely leading to an under-representation of As and Fe mass in the domain.

Mass partitioning of As and Fe between sediment and groundwater

This study shows that sediment is the main reservoir for nearly all (>99%) of the As and Fe mass in the domain. Calculations of mass distribution of Fe support results from a previous mass balance study on Fe, DO, and C fate and transport at the Bemidji site (Ng et al., 2014). For As, more than 69% of the domain area had dissolved As concentrations that exceed the 10 μg/L drinking water standard, yet the elevated dissolved As accounts for only a minute fraction of As in the domain. A calculation in Cozzarelli et al. (2016) showed that if all background sediment-bound As were released to groundwater, a maximum possible concentration would be 14,480 μg/L, yet the maximum observed As in groundwater was 0.15% of this value (230 μg/L). A study of As in glacially derived alluvial aquifers in the Midwest showed that, on average, <0.1% of sediment-associated As must be mobilized to elevate concentrations above 10 μg/L (Erickson and Barnes, 2005). Crustal As concentrations range from 1 to 20 mg/kg (Nordstrom, 2002), with U.S. sediments and soils averaging 5.2 mg/kg (Reimann et al., 2009; Shacklett and Boerngen, 1984). At the Bemidji site, As sediment concentrations were on the lower end of the reported range, underscoring that it is not necessary to have high sediment concentrations of As to elevate groundwater above the 10 μg/L drinking water standard. In fact, calculations using sediment porosity of 0.38 and assumed bulk density of 2.65 g/cm3 show that As concentrations in groundwater could exceed the drinking water standard even when the sediment concentration is as low as 0.02 mg/kg, well below the 0.44 mg/kg detection limit for this study. Thus, virtually any aquifer containing As associated with bioavailable Fe-hydroxides is vulnerable to unsafe As levels in groundwater if geochemical conditions become reducing through introduction of a bioavailable carbon source. Although only a very small percentage of As is in groundwater at a

given time, this study shows that a large (~78%) mass of As has been mobilized from sediment and redistributed in the aquifer over the plume's history.

Mass calculation design and sensitivity analysis

There are two factors critical for developing a robust calculation of mass partitioning between sediment and groundwater in perturbed aquifers. First, the accuracy of the calculated masses is highly dependent on well characterized background conditions, as these are used to calculate the initial mass totals in the domain. For the Bemidji site, background wells upgradient from the hydrocarbon plume are oxygenated and have non-detectable Fe and As. To best describe background sediment conditions, we used two cores to establish background concentrations for Fe and As. Although it is not ideal to have one of the two cores used collected downgradient from the hydrocarbon plume, we are confident that the sediment-bound Fe and As values reflect background conditions, because the core location is 70 m downgradient from the leading edge of the dissolved Fe and As plume. However, we would caution against using a downgradient core for background values for some other parameters. For example, Bekins et al. (2016) showed that some crude oil metabolites can be transported in oxygenated groundwater beyond the leading edge of a hydrocarbon plume. Thus, sediment at this location might not be well-suited for background values in studies related to organic matter.

The downgradient core was important for quantifying background Fe and As, because the upgradient core alone would not have provided a sufficiently large sample size of concentrations, allowing its relatively high mean As value (2.6 mg/kg) to skew estimates. Using just the upgradient core, the highest As value of 4.8 mg/kg sample was not omittable as an outlier (α = 0.05) using Grubbs' test ($p = 0.0523$). However, in a Grubbs' test including the downgradient core, the 4.8 mg/kg sample was confidently rejected as an outlier ($p = 0.003655$), reducing

background value for As from 2.6 mg/kg to 2.0 mg/kg. Although only a 0.6 mg/kg decrease resulted from including the downgradient core, the resulting total domain mass was reduced 23% from 4.3 kg/m to 3.3 kg/m. Because the As concentrations are so low in background sediment, a difference of 0.6 mg/kg for the assigned background sediment concentration strongly influences the resulting domain totals.

A second factor important for an accurate mass partitioning calculation is addressing data sparsity. Groundwater and sediment data were sparse upgradient from well 421 because the presence of the oil body complicated sample collection. Multiple approaches can be used to estimate mass in areas of sparse data. In this study, we followed the method of Ng et al. (2014), which applied the 90th percentile values to the coordinates corresponding to the upgradient corner of the rectangle in Figure 3.1B in mass balance models for C, Fe, and DO. Although this approach adds unknown artificial mass to dissolved phase based on unknown data, the method is more appropriate than assuming that no Fe or As is in groundwater upgradient from well 421 because this is the most reducing groundwater in the plume. To test the sensitivity of the calculations to this approach, we applied a variety of artificial values to the coordinates described in Ng et al. (2014), with zero and the maximum observed value (100th percentile) as end-members. Because in this system, the overwhelming majority (>99%) of As mass was in the sediment and not in groundwater, we concluded that the calculation was not sensitive to the approach used to quantify dissolved mass.

Conclusions and implications

Even under reducing conditions that promote reductive dissolution of Fe(III) hydroxides and mobilization of As, aquifer sediments are the main reservoir for Fe and As mass at the Bemidji site, accounting for 99.9% and 99.5% of Fe and As masses, respectively. However, long term

biodegradation of organic matter coupled with Fe reduction and As mobilization have caused significant redistributions of As mass in aquifer sediments. Although the current mass distribution estimate suggests that only a small percentage of the total As mass (~0.5%) is present in groundwater at a given time, prolonged Fe reduction and As mobilization over the plume's 35 year history has resulted in removal of As in sediment near the oil body to concentrations below the detection limit (<0.44 mg/kg), showing that a minimum of 78% of the original sediment As mass has been mobilized. At the leading edge of the plume, aquifer sediments have the capacity to naturally attenuate As; As has accumulated to concentrations 5.6 times greater than the mean background concentration. However, this As can potentially be re-mobilized if the hydrocarbon plume expands and reducing conditions are established where sediment As is concentrated. Last, this study highlights the importance of identifying aquifers susceptible to contamination from naturally occurring As. Because As can have negative health impacts at concentrations as low as 10 μg/L in drinking water, our calculations show that sediment As concentrations need only be 0.02 mg/kg (22 times less than the detection limit for this study) for groundwater As concentrations to exceed 10 μg/L if all As is mobilized from sediment. Thus, aquifers with low or non-detectable concentrations of natural As in sediment are still potentially vulnerable to levels of As in groundwater that exceed drinking water standards if bioavailable organic carbon is introduced to the aquifer.

Acknowledgements

We thank Jeanne Jaeschke for her help collecting and analyzing samples and the team of scientists at the USGS Minnesota Water Science Center, including Jared Trost for field site coordination and support, Melinda Erickson for discussions about the study design, and Andrew Berg, Brent Mason, and John Greene for core collection. We also thank Barbara Bekins for

helpful discussions about biodegradation and Fe reduction, Katie Krueger, Spencer Kleptazki, Ricardo Fernandez, and Autumn Parker for laboratory assistance, and Athena Tilley for ICP analyses. We thank Doug Kent and four anonymous reviewers for their guidance and helpful suggestions.

This project was supported by the USGS Toxic Substances Hydrology Program and the National Research Program. Additional funding was provided by a collaborative venture of the USGS, Enbridge Energy Limited Partnership, the Minnesota Pollution Control Agency, and Beltrami County, MN, the Virginia Water Resources Research Center, the American Association of Petroleum Geologists, and the Geological Society of America. Any use of trade, product, or firm names in this publication is for descriptive purposes only and does not imply endorsement by the U.S. Government. A data-release product companion to this journal article (Ziegler et al., 2017b) contains all the data and metadata associated with this article and can be found at https://doi.org/10.5066/F7280648.

References

Amirbahman, A., Kent, D.B., Curtis, G.P., Davis, J.A., 2006. Kinetics of sorption and abiotic oxidation of arsenic(III) by aquifer materials. Geochim. Cosmochim. Acta 70, 533-547.
Baedecker, M.J., Cozzarelli, I.M., Eganhouse, R.P., Siegel, D.E., Bennett, P.C., 1993. Crude oil in a shallow sand and gravel aquifer-III. Biogeochemical reactions and mass balance modeling in anoxic groundwater. Appl. Geochem. 8, 569-586.

Bekins, B.A., Cozzarelli, I.M., Erickson, M.L., Steenson, R.A., Thorn, K.A., 2016. Crude oil metabolites in groundwater at two spill sites. Groundwater 54, 681-691.

Bekins, B.A., Cozzarelli, I.M., Godsy, E.M., Warren, E., Essaid, H.I., Tuccillo, M.E., 2001. Progression of natural attenuation processes at a crude oil spill site: II. Controls on spatial distribution of microbial populations. J. Contam. Hydrol. 53, 387-406.

Bekins, B.A., Hostettler, F.D., Herkelrath, W.N., Delin, G.N., Warren, E., Essaid, H.I., 2005. Progression of methanogenic degradation of crude oil in the subsurface. Environ. Geosci. 12, 139-152.

Bennett, P.C., Siegel, D.E., Baedecker, M.J., Hult, M.F., 1993. Crude oil in a shallow sand and gravel aquifer-I. Hydrogeology and inorganic geochemistry. Appl. Geochem. 8, 529-549.

Borden, R.C., Bedient, P.B., 1986. Transport of dissolved hydrocarbons influenced by oxygen-limited biodegradation: 1. Theoretical development. Water Resour. Res. 22, 1973-1982.

Brusseau, M.L., Rao, P., Gillham, R.W., 1989. Sorption non-ideality during organic contaminant transport in porous media. Crit. Rev. Environ. Sci. Technol. 19, 33-99.

Cerniglia, C.E., 1993. Biodegradation of polycyclic aromatic hydrocarbons. Curr. Opin. Biotechnol. 4, 331-338.

Chaplin, B.P., Delin, G., Baker, R., Lahvis, M., 2002. Long-term evolution of biodegradation and volatilization rates in a crude oil-contaminated aquifer. Biorem. J. 6, 237-255.

Cozzarelli, I.M., Baedecker, M.J., Eganhouse, R.P., Goerlitz, D.F., 1994. The geochemical evolution of low-molecular-weight organic acids derived from the degradation of petroleum contaminants in groundwater. Geochim. Cosmochim. Acta 58, 863-877.

Cozzarelli, I.M., Bekins, B.A., Baedecker, M.J., Aiken, G.M., Eganhouse, R.P., Tuccillo, M.E., 2001. Progression of natural attenuation processes at a crude-oil spill site: I. Geochemical evolution of the plume. J. Contam. Hydrol. 53, 369-385.

Cozzarelli, I.M., Bekins, B.A., Eganhouse, R.P., Warren, E., Essaid, H.I., 2010. In situ measurements of volatile aromatic hydrocarbon biodegradation rates in groundwater. J. Contam. Hydrol. 111, 48-64.

Cozzarelli, I.M., Eganhouse, R.P., Baedecker, M.J., 1990. Transformation of monoaromatic hydrocarbons to organic acids in anoxic groundwater environment. Environ. Geol. Water Sci. 16, 135-141.

Cozzarelli, I.M., Schreiber, M.E., Erickson, M.L., Ziegler, B.A., 2016. Arsenic cycling in hydrocarbon plumes: secondary effects of natural attenuation. Groundwater 54, 35-45.

Datry, T., Malard, F., Gibert, J., 2004. Dynamics of solutes and dissolved oxygen in shallow urban groundwater below a stormwater infiltration basin. Sci. Total Environ. 329, 215-229.

deLemos, J.L., Bostick, B.C., Renshaw, C.E., StÜrup, S., Feng, X., 2005. Landfill-stimulated iron reduction and arsenic release at the Coakley Superfund Site (NH). Environ. Sci. Technol. 40, 67-73.

Dixit, S., Hering, J.G., 2003. Comparison of arsenic(V) and arsenic(III) sorption onto iron oxide minerals: implications for arsenic mobility. Environ. Sci. Technol. 37, 4182-4189.

Dojka, M.A., Hugenholtz, P., Haack, S.K., Pace, N.R., 1998. Microbial diversity in a hydrocarbon-and chlorinated-solvent-contaminated aquifer undergoing intrinsic bioremediation. Appl. Environ. Microbiol. 64, 3869-3877.

Eganhouse, R.P., Baedecker, M.J., Cozzarelli, I.M., Aiken, G.M., Thorn, K.A., Dorsey, T.F., 1993. Crude oil in a shallow sand and gravel aquifer-II. Organic geochemistry. Appl. Geochem. 8, 551-567.

Eganhouse, R.P., Cozzarelli, I.M., Scholl, M.A., Matthews, L.L., 2001. Natural attenuation of volatile organic compounds (VOCs) in the leachate plume of a municipal landfill: using alkylbenzenes as process probes. Ground Water 39, 192-202.

Erickson, M.L., Barnes, R.J., 2005. Glacial sediment causing regional-scale elevated arsenic in drinking water. Ground Water 43, 796-805.

Essaid, H.I., Bekins, B.A., Herkelrath, W.N., Delin, G.N., 2011. Crude oil at the Bemidji site: 25 years of monitoring, modeling, and understanding. Ground Water 49, 706-726.

Essaid, H.I., Cozzarelli, I.M., Eganhouse, R.P., Herkelrath, W.N., Bekins, B.A., Delin, G.N., 2003. Inverse modeling of BTEX dissolution and biodegradation at the Bemidji, MN crude-oil spill site. J. Contam. Hydrol. 67, 269-299.

Gibbs, M.M., 1979. A simple method for the rapid determination of iron in natural waters. Water Res. 13, 295-297.

Grubbs, F.E., 1950. Sample criteria for testing outlying observations. Ann. Math. Stat. 21, 27-58.

Harper, T.R., Kingham, N.W., 1992. Removal of arsenic from wastewater using chemical precipitation methods. Water Environ. Res. 64, 200-203.

Hering, J.G., O'Day, P.A., Ford, R.G., He, Y.T., Bilgin, A., Reisinger, H.J., Burris, D.R., 2009. MNA as a remedy for arsenic mobilized by anthropogenic inputs of organic carbon. Ground Water Monit. Remediat. 29, 84-92.

Heron, G., Crouzet, C., Bourg, A.C., Christensen, T.H., 1994. Speciation of Fe (II) and Fe (III) in contaminated aquifer sediments using chemical extraction techniques. Environ. Sci. Technol. 28, 1698-1705.

Jones, J.G., Gardener, S., Simon, B.M., 1984. Reduction of ferric iron by heterotrophic bacteria in lake sediments. Microbiology 130, 45-51.

Keimowitz, A.R., Zheng, Y., Chillrud, S.N., Mailloux, B., Jung, H.B., Stute, M., Simpson, H.J., 2005. Arsenic redistribution between sediments and water near a highly contaminated source. Environ. Sci. Technol. 39, 8606-8613.

Kent, D.B., Fox, P.M., 2004. The influence of groundwater chemistry on arsenic concentrations and speciation in a quartz sand and gravel aquifer. Geochem. Trans. 5, 1.

Kirk, M.F., Holm, T.R., Park, J., Jin, Q., Sanford, R.A., Fouke, B.W., Bethke, C.M., 2004. Bacterial sulfate reduction limits natural arsenic contamination in groundwater. Geology 32, 953-956.

Knobeloch, L.M., Zierold, K.M., Anderson, H.A., 2006. Association of arsenic-contaminated drinking-water with prevalence of skin cancer in Wisconsin's Fox River Valley. J. Health, Popul. Nutr. 206-213.

Kocar, B.D., Herbel, M.J., Tufano, K.J., Fendorf, S., 2006. Contrasting effects of dissimilatory iron(III) and arsenic(V) reduction on arsenic retention and transport. Environ. Sci. Technol. 40, 6715-6721.

Lovley, D.R., Baedecker, M.J., Lonergan, D.J., Cozzarelli, I.M., Phillips, E.J., Siegel, D.I., 1989. Oxidation of aromatic contaminants coupled to microbial iron reduction. Nature 339, 297-300.

McArthur, J., Ravenscroft, P., Safiulla, S., Thirlwall, M., 2001. Arsenic in groundwater: testing pollution mechanisms for sedimentary aquifers in Bangladesh. Water Resour. Res. 37, 109-117.

McArthur, J.M., Banerjee, D.M., Hudson-Edwards, K.A., Mishra, R., Purohit, R., Ravenscroft, P., Cronin, A., Howarth, R.J., Chatterjee, A., Talukder, T., Lowry, D., Houghton, S., Chadha, D.K., 2004. Natural organic matter in sedimentary basins and its relation to arsenic in anoxic ground water: the example of West Bengal and its worldwide implications. Appl. Geochem. 19, 1255-1293.

Murphy, F., Herkelrath, W., 1996. A sample-freezing drive shoe for a wire line piston core sampler. Ground Water Monit. Remediat. 16, 86-90.

National Research Council, 2000. Natural Attenuation for Groundwater Remediation. National Academies Press.

Neumann, R.B., Ashfaque, K.N., Badruzzaman, A.B.M., Ashraf Ali, M., Shoemaker, J.K., Harvey, C.F., 2010. Anthropogenic influences on groundwater arsenic concentrations in Bangladesh. Nat. Geosci. 3, 46-52.

Neumann, R.B., Pracht, L.E., Polizzotto, M.L., Badruzzaman, A.B.M., Ali, M.A., 2014. Biodegradable organic carbon in sediments of an arsenic-contaminated aquifer in Bangladesh. Environ. Sci. Technol. Lett. 1, 221-225.

Ng, G.H.C., Bekins, B.A., Cozzarelli, I.M., Baedecker, M.J., Bennett, P.C., Amos, R.T., 2014. A mass balance approach to investigating geochemical controls on secondary water quality impacts at a crude oil spill site near Bemidji, MN. J. Contam. Hydrol. 164, 1-15.

Nordstrom, D.K., 2002. Worldwide occurrences of arsenic in ground water. Science 296, 2143-2145.

Pfannkuch, H.O., 1979. Interim Report and Recommendations on Monitoring Program for Site M.P. 9265. Report prepared for Lakehead Pipe Line Company, Inc., (Available for inspection at the Minnesota Pollution Control Agency, St. Paul, MN; U.S. Geological Survey, Mounds View, MN, University of Minnesota, Department of Geology and Geophysics, Minneapolis, MN).

Pierce, M.L., Moore, C.B., 1982. Adsorption of arsenite and arsenate on amorphous iron hydroxide. Water Res. 16, 1247-1253.

Polizzotto, M.L., Kocar, B.D., Benner, S.G., Sampson, M., Fendorf, S., 2008. Near-surface wetland sediments as a source of arsenic release to ground water in Asia. Nature 454, 505-508.

Poulton, S.W., Canfield, D.E., 2005. Development of a sequential extraction procedure for iron: implications for iron partitioning in continentally derived particulates. Chem. Geol. 214, 209-221.

Raven, K.P., Jain, A., Loeppert, R.H., 1998. Arsenite and arsenate adsorption on ferrihydrite: kinetics, equilibrium, and adsorption envelopes. Environ. Sci. Technol. 32, 344-349.

Ravenscroft, P., Brammer, H., Richards, K., 2009. Arsenic Pollution: A Global Synthesis. John Wiley & Sons.

Rees, J.F., 1980. The fate of carbon compounds in the landfill disposal of organic matter. J. Chem. Technol. Biotechnol. 30, 161-175.

Reimann, C., Matschullat, J., Birke, M., Salminen, R., 2009. Arsenic distribution in the environment: the effects of scale. Appl. Geochem. 24, 1147-1167.

Root, T.L., Gotkowitz, M.B., Bahr, J.M., Attig, J.W., 2010. Arsenic geochemistry and hydrostratigraphy in midwestern U.S. glacial deposits. Ground Water 48, 90-912.

Schreiber, M., Simo, J., Freiberg, P., 2000. Stratigraphic and geochemical controls on naturally occurring arsenic in groundwater, eastern Wisconsin, USA. Hydrogeol. J. 8, 161-176.

Shacklett, H.T., Boerngen, J.G., 1984. Element Concentrations in Soils and Other Surficial Materials of the Conterminous United States. U.S. Geological Survey Professional Paper, p. 1270.

Smedley, P., Kinniburgh, D., 2002. A review of the source, behaviour and distribution of arsenic in natural waters. Appl. Geochem. 17, 517-568.

Smedley, P.L., 2003. Arsenic in groundwater south and east Asia. In: Welch, A.H., Stollenwerk, K.G. (Eds.), Arsenic in Ground Water. Springer, pp. 179-209.

Smith, A.H., Lingas, E.O., Rahman, M., 2000. Contamination of drinking-water by arsenic in Bangladesh: a public health emergency. Bull. World Health Organ. 78, 1093-1103.

Stucker, V.K., Silverman, D.R., Williams, K.H., Sharp, J.O., Ranville, J.F., 2014. Thioarsenic species associated with increased arsenic release during biostimulated subsurface sulfate reduction. Environ. Sci. Technol. 48, 13367-13375.

Tuccillo, M.E., 1998. Processes and Effects of Iron Reduction in Anoxic Surficial Aquifers. Ph.D. dissertation. Department of Environmental Sciences. University of Virginia, Charlottesville, VA.

CHAPTER 4. A REACTIVE TRANSPORT MODEL OF ARSENIC CYCLING IN A PETROLEUM-CONTAMINATED AQUIFER

Introduction

A global analysis of arsenic (As) in drinking water estimates that 150 million people are at risk of developing diseases due to chronic exposure to unsafe concentrations of As (Ravenscroft et al., 2009). Arsenic is a toxin and carcinogen regulated by the U.S. Environmental Protection Agency and the European Union at a threshold of 10 µg/L in drinking water. Consumption of water containing As above this threshold has been linked to development of skin, lung, and bladder cancers, (Knobeloch et al., 2006; Nordstrom, 2002; Smith et al., 2000).

South and Southeast Asia continue to struggle with health effects due to widespread prevalence of As in fluviodeltaic and alluvial drinking water aquifers (Bhowmick et al., 2018; Ravenscroft et al., 2009). In Bangladesh alone, an estimated 5.6% of all non-accidental deaths are attributed to chronic exposure to As in drinking water (Flanagan et al., 2012). Dissolved As in these aquifers is most commonly due to reductive dissolution of As-bearing ferric (Fe)-oxides coupled with microbial oxidation (i.e., biodegradation) of organic carbon (C) (McArthur et al., 2001; Nickson et al., 1998; Nordstrom, 2002). This mechanism is thought to be the driver for As in groundwater in other regions, including northern China (Luo et al., 1997; Ma et al., 1999), Hungary and Romania (Lindberg et al., 2006; Varsányi and Kovács, 2006), Argentina (Bhattacharya et al., 2006), and the Midwestern U.S (Erickson and Barnes, 2005; Root et al., 2010).

Reactive transport models have been developed over the past decade to simulate As mobilization due to biodegradation of natural (Charlet et al., 2007; Jung et al., 2012; Postma et al., 2007; Rotiroti et al., 2015) and anthropogenic (Jung et al., 2009; Rawson et al., 2017) organic

C. Recently, Sø et al. (2018) highlighted four factors that are critical for accurate long-term assessment of As-affected groundwater: 1) the source and biodegradability of organic C that drive Fe-reduction and subsequent As mobilization (Harvey et al., 2002; McArthur et al., 2004; Neumann et al., 2010; Neumann et al., 2014; Polizzotto et al., 2008; Whaley-Martin et al., 2017); 2) mineralogy, reactivity, and As content of Fe-oxides (Kocar and Fendorf, 2009; Postma et al., 2012; Stuckey et al., 2015; Stuckey et al., 2016); 3) retention of mobilized As by incorporation in secondary mineral phases and/or resorption of As to sediment mineral surfaces (Harvey et al., 2002; Radloff et al., 2011; van Geen et al., 2008); and 4) groundwater flow rate (McArthur et al., 2004; Postma et al., 2017; Smedley and Kinniburgh, 2002; Stute et al., 2007; van Geen et al., 2008). Collecting accurate data to adequately characterize the hydrologic and geochemical interactions of these four factors is challenging and complicates efforts to create meaningful transport models that can be used to simulate long-term cycling of As in groundwater.

We have developed a reactive transport model for As cycling coupled to Fe-reduction at the Bemidji, MN oil spill site, which has a breadth of historic biogeochemical data from long-term monitoring as a U.S. Geological Survey site through the Toxics Program. One benefit of developing a model with a historic database is that important factors controlling As cycling are reasonably well constrained by decades of monitoring and analyses. Using historic data published in the literature, we are well equipped to address the four factors highlighted by Sø et al. (2018) to develop a reactive transport model for As cycling: 1) extensive research has characterized the composition, distribution, and biodegradation of organic carbon (petroleum hydrocarbons and biodegradation products) (Bekins et al., 2005; Cozzarelli et al., 1994; Cozzarelli et al., 2010; Eganhouse et al., 1993; Essaid et al., 2011; Essaid et al., 2003; Ng et al., 2015); 2) sequential chemical extraction methods have been used to estimate Fe mineral

reactivity in background sediment and in different locations in the contaminant plume (Lovley et al., 1989; Tuccillo et al., 1999; Ziegler et al., 2017a) and studies of Fe mineralogy have quantified the mechanisms and limits of Fe-reduction (Baedecker, 1992; Zachara et al., 2004); 3) chemical extraction methods have also been used to describe quasi-mechanistically the spatial and temporal association of As with Fe-oxides during plume evolution (Ziegler et al., 2017a; Ziegler et al., 2017b); and 4) groundwater flow rates and hydraulic conductivity have been well evaluated to monitor contaminant transport in the aquifer (Bennett et al., 1993; Essaid et al., 2003).

Here, we build upon a reactive transport model previously developed for the Bemidji site (Ng et al., 2015) by incorporating surface complexation reactions to simulate As cycling in the aquifer. The original model took a comprehensive approach to describe biodegradation of a suite of petroleum hydrocarbons, including benzene, ethylbenzene, xylenes (B, E, X), toluene, non-volatile dissolved organic C, short-chain *n*-alkanes, and long-chain *n*-alkanes, coupled with different terminal electron accepting processes (e.g., aerobic respiration, manganese reduction, Fe-reduction, and methanogenesis). Other biogeochemical processes accounted for in the model included inorganic reactions such as sinks for reduced Fe, explicit mineral dissolution and precipitation, outgassing of dissolved gases, and multidimensional domain spatial effects. The addition of surface complexation reactions to simulate As sorption/desorption to a ferrihydrite-like phase ($Fe(OH)_3$) to the model allows for a more holistic picture of the consequences of biogeochemical reactions triggered by bioavailable organic C, and it also provides a framework for developing reactive transport models better equipped to address the long-term fate of As in groundwater.

Study site

The study site, located near Bemidji, Minnesota, is a glacially-derived surficial alluvial aquifer consisting mostly of sand and gravel with discontinuous low permeability silt layers and lenses (Dillard et al., 1997). Groundwater velocity estimates range from 0.05 m/d in low conductivity sediments to 0.5 m/d in coarser units (Bennett et al., 1993).

A pipeline rupture in 1979 released 10,700 barrels of crude oil to the land surface (Phannkuch, 1979). After initial clean-up efforts, approximately 25% of the spilled oil infiltrated into the subsurface and settled on the water table. The oil body remains a source of dissolved organic C in groundwater. Biodegradation of petroleum is coupled with anaerobic terminal electron accepting processes (TEAPs) including manganese-reduction, Fe-reduction, and methanogenesis (Baedecker et al., 1993; Cozzarelli et al., 1994; Cozzarelli et al., 2001; Essaid et al., 1995; Essaid et al., 2011; Ng et al., 2015). Since 1984, the site has been studied extensively to monitor the long-term evolution of the hydrocarbon plume, the natural attenuation capacity of the aquifer, and secondary water quality impacts such as depleted DO, elevated Fe, and pH changes triggered by biodegradation of organic C (for review of Bemidji research, see Essaid et al. (2011)).

Recently, Cozzarelli et al. (2016) documented As mobilization due to biodegradation coupled with Fe-reduction at the Bemidji site. Groundwater sampling results showed a secondary plume of dissolved As that overlapped with plumes of benzene, depleted dissolved oxygen (DO), and elevated dissolved Fe. The maximum observed As concentration in groundwater was 230 µg/L. Sediment and groundwater surveys along the plume transect showed Fe and As depletion in sediment near the oil, corresponding to elevated Fe and As in groundwater. Dissolved Fe and As decrease along the groundwater flowpath to the leading edge of the hydrocarbon plume (i.e.,

transition zone). At the transition zone, As accumulates in sediment by association with Fe in an Fe-rich "curtain" (Ziegler et al., 2017a; Ziegler et al., 2017b). Long-term studies have suggested that the Fe curtain can be reduced as the plume expands downgradient (Tuccillo et al., 1999; Ziegler et al., 2017a), releasing Fe and As from the curtain into groundwater.

Methods

The model presented here is built upon the comprehensive reactive transport model of the Bemidji site described in Ng et al. (2015). The original model compiled reactions from previous Bemidji models, which are described in detail in Ng et al. (2015). Here, we add a surface complexation model to simulate As sorption and desorption from $Fe(OH)_3$ during biodegradation to simulate As cycling in the two-dimensional cross section along the plume transect. Model simulations are performed using PHT3D (Prommer et al., 2003), which combines groundwater flow from MODFLOW2005 (Harbaugh, 2005), solute transport from MT3DMS (Zheng and Wang, 1999), and geochemical reactions from PHREEQC-3 (Parkhurst and Appelo, 2013).

Model domain and hydrogeologic parameters

The initial model simulation covers a 37-year period from the occurrence of the spill (August 1979) to July 2016. The model domain extends horizontally from 45 m upgradient of well 421, a reference point for the center of the oil body, to 215 m downgradient. The vertical dimension of the domain covers an elevation of 417-424 m above mean sea level. In order to avoid boundary effects during model simulations, the computational grid was extended to 475 m downgradient and down to an elevation of 410 m. Individual cells in the computational grid had dimensions of 4.3 m (horizontal) by 0.47 m (vertical).

Hydrogeologic parameters determined from inverse modeling were used to inform physical flow (Essaid et al., 2003) The mean porosity for the study area (0.38) was applied uniformly to the model. Longitudinal and transverse dispersivities were applied uniformly at values of 1 and 0.04 m, respectively. A constant head boundary condition of 424 m was applied to the left boundary, and a constant hydraulic gradient of 0.0035 was applied across the model domain. A constant recharge rate of 4.88 $x10^{-4}$ m/d was applied to the water table boundary. Hydraulic conductivity (K) was applied heterogeneously to the model based on permeability values calculated from grain size data (Dillard et al., 1997). K values were then increased by a factor of two in the Ng et al. (2015) model to achieve better agreement with the homogeneous K determined from inverse modeling (Essaid et al., 2003).

Geochemical formulation

A comprehensive list of the modeled inorganic constituents includes aqueous phases (carbonate species, As(V), As(III), CH_4, DO, Mn, Fe, Ca, Cl, Na, H, and inert N), mineral phases including electron acceptors (MnO_2 and $Fe(OH)_3$) and carbonate precipitates ($CaCO_3$, $MnCO_3$, and $FeCO_3$), dissolved gases (CO_2, CH_4, O_2, and inert N_2) to simulate outgassing, species sorbed via cation exchange (HX, FeX_2, and MnX_2), and surface complexes for arsenate, arsenite, and HCO_3^-. Here, we focus on Fe, As, and DO species and hydrocarbons; results for other species can be found in Ng et al. (2015).

Ng et al. (2015) describes in detail the model formulation for biodegradable organic molecules. Benzene, ethylbenzene, and xylenes were modeled as one component (BEX); toluene, non-volatile dissolved organic C, short-chain *n*-alkanes, and long-chain *n*-alkanes were the other modeled organics. Information regarding chemical composition of the non-aqueous

phase liquid (NAPL), molecule dissolution rates from the NAPL, and biodegradation rates are reported in Ng et al. (2015).

The model uses a partial equilibrium approach, which assumes that organic C oxidation is the rate-limiting step, and the associated reduction reaction proceeds as an equilibrium reaction. Using this approach, an organic molecule is irreversibly broken down into its constitutive elements and oxidation states (in parentheses) at a specified rate, *r*. An example for benzene is shown in Eq. 4.1:

$$C_6H_6 \xrightarrow{r} 6C(-1) + 6H(+1) \qquad \text{Eq. 4.1}$$

The six moles of C(-1) and H(+1) are then reintroduced into the equilibrium solution. C(-1) is converted into HCO_3^- by equilibrium reactions using the most thermodynamically favorable TEAP.

Initial conditions

Initial concentrations for dissolved constituents were determined from well 310E, located upgradient of the spill site in an uncontaminated area of the aquifer. During model equilibration, average concentrations from well 310E from six samplings from 1985-1995 were equilibrated with calcite in the model and charged balanced using PHREEQC-3. Constant concentration flux boundaries with the initial solution chemistry (arsenic species were removed from recharge) were imposed at the left boundary and water table boundary of the model domain.

Initial mineral concentrations for a ferrihydrite-like phase, $Fe(OH)_3$, were determined by 0.5 M HCl extraction (Heron et al., 1994; Tuccillo et al., 1999; Ziegler et al., 2017a), which extracts operationally defined "easily reducible" Fe(III) from aquifer sediments thought to be a reasonable proxy for $Fe(OH)_3$. Average background Fe(III) concentrations reported from

samples collected in 1993 (Tuccillo et al., 1999) and 2013 (Ziegler et al., 2017a) were in close agreement (0.0393 mol/L_v where L_v is the total aquifer volume, and 0.0420 mol/L_v, respectively). Ziegler et al. (2017a) observed low but detectable concentrations (0.004 mol/L_v) of residual Fe(III) near the oil body where the dominant TEAP is methanogenesis, suggesting that some HCl-extractable Fe(III) may not be microbially reducible. Thus, the difference between measured average background Fe(III) and residual Fe(III) (0.037 mol/L_v) was used as the initial concentration for $Fe(OH)_3$. This is an adjustment from Ng et al. (2015), who used an initial concentration of 0.0288 mol/L_v based on higher measured residual Fe(III) near the oil body observed in 1993 (Tuccillo et al., 1999).

Two sorption models were equilibrated to the initial solution chemistry. The first is a cation exchange model used by Ng et al. (2015) to simulate sorption of reduced Fe(II), which was shown to be an important mechanism to close the Fe mass balance (Ng et al., 2014). The surface complexation model introduced for this study (described below) was equilibrated with dissolved As in the initial solution. Although As is below detection (< 1 μg/L; < 1.3 $x10^{-8}$ mol/L_w) in background wells at the Bemidji site, an initial dissolved As concentration is necessary to create initial As complexes on $Fe(OH)_3$ for an initial condition of sorbed As. Thus, we chose an initial As solution concentration of 3 $x10^{-10}$ M, so that it was well below the detection limit, would not contribute appreciably to As mass in the model, and would generate reasonable initial concentrations of As complexed to $Fe(OH)_3$ based on chemical extractions from Ziegler et al., (2017a) (1.62 $x10^{-5}$ mol/L_v).

We used the generalized two-layer surface complexation model and database described in Dzombak and Morel (1990) for modeling As complexes on hydrous ferric oxide (HFO). The two-layer model defines “Type 1” and “Type 2” sites, alternatively strong and weak sites. Type 1

sites, defined in the PHREEQC database as Hfo_s (_s denotes "strong"), correspond to a smaller subset of surface sites with high affinity for cation sorption. Type 2 sites, defined as Hfo_w in the PHREEQC database (_w denotes "weak"), are the total reactive sites available for sorption of protons, cations and anions as determined by observed sorption maxima (Dzombak and Morel, 1990). Because Type 1 sites do not sorb As oxyanions, they were excluded from this model. In our model, HFO is user-defined as $Fe(OH)_3$. The specific surface area (600 m^2/g) and surface site density for Hfo_w (0.2 mol/mol Fe) were taken from the Dzombak and Morel (1990) database.

Arsenic complexation to $Fe(OH)_3$ is described thermodynamically by empirically derived intrinsic surface complexation constants. Complexation of both arsenate and arsenite are simulated. Acid dissociation constants and intrinsic surface complexation constants for reactions used in this model are listed in Table 4.1. Note that the complexes are all represented as monodentate complexes. Using Eq. 4.8 in Table 4.1 as an example, Hfo_wOH represents a single Type 2 sorption site on HFO, and the formation of $Hfo\_wH_2AsO_4$ represents the sorption of a single arsenate molecule to one Type 2 site on HFO. Carbonate complexation is also considered as carbonate has been shown to outcompete As for sorption sites and displace already-sorbed As (Appelo et al., 2002). Phosphate is not included because it is not detected in groundwater at the Bemidji site.

Table 4.1 Surface complexation constants and reactions for arsenate, arsenite, and bicarbonate

		logK	$logK^-$ 95% CI	$logK^+$ 95% CI	reference
Acid dissociation reaction[a]					
Eq. 4.2	$H_3AsO_4 = H_2AsO_4^- + H^+$	2.24			Smith and Martel (1976)
Eq. 4.3	$H_2AsO_4^- = HAsO_4^{2-} + H^+$	6.96			Smith and Martel (1976)
Eq. 4.4	$HAsO_4^{2-} = AsO_4^{3-} + H^+$	11.5			Smith and Martel (1976)

Eq. 4.5	$H_3AsO_3 = H_2AsO_3^- + H^+$	9.29			
surface (de)protonation reaction					
Eq. 4.6	$Hfo\_wOH + H^+ = Hfo\_wOH_2^+$	7.29			Dzombak and Morel (1990)
Eq. 4.7	$Hfo\_wOH = Hfo\_wO^- + H^+$	-8.93			Dzombak and Morel (1990)
	arsenate reaction				
Eq. 4.8	$Hfo\_wOH + AsO_4^{3-} + 3H^+ = Hfo\_wH_2AsO_4 + H_2O$	29.31	28.29	30.34	Dzombak and Morel (1990)
Eq. 4.9	$Hfo\_wOH + AsO_4^{3-} + 2H^+ = Hfo\_wHAsO_4^- + H_2O$	23.51	23.33	23.7	Dzombak and Morel (1990)
Eq. 4.10	$Hfo\_wOH + AsO_4^{3-} + H^+ = Hfo\_wAsO_4^{2-} + H_2O$	18.1			Dixit and Hering (2003)
Eq. 4.11	$Hfo\_wOH + AsO_4^{3-} = Hfo\_wOHAsO_4^{3-}$	10.58	10.01	11.15	Dzombak and Morel (1990)
arsenite reactions					
Eq. 4.12	$Hfo\_wOH + H_3AsO_3 = Hfo\_wH_2AsO_3 + H_2O$	5.41	5.11	5.71	Dzombak and Morel (1990)
bicarbonate reaction					
Eq. 4.13	$Hfo\_wOH + CO_3^{2-} + 2H^+ = Hfo\_wHCO_3 + H_2O$	20.37	19.39	21.35	Apello et al. (2002)
Eq. 4.14	$Hfo\_wOH + CO_3^{2-} + H^+ = Hfo\_wCO_3^- + H_2O$	12.78	12.58	12.98	Apello et al. (2002)

[a]Acidity constants correspond to T = 20-25 C and I = 0.

Results and Discussion

Model calibration

The reactive transport model was calibrated to reasonably simulate three parameters important for As cycling: the maximum concentration of dissolved As, the total dissolved As mass, and the location of the 10 μg/L front for As, representing the plume's leading edge. Because 10 μg/L is the regulated drinking water standard in the U.S., priority was given to accurately simulating the location of the 10 μg/L front. Only three parameters were allowed to be adjusted during the calibration process. First was the initial concentration of $Fe(OH)_3$ in aquifer sediments. Second was the initial input concentration for dissolved As. During calibration, the initial dissolved As was equilibrated with surface sites for $Fe(OH)_3$ to create the initial concentration for sorbed As. The initial input As concentration was always held at least two orders of magnitude below the

detection limit for As in groundwater (1 μg/L) to ensure we were not creating falsely high concentrations of sorbed As. The third adjustable parameter was the intrinsic complexation constants (logK) for As complexes on $Fe(OH)_3$. Constants were allowed to be adjusted to the +95% and -95% confidence intervals (Table 4.1). The results presented below are for the calibrated base case simulation. For the base case, the initial $Fe(OH)_3$ was 0.037 mol/L_v, corresponding to the average background concentration for Fe(III) from field sampling, minus the lowest observed residual Fe(III) near the oil body (Ziegler et al., 2017a). Initial dissolved As was 3 $x10^{-10}$ M. Complexation logK values used in the base case were the mean reported values (Table 4.1).

Groundwater chemistry

Aqueous species that are important for As cycling (pH, DO, Fe^{2+}, and total As (As_T)) are shown in Figure 4.1 for 37 years after the oil spill (year 2016). Overall, pH has decreased in the plume due to a number of reactions, including cation exchange of dissolved cations with surficial H^+ (Ng et al., 2015) and the production of H^+ (Ng et al., 2015) and organic acids (Cozzarelli et al., 1994) during biodegradation. For an in-depth discussion of reactions affecting pH in the aquifer, see (Bennett et al., 1993). pH is included here because the forms of dissolved and sorbed As species and the charge on surficial hydroxyls of $Fe(OH)_3$ are pH-dependent.

DO and Fe^{2+} in groundwater are shown because of their importance in electron accepting processes, aerobic respiration and Fe-reduction, respectively. DO is depleted from groundwater near the oil due to extensive aerobic biodegradation over the plume's lifespan. Fe^{2+} is an electron acceptor byproduct of biodegradation coupled with reductive dissolution of $Fe(OH)_3$. As such, Fe^{2+} is elevated in groundwater. The shape of the Fe^{2+} plume in our 2016 simulation in comparison of plumes in previous model simulations for 1986, 1993, and 2007 (Ng et al., 2015)

suggest that Fe^{2+} continues to advance downgradient over time. The dissolved Fe^{2+} front has advanced downgradient from 110 m to 140 m from the simulation for 2007 to 2016. However, this may be due in part to the increased initial $Fe(OH)_3$ of 0.037 mol/L_v used in this simulation compared to 0.0288 mol/L_v used for the Ng et al. (2015) 2007 simulation.

Dissolved As is shown in Figure 4.1 as total dissolved As (As(III) + As(V)), though virtually all dissolved As is As(III) in the model; nowhere in the model did As(V) exceed 1 μg/L in 2016. Field measurements also show that most As in groundwater (>80%) is As(III) (Cozzarelli et al., 2016). In the simulation, the center of As mass occurs at approximately 65 m downgradient (Figure 4.1), with the As maximum (428 μg/L) located at 74 m downgradient. The maximum simulated As concentration was within a factor of two of the field-measured maximum of 230 μg/L (Cozzarelli et al., 2016). Near the oil, As mass was completely removed from sediment and transported downgradient by 2016. From field sampling, the estimated center of mass of the As plume was ~40 m downgradient (Cozzarelli et al., 2016). The model does accurately simulate the location of 10 μg/L As front (124 m), in comparison with 122 m from field sampling (Cozzarelli et al., 2016).

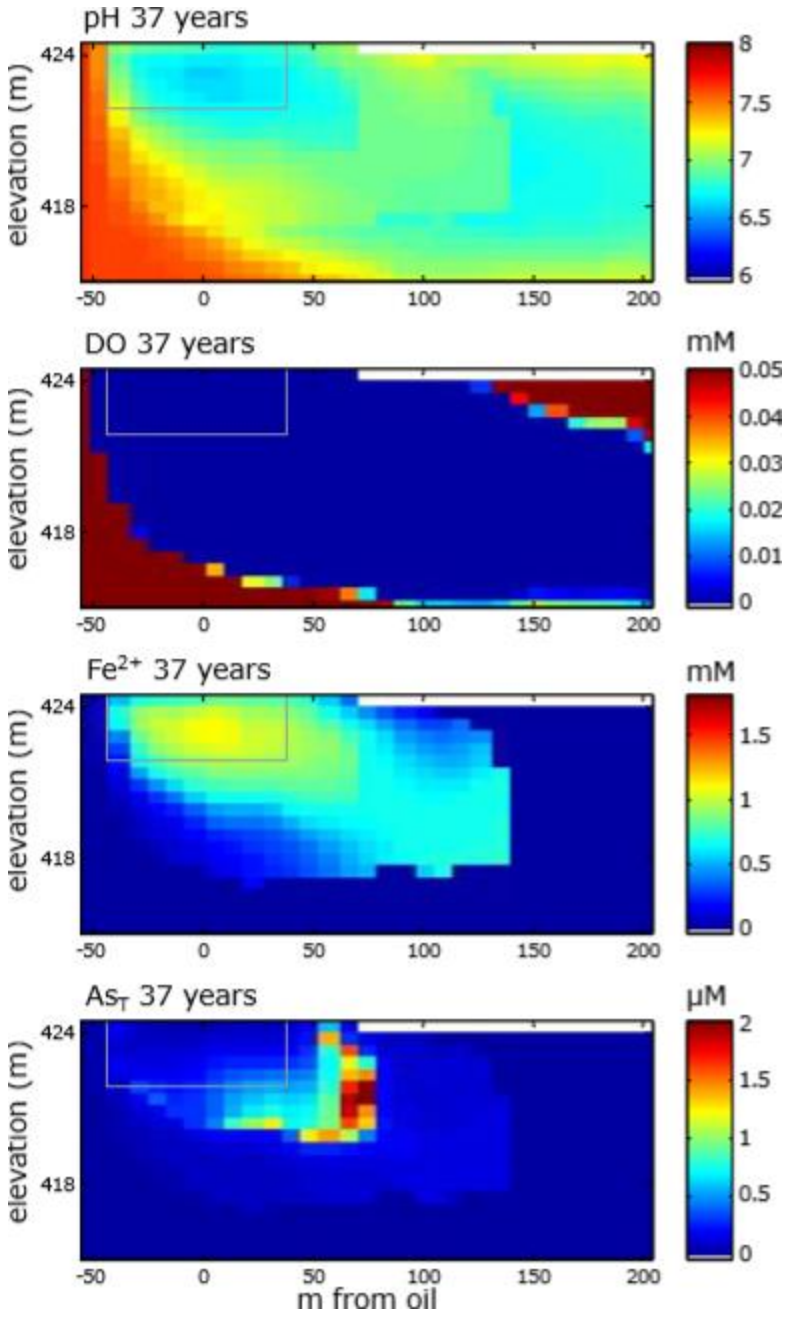

Figure 4.1. Model simulation results from the base case model for pH, DO, Fe^{2+}, and total dissolved As (As_T) for 37 years after the oil spill (2016). The gray box is the reference for the extent of the oil body.

Sediment and surface chemistry

Figure 4.2 shows the depletion of $Fe(OH)_3$ as a result of Fe-reduction. Most $Fe(OH)_3$ mass has been depleted from aquifer sediments near the oil body due to extensive biodegradation

coupled with Fe-reduction. Further downgradient, active Fe reduction occurs in the plume, as is evident from the remaining $Fe(OH)_3$ that has not been fully depleted.

The regions of depleted $Fe(OH)_3$ and active Fe-reduction correspond to elevated Fe^{2+} in groundwater due to dissolution of reduced $Fe(OH)_3$ (Figure 4.1). Despite Fe^{2+} reaching concentrations as high as 1.1 mM, dissolved Fe^{2+} only accounts for ~0.1% of the Fe mass in the aquifer (Ng et al., 2014). Ng et al. (2015) discusses in detail multiple solid-phase mechanisms that serve as sinks for reduced Fe(II), including sorbed Fe(II) in sediment and precipitation of Fe(II)-carbonates.

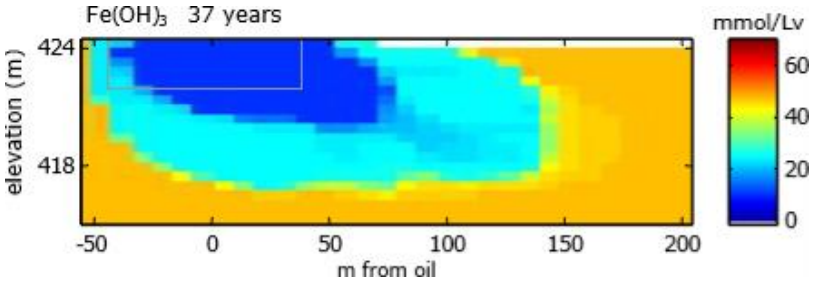

Figure 4.2. Model simulation results for solid phase concentrations of $Fe(OH)_3$ in 2016 (37 years after the oil spill). The gray box is the reference for the extent of the oil body.

Arsenic mobilization and attenuation

Sorbed As complexes on $Fe(OH)_3$ function as the source for As in groundwater. In the equilibrated model, background As sorbed complexes are dominated by two As(V) complexes: $Hfo\_wAsO_4^{2-}$ and $Hfo\_wOHAsO_4^{3-}$. Combined, these two forms account for 99.8% of the initial As mass. More protonated forms of sorbed As(V) and sorbed As(III) contribute minimally to the background As mass.

After the introduction of petroleum hydrocarbons (time 0 in the model), biodegradation coupled with Fe reduction begins within 100 days of the model simulation, allowing $Fe(OH)_3$ to be reductively dissolved, and As(V) to be desorbed into groundwater to create a plume of

dissolved As. The reducing conditions in the plume also promote the abiotic transformation of As(V) to As(III). After 37 years of hydrocarbon presence in the aquifer, the region from 45 m upgradient from well 421 to ~65 m downgradient has sorbed As concentrations near zero due to extensive mobilization (Figure 4.3).

Beneath the As plume and at its leading edge, As is removed from groundwater by resorption onto $Fe(OH)_3$ surface sites (Figure 4.3). Certain complexes contribute more to As attenuation than others. Specifically, sorption of As(III) in the form $Hfo\_wH_2AsO_3$ occurs at the plume boundaries and accumulates high concentrations of As. However, some dissolved As is transported beyond this zone and breaks through the zone of elevated $Hfo\_wH_2AsO_3$ (Figure 4.3). Further downgradient, groundwater is slightly more oxic, allowing As to be oxidized and form As(V) complexes on $Fe(OH)_3$ as $Hfo\_wAsO_4^{2-}$, which increases by a factor of two relative to background concentrations (Figure 4.3). Other As(V) complexes do not contribute to As retention. In fact, the other dominant form from background sediments, $Hfo\_wOHAsO_4^{3-}$, decreases by a factor of two relative to background.

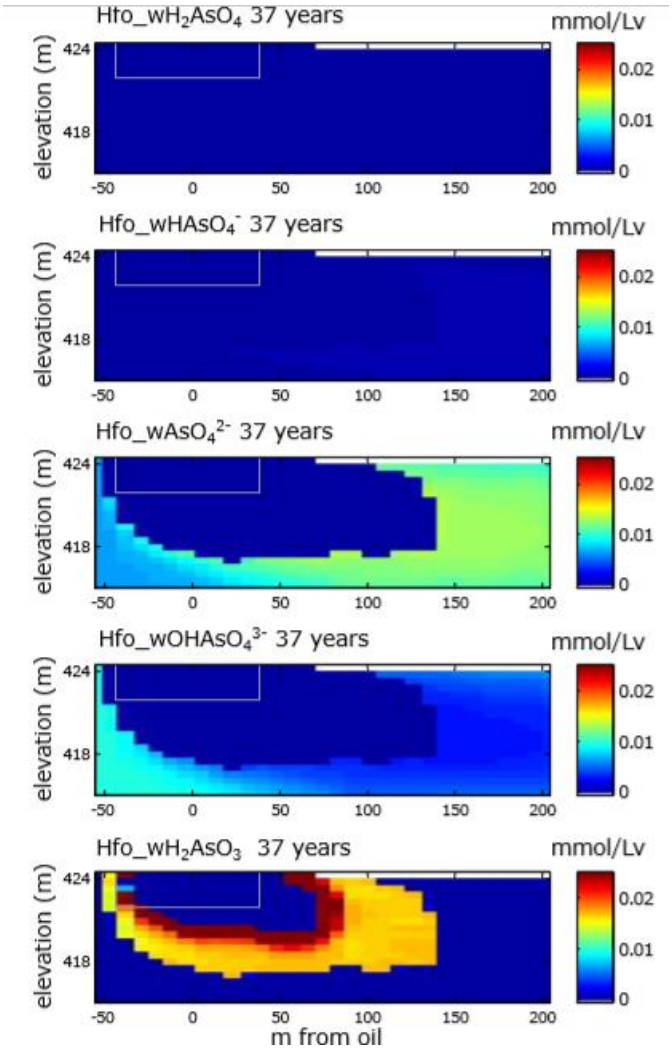

Figure 4.3. Model simulation results for As(V) and As(III) species sorbed to $Fe(OH)_3$ in 2016 (37 years after the oil spill). The gray box is the reference for the extent of the oil body. As(V) species are shown in the top four panels: Hfo_wH_2AsO_4, Hfo_w$HAsO_4^-$, Hfo_wAsO_4^{2-}, and Hfo_w$OHAsO_4^{3-}$. The As(III) species is shown in the bottom panel: Hfo_wH_2AsO_3.

Long-term cycling

After calibration, the base case simulation was run for 400 years to provide insight into the long-term cycling of As and other important reactions in the plume. The long-term simulation results are presented as cross section heatmaps for pH, DO, benzene, ethylbenzene, and xylenes (BEX), non-volatile dissolved organic carbon (NVDOC), Fe^{2+}, $Fe(OH)_3$, sorbed Fe(II), and siderite

($FeCO_3$). (Figure 4.4). A series of four times are shown: 18,200 days (50 years; 2029), 36,000 days (100 years; 2079), 54,700 days (150 years; 2129), and 76,000 days (200 years; 2179). Simulation results after 200 years are not shown because the As plume stabilizes at 300 m by 200 years.

pH, DO, Fe, and hydrocarbons

Evolution of the hydrocarbon plume lowers the pH in groundwater through 100 years, with a pH minimum of ~6.5 occurring in near the oil body (Figure 4.4). However, between 100 and 150 years, the pH begins to revert to its background condition due to the near complete degradation of NVDOC, which produces acidity as it biodegrades. Without the added acidity from NVDOC biodegradation, recharging groundwater from the constant flux boundary at the left and the water table recharge boundary allow pH to revert to near-background conditions.

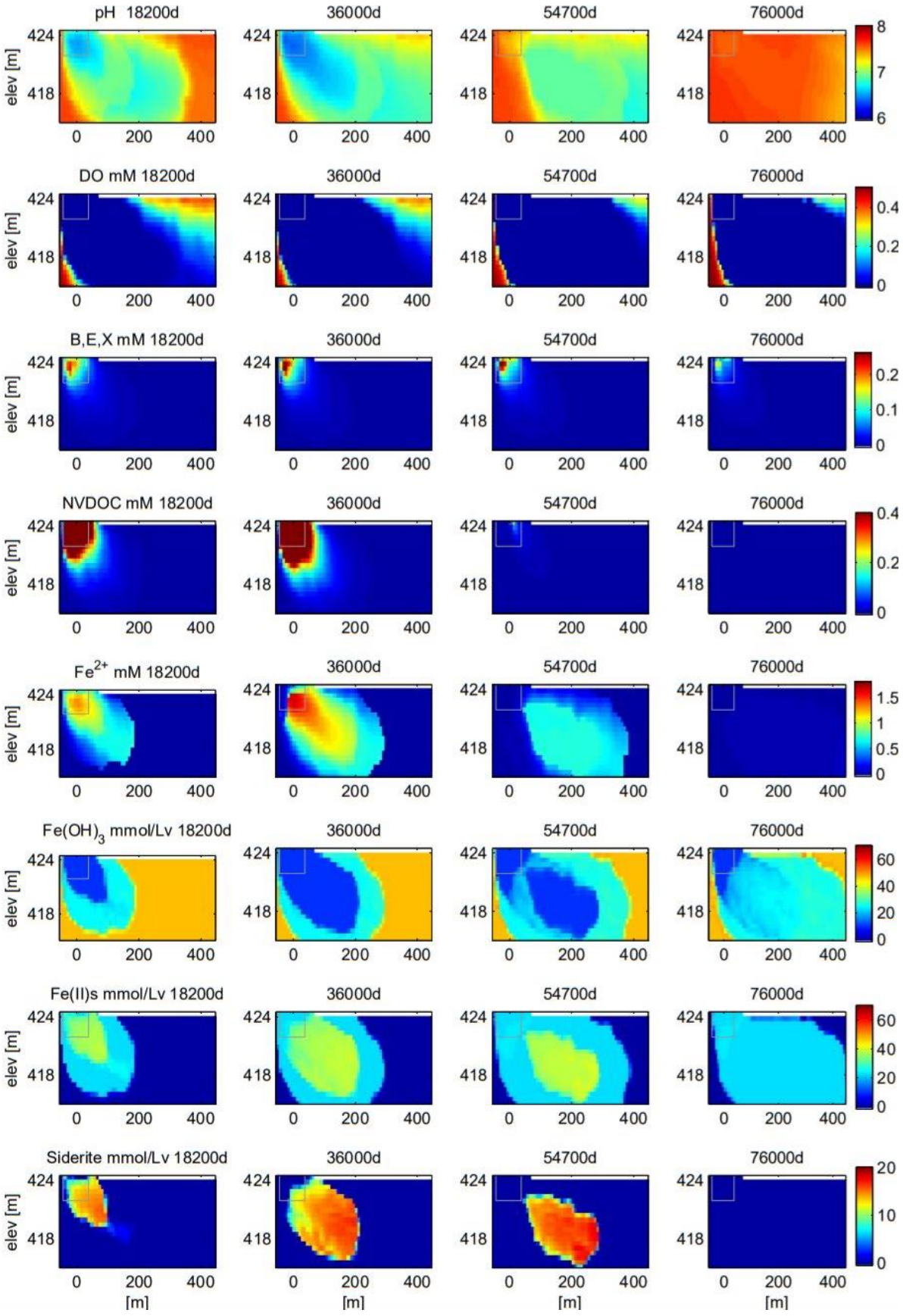
pH 18200d
36000d
54700d
76000d
DO mM 18200d
B,E,X mM 18200d
NVDOC mM 18200d
Fe2+ mM 18200d
Fe(OH)3 mmol/Lv 18200d
Fe(II)s mmol/Lv 18200d
Siderite mmol/Lv 18200d
elev [m]
424
418
0
200
400
[m]
8
7
6
0.4
0.2
0
0.1
1.5
1
0.5
60
40
20
10

Figure 4.4. Model simulation results for selected species for the time periods of 18,200 days (50 years; 2029), 36,000 days (100 years; 2079), 54,700 days (150 years; 2129), and 76,000 days (200 years; 2179) after the spill. Modeled species include pH, DO, cumulative benzene, ethylbenzene, and xylene (BEX), non-volatile dissolved organic carbon (NVDOC), Fe^{2+}, $Fe(OH)_3$, sorbed Fe(II), and siderite ($FeCO_3$). The gray box is the reference for the extent of the oil body.

The plume of depleted DO also expands downgradient as the plume evolves over time. Unlike pH, DO does not revert to background conditions quickly. The depleted DO plume extends well past the 400 m model domain through at least 200 years; background concentrations for DO are not attained by the end of the 400-year simulation (data not shown). This is likely due to DO being consumed through a variety of processes, including aerobic respiration of residual BEX and NVDOC near well 421. Immediately downgradient from where organics are still in place, the long-term reducing conditions in the plume have created substantial chemical oxygen demand, and DO is likely consumed via oxidation of dissolved electron donors (Fe^{2+}), reduced minerals (siderite; $FeCO_3$) and sorbed phases (Fe(II)). The effect of DO in oxidizing these reduced Fe(II) phases is shown by the halo of increased $Fe(OH)_3$ at 150 years from ~0-100 m downgradient from well 421 (Figure 4.4). Recharging oxygen from the water table boundary that is not consumed via biodegradation oxidizes reduced Fe(II) phases from the surface and gradually penetrates to greater depths. Similarly, DO recharging from the constant flux boundary at left oxidizes the upgradient edge of reduced Fe(II) phases along the groundwater flow path as is evident from the loss of Fe^{2+}, Fe(II), and $FeCO_3$ corresponding to a "halo" of increased $Fe(OH)_3$ (panels 5-8 in Figure 4.4). By 200 years, the halo of increased $Fe(OH)_3$ has encroached downward from the top and rightward from the left. Within 200 years, sorbed Fe(II) is depleted, and $FeCO_3$ is completely oxidized from the aquifer. Based on these simulations, we suspect that background DO concentrations will not be reestablished until both biologic and chemical oxygen

demand in the aquifer have been satisfied and organic and inorganic electron donors have been oxidized, which is predicted to take more than 400 years in the Bemidji aquifer.

Arsenic cycling

As the hydrocarbon plume evolves over time, the center of dissolved As is transported downgradient (Figure 4.5). At 50 years, the center of As mass is located ~80 m downgradient from well 421. By 100 years, the center of mass has migrated downward in the aquifer to 200 m from well 421. During this time, the 10 μg/L front also migrated from 128 to 225 m. Based on these observations, the center of mass migrated at a slightly faster rate of 2.4 m/y compared to the 10 μg/L front, which advanced at 1.9 m/y.

Over 100 years, the amount of dissolved As mass increased by a factor of two to its observed maximum of 0.4 moles (Figure 4.6). From 100 to 150 years, the advancement of the center of mass and the 10 μg/L front slows down and corresponds to a substantial loss of dissolved As mass; by 150 years, the total As mass in groundwater was 0.08 moles (Figure 4.6), though concentrations at the center of mass still remain relatively high (>100 μg/L in some cells). After 150 years, the dissolved As plume begins to stabilize, and the 10 μg/L front reaches 300 m downgradient. The front remains fixed at 300 m for the remainder of model simulations until 387 years, after which dissolved As in all cells is < 10 μg/L. During this period, the total amount of dissolved As also stabilizes at 0.02 moles.

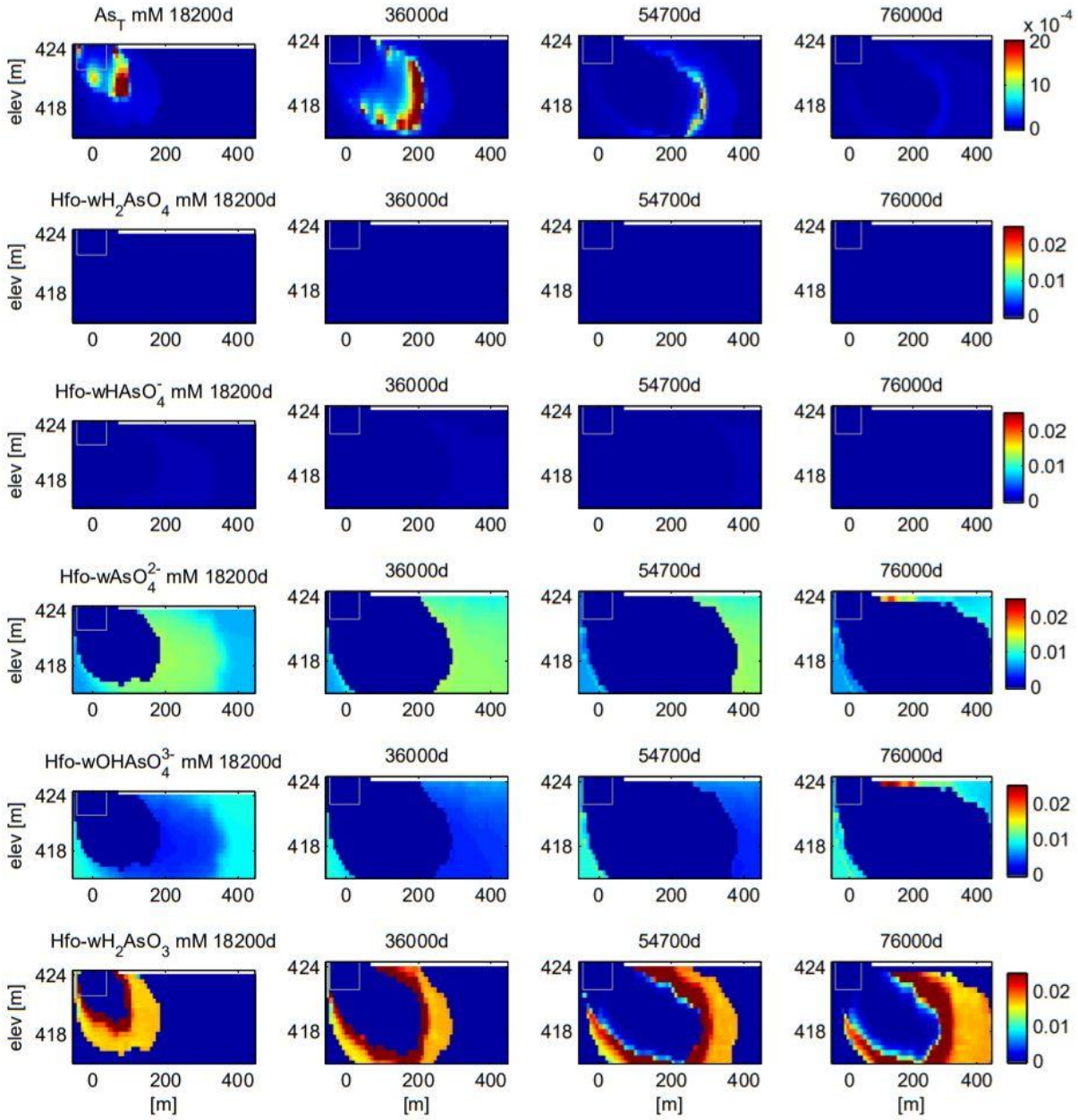

Figure 4.5. Model simulation results for several As species for the time periods of 18,200 days (50 years; 2029), 36,000 days (100 years; 2079), 54,700 days (150 years; 2129), and 76,000 days (200 years; 2179) after the spill. Modeled species include dissolved As (top panel) and sorbed species Hfo_wH_2AsO_4, Hfo_w$HAsO_4^-$, Hfo_wAsO_4^{2-}, Hfo_w$OHAsO_4^{3-}$, and Hfo_wH_2AsO_3 (bottom five panels). The gray rectangle is the reference for the extent of the oil body.

Similar to the modern-day simulation, the long-term model simulation suggests that the primary mechanism responsible for As retention is sorption of As(III) in the form of Hfo_wH_2AsO_3, which forms a ring around the plume fringes (bottom panel of Figure 4.5). Beyond the ring of

sorbed As(III), some oxidized As(V) is also sorbed to $Fe(OH)_3$ (panel 4 of Figure 4.5), similar to the modern-day simulation. The predominant sorbed As(V) form is $Hfo\_wAsO_4^{2-}$.

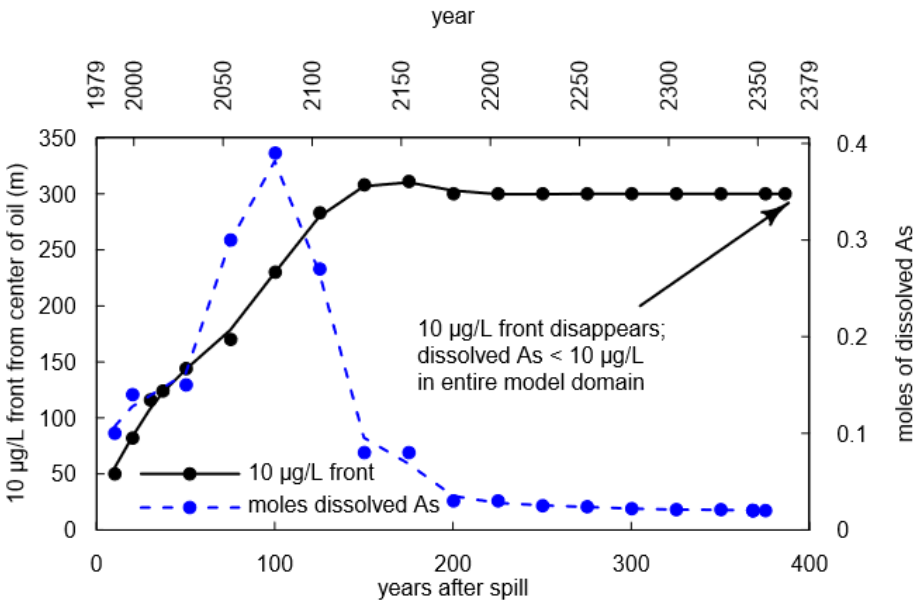

Figure 4.6. Model simulation results for the location of the 10 µg/L front (black) and the total mass of dissolved As (blue) over the entire model simulation.

We suspect that the pervasive nature of the simulated dissolved As mass through 100 years, followed by a steep decline thereafter (Figure 4.6), is controlled by the presence of NVDOC in groundwater. NVDOC is also rapidly lost between 100 and 150 years (Figure 4.4). We propose that the prolonged biodegradation of NVDOC sustains the reducing conditions that promote Fe-reduction and As mobilization, resulting in continued release of Fe^{2+} and As into groundwater. However, after NVDOC becomes (nearly) completely biodegraded after 100 years, the dissolved As mass rapidly declines, most likely because $Fe(OH)_3$ no longer is reductively dissolved because NVDOC has been depleted. In other words, our simulations suggest that no additional As will be added to groundwater after NVDOC is attenuated, and over time, the already dissolved As will become sequestered over time via sorption to $Fe(OH)_3$, resulting in the decline in dissolved As mass after 100 years.

Model sensitivity

A discussion of calibration and sensitivity of the original model can be found in (Ng et al., 2015). In this new edition of the model, we only added or changed three input parameters, initial $Fe(OH)_3$, initial dissolved As used for equilibration with $Fe(OH)_3$ to generate initial sorbed As concentrations, and the logK values for surface complexation of As. For a test of model sensitivity, we employed the sensitivity coefficient approach of Zheng and Bennett (2002). Using this approach, the sensitivity of a dependent variable to a model parameter is the partial derivative of the dependent variable with respect to the model parameter. For easier comparison of different model parameters, the sensitivity coefficient can be normalized to a dimensionless form (Eq. 4.15):

$$X_{i,k} = \frac{\frac{\partial y_i}{y_i}}{\frac{\partial \alpha_k}{a_k}} = \frac{\frac{y_{i,2}-y_{i,1}}{y_{i,1}}}{\frac{\alpha_{k,2}-\alpha_{k,1}}{a_{k,1}}} \qquad \text{(Eq. 4.15)}$$

where $X_{i,k}$ is the sensitivity coefficient of the dependent variable y with respect to the kth parameter at the ith observation point. $y_{i,2}$ is the altered dependent variable. $y_{i,1}$ is the base case dependent variable. $\alpha_{k,2}$ is the manipulated independent variable. $\alpha_{k,1}$ is the base case independent variable. Table 4.2 summarizes the sensitivity coefficients for independent variables logK's, initial $Fe(OH)_3$, and initial sorbed As on the following dependent parameters: location of 10 μg/L front, total dissolved As mass, and maximum dissolved As concentration.

Table 4.2 Sensitivity coefficients model parameters

Sensitivity of:	logK		Initial $Fe(OH)_3$ (mol/L_v)		Initial sorbed As	
	base: mean		base: 0.0370		base: 1.62 x10^{-5} (mol/L_v)	
	decrease	increase	decrease	increase	decrease	increase

	$\log(K)^-$ 95% C.I.	$\log(K)^+$ 95% C.I.	lowest measured background: 0.0228	greatest measured background: 0.0657	half: 3.7×10^{-5}	double: 3.24×10^{-5}
Location of 10 μg/L As front	-0.46	-0.09	-0.43	-1.05	0.08	0.79
total dissolved As mass	-0.06	-0.12	-14.36	-0.12	1.01	1.00
maximum dissolved As	0.08	-0.09	-11.75	2.27	1.02	1.05

Of the three dependent parameters considered, the location of the 10 μg/L front was relatively insensitive to the any of the independent variables assessed. The total dissolved As mass and the maximum dissolved As concentration were about equally sensitive. Adjusting the intrinsic surface complexation constants for As sorption to the upper and lower 95% confidence intervals has little effect on any of the dependent parameters. Doubling and halving the initial sorbed As concentration was somewhat sensitive with respect to the total dissolved mass and the maximum dissolved As, but it had little effect on the location of the 10 μg/L front, which we considered our most important dependent parameter based on drinking water regulations. By far, the most sensitive independent variable was the initial $Fe(OH)_3$ concentration. In our sensitivity tests, we set the lower and upper bounds for $Fe(OH)_3$ as the minimum and maximum measured field concentrations for a single background sample (Ziegler et al., 2017a), respectively. The sensitivity analysis shows that for this model, it is crucial to have an accurate estimate for $Fe(OH)_3$ to accurately simulate total dissolved As mass and the maximum dissolved As. The model is particularly sensitive to underestimations of initial $Fe(OH)_3$; when initial $Fe(OH)_3$ is decreased, dependent variables have large sensitivity coefficients. Because sorption to $Fe(OH)_3$ is the main retention mechanism for As, a poorly quantified initial condition for $Fe(OH)_3$ can

cause substantial errors in simulating As transport by either over- or underestimating sorption sites for As, which then either incorrectly enhance or lessen As retention.

Concentration profiles of dissolved As for two discrete elevations (422 m and 419 m) show the sensitivity of our model parameters to changes in logK, initial $Fe(OH)_3$ and initial sorbed As and two binary scenarios (i.e., "on" vs. "off") to evaluate how 1) allowing HCO_3^- to form surface complexes, and 2) the incorporation of a commonly disregarded As(V) surface complexation reaction (Eq. 4.10 in Table 4.1) affect As cycling (Figure 4.7). Previous studies have reported that the formation of HCO_3^- surface complexes on $Fe(OH)_3$ is crucial to simulating As cycling because it is an important competing ion for As on $Fe(OH)_3$ surface sites (Anawar et al., 2004; Appelo et al., 2002; Charlet et al., 2007; Dixit and Hering, 2003). Surface complexation of HCO_3^- was permitted in the base case, but a separate simulation was conducted in which HCO_3^- was not allowed to form surface complexes.

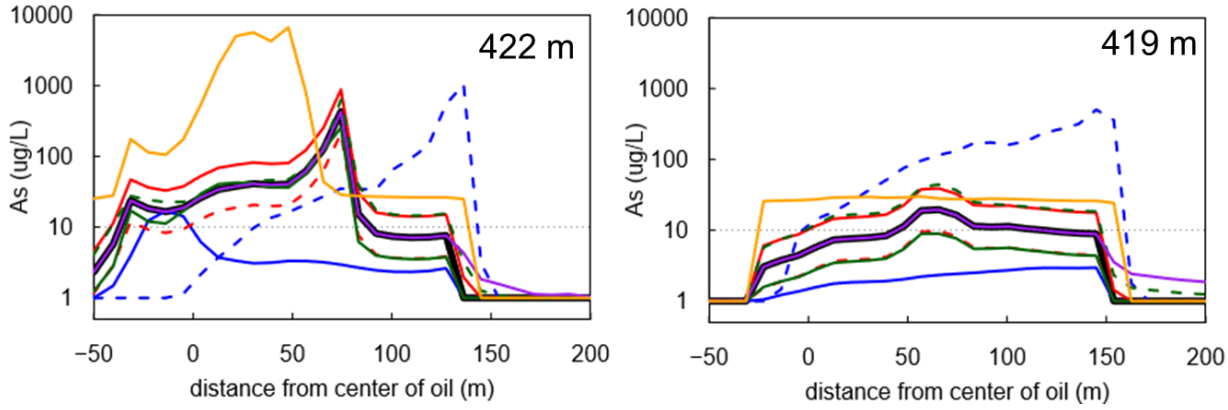

Figure 4.7. Concentration profiles for dissolved As at elevations of 422 m (top), and 419 m (bottom). Scenarios shown include the base case (black), doubled initial sorbed As (red, solid), halved initial sorbed As (red, dashed), upper 95% confidence interval for intrinsic As surface complexation constants (green, solid), lower 95% confidence interval for intrinsic As surface complexation constants (green, dashed), maximum measured background $Fe(OH)_3$ concentration (blue, solid), minimum measured background $Fe(OH)_3$ concentration (blue, dashed), no complexation of HCO_3^- (yellow), and omission of an As(V) surface complexation reaction (Eq. 4.10 in Table 4.1) (purple).

The As concentration profiles at 422 m and 419 m elevation show that doubling and halving the initial sorbed As had minimal effect on the distribution of As at these two depths (Figure 4.7). Similarly, increasing and decreasing the logK values did not significantly alter the concentration profiles.

The profiles show the substantial effect of changing initial concentration of $Fe(OH)_3$ (Figure 4.7). When overestimating the initial concentration, the As plume becomes over-attenuated, with the As maximum at 422 m occurring at 15 m upgradient of well 421 compared to the base case, where the maximum occurs at 65 m downgradient. Additionally, the maximum As concentration is an order of magnitude less than the base case and barely exceeds the 10 μg/L threshold. At 419 m elevation, dissolved As never exceeds the 10 μg/L threshold, whereas the base case 10 μg/L front extends to 122 m. These simulated phenomena occur because there is an excess of $Fe(OH)_3$, and thus, an excess of surface sites to sorb As, which amplifies As attenuation. Conversely, underestimating initial $Fe(OH)_3$ has the opposite effect. At 422 m, the dissolved As maximum occurs at 145 m, 23 m further than the base case, though the As maximum is roughly similar. At a depth of 419 m, the magnitude of As in groundwater is grossly overestimated. These trends occur because there is too little $Fe(OH)_3$, and thus fewer surface sites to sorb As which allows for more As in groundwater and further As transport. These two scenarios illustrate the critical importance of a well sampled and well characterized background sediment chemistry, as an overestimation or underestimation of $Fe(OH)_3$ can have critical effects on model output for As mobility.

Excluding complexation of HCO_3^- also has critical effects on simulating As (Figure 4.7). Surprisingly, prohibition of HCO_3^- complexation increases dissolved As at 422 m and 419 m elevation, though the effect is particularly pronounced at 422 m, where As concentrations are

approximately 80 times greater than the base case. At both depths, the location of the 10 μg/L front is approximately 45 m further downgradient compared to the base case. These results corroborate the findings of other studies that have identified sorption of HCO_3^- as crucial to accurately simulate As cycling (Anawar et al., 2004; Appelo et al., 2002; Charlet et al., 2007; Dixit and Hering, 2003).

Importance of a complete database

In addressing the importance of HCO_3^- surface complexation on As mobility, Appelo et al. (2002) caution against surface complexation models to simulate As sorption because databases are incomplete and can lead to incorrect results. The majority of reactive transport models in the published literature that simulate As sorption to $Fe(OH)_3$ as surface complexation reactions exclude the formation of the $Hfo\_wAsO_4^{2-}$ (Eq. 4.10 in Table 4.1). We suspect this is because most models employ the surface complexation database from Dzombak and Morel (1990). Although Dzombak and Morel (1990) has become the standard for surface complexation modeling, it is crucial to recognize that the database is missing a logK value for Eq. 4.10. Dzombak and Morel (1990) did not report a logK for the surface species $Hfo\_wAsO_4^{2-}$ because it had no influence fitting of available experimental data. However, when we consider the predominant species of dissolved and surface species for As(V) based on thermodynamic data (Table 4.1), the As(V) species not reported in Dzombak and Morel (1990) is the most dominant As(V) species at the pH range of groundwater (Figure 4.8), suggesting the database may be limited in simulating As surface complexation in aquifers. To address the lack of a logK for Eq. 4.10, we included a value from Dixit and Hering (2003).

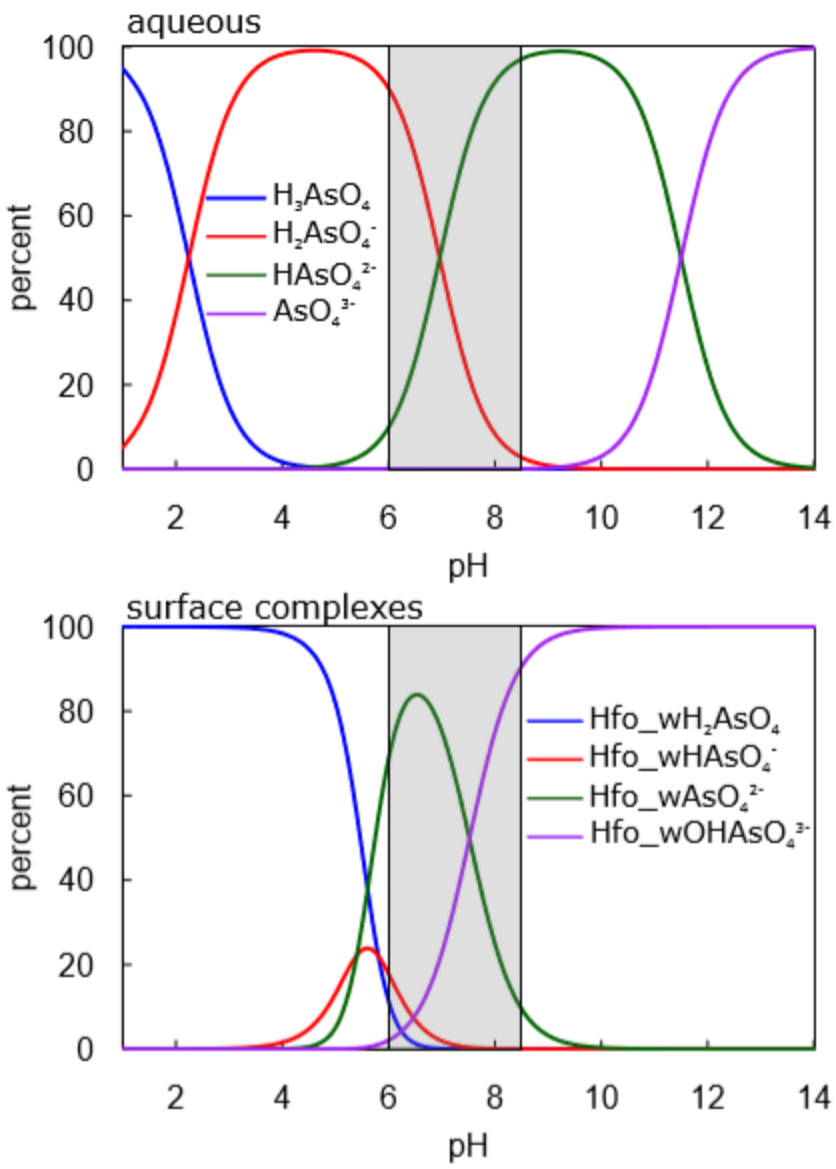

Figure 4.8. Generalized relative abundances of aqueous As(V) species (top) and As(V) surface complexes on $Fe(OH)_3$ (bottom). Aqueous species are determined from acid dissociation constants in Table 4.1. Surface species are determined from intrinsic complexation constants in Table 4.1. Modeled As(V) species are triprotic (blue; H_3AsO_4/Hfo_wH_2AsO_4), diprotic (red; $H_2AsO_4^-$/Hfo_w$HAsO_4^-$), monoprotic (green; $HAsO_4^{2-}$/Hfo_wAsO_4^{2-}), and unprotonated (purple; AsO_4^{3-}/Hfo_w$OHAsO_4^{3-}$). The monoprotic surface species (green) is omitted from Dzombak and Morel (1990). The gray box indicates the pH range of most groundwaters (6-8.5).

The more protonated species (H_3AsO_4/Hfo_wH_2AsO_4 and $H_2AsO_4^-$/Hfo_w$HAsO_4^-$) are essentially irrelevant for As attenuation because the pKa's for the dissolved species are so low, and the species are important only at low pH. Although dissolved As at our site is predominantly

controlled by As(III) sorption, the downgradient reaches of the model domain show that the only As(V) surface species that increases is Hfo_wAsO_4^{2-} (Figure 4.8). Based on this result, we infer that reactive transport models that simulate As surface complexation reactions at circumneutral pH but do not include formation of the Hfo_wAsO_4^{2-} species will likely miss the most important sorbed As(V) species, which can potentially lead to errors in modeling results. This is especially critical when dissolved As is limited primarily by sorption of As(V). For our model, As(III) sorption is the dominant process limiting As transport, and we observe no deviation from the base case when Eq. 4.10 is omitted up to 140-150 m (Figure 4.7). However, downgradient from 140-150 m, As is fully removed from groundwater in the base case due to formation of the Hfo_wAsO_4^{2-} complex. When Eq. 4.10 is omitted, As is pervasive in groundwater beyond 200 m at both depths. We suspect this problem would be especially amplified if As(V) sorption was the main attenuation mechanism, and Eq. 4.10 was omitted.

Long-term As attenuation mechanisms

Immediate As over the entirety of the model simulation show that sorption of As(III) is the dominant mechanism that attenuates dissolved As (Figure 4.6). However, close examination of the time series evolution of As surface species (Figure 4.5) provides hints that the As(III) complex will not be stable over several centuries. First, the bulk of aquifer still has very low DO, and we suspect that a return to background DO concentrations cannot be established until electron donors, organic and inorganic, are oxidized in the aquifer. Evidence of this phenomenon can be seen in the simulated gradual increase of $Fe(OH)_3$ corresponding to the gradual loss of Fe(II) and complete oxidation of $FeCO_3$ (Figure 4.4). In examining the upgradient edge of the Hfo_wH_2AsO_3 species (Figure 4.5) from approximately -50 to -15 m, we see that from 50 years to 200 years, there is a loss of Hfo_wH_2AsO_3. This is also observed near the water table

boundary 100 to 250 m downgradient. However, the loss of this As(III) complex does not correspond to increased dissolved As but instead to increases in As(V) complexes. This is especially noticeable at the water table, where increases in the Hfo_wAsO_4^{2-} and Hfo_w$OHAsO_4^{3-}$ are observed. Based on these signatures, we suggest that recharging DO is causing the early stage of the transformation of the reduced As(III) complexes to oxidized As(V) complexes. Eventually all As in the model domain will be transformed to As(V) complexes, where the predominant complex is determined by the pH of groundwater. However, the time until this transformation is complete is unclear. We suspect it to take several hundreds, if not thousands, of years to occur. In effect, the model suggests that the final step in As cycling is the return of As to its original form, As(V) sorbed to $Fe(OH)_3$. Biodegradation of petroleum has caused a redistribution of As mass in the aquifer, with virtually no As existing in sediment from the location of the oil spill to 300 m downgradient. However, beyond 300 m, As is sorbed to $Fe(OH)_3$, is substantially enriched relative to the original background concentration, and could be remobilized given an introduction of biodegradable organic carbon.

Model limitations

While the model used in this study accounts for biodegradation and secondary reactions that affect water quality, there are some limitations that must be considered that could have confounding effects on As transport.

First, Ng et al. (2015) discusses that the model does not re-oxidize dissolved Fe^{2+} to form Fe(III)-rich sediments at the plume's leading edge as observed in field observations (Tuccillo et al., 1999; Ziegler et al., 2017a). This may have an effect on As transport in that the model's omission of reprecipitation of $Fe(OH)_3$ causes an underrepresentation of simulated sorption sites compared to reality. Thus, the model would underestimate the aquifer's natural attenuation

capacity for As, resulting in the model allowing As to be transported further than would likely occur than if reprecipitation of $Fe(OH)_3$ occurred.

Conversely, the model does not account for biodegradation products recently documented in the aquifer (Bekins et al., 2016) that could serve as additional electron donors that drive the aquifer more reducing. Biodegradation of these molecules could potentially lower the redox potential of the aquifer, allowing for further transport of As over the long-term.

The model also omits microbially mediated As(V)-reduction reactions. Microbes have the potential to use As(V) as an electron acceptor, reducing it to As(III) and promoting reductive desorption into groundwater (Tufaco et al., 2008; Kocar et al., 2006). Although these reactions are possible, they would be dwarfed in comparison to As mobilization due to Fe-reduction.

Last, the model assumes a homogeneous distribution of $Fe(OH)_3$ in background sediments prior to the oil spill. Based on sampling of background sediment, $Fe(OH)_3$ concentrations can be heterogeneous, though average background Fe(III) concentrations from two different locations were in close agreement, 1330 mg/kg (Tuccillo et al. 1999) and 1390 mg/kg (Ziegler et al. 2017a). As previously discussed, $Fe(OH)_3$ is the primary control on As transport. By invoking a homogeneous distribution of $Fe(OH)_3$ as an initial condition, the model likely neglects some of the fine-scale nuances in Fe cycling that result from natural heterogeneity, which could affect As cycling. We expect these fine-scale nuances are likely unimportant considering the overall spatial and temporal bounds of these model simulations.

Human health consequences

To assess the relative threat posed by As in groundwater, we compared the aquifer volume that exceeds the respective maximum contaminant levels (MCL) for benzene (5 μg/L) and As (10

µg/L) (Figure 4.9). We assumed a 1 m aquifer thickness, so one grid cell has a volume of 2.021 m^3: cell width (4.3 m) x cell height (0.47 m) x cell thickness (assumed 1 m). Because benzene, ethylbenzene, and xylene are modeled under a common parameter (BEX), we assumed that 90% of BEX was benzene based on groundwater saturation experiments (Eganhouse et al., 1996). Simulation results show that 20 years after the spill, significantly more aquifer volume is contaminated with respect to As than to benzene. Exceedance of the As MCL occurs at a significantly greater magnitude for a longer duration compared to benzene. Based on this analysis, As poses a threat to far more groundwater over a longer period of time than benzene.

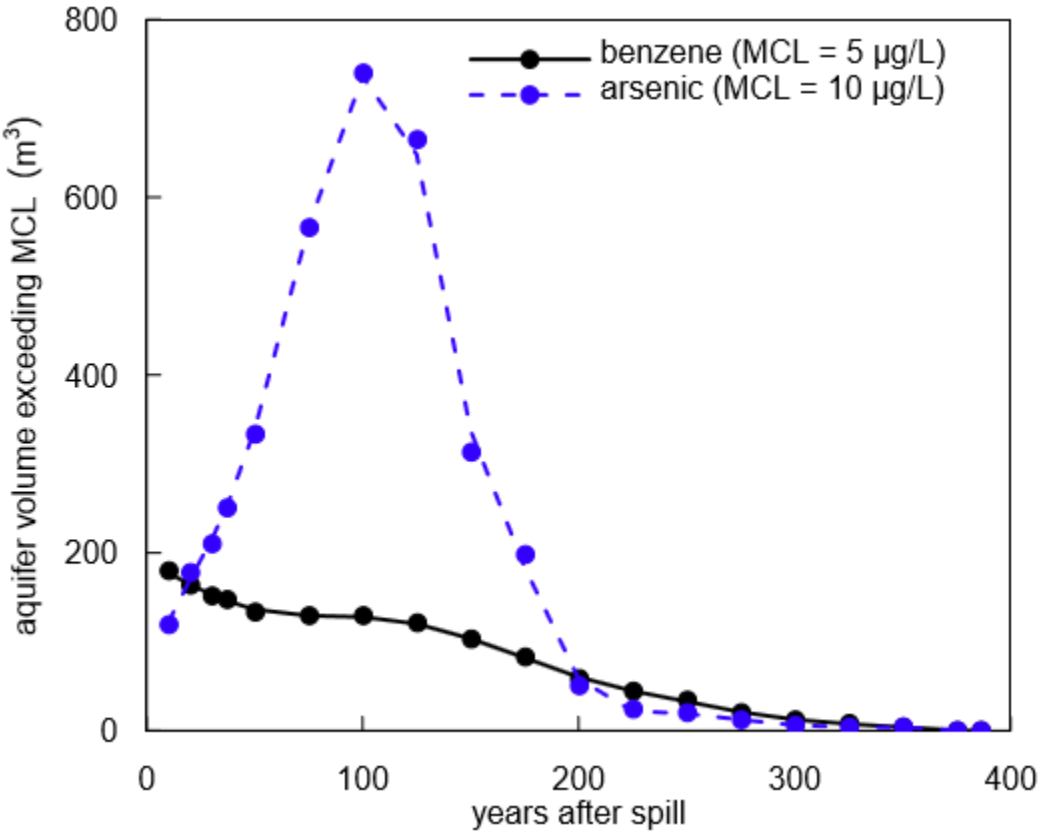

Figure 4.9. Model simulations for the total aquifer volume, assuming 1 m aquifer thickness, exceeding the maximum contaminant level for benzene (5 µg/L; blue) and arsenic (10 µg/L; orange) over time.

This modeling study provides support that over the long-term plume evolution, the legacy of As in groundwater is likely a greater threat than petroleum hydrocarbons from a human health perspective for four reasons: 1) arsenic is transported further downgradient from the oil body than hydrocarbons, which biodegrade and retract to the source. Thus, As contaminates groundwater further from the oil source; 2) the aquifer volume above the respective MCLs for benzene is dwarfed in comparison to the aquifer volume exceeding the As MCL over the simulation period; 3) after biodegradation, hydrocarbons are fully removed from the aquifer, whereas sorbed As can be remobilized if a new source of biodegradable organic carbon is introduced; and 4) oil spills are well documented, and regulatory agencies are charged with monitoring petroleum near oil spill sites. Because As released from oil spills is sourced from sediments and not from the oil, As is much less likely to be monitored. Given these factors, it is crucial that the mobilization of As be considered at sites impacted by organic carbon. At this site, As appears to pose a greater threat to groundwater quality than hydrocarbons.

The number of sites with elevated As concentrations in groundwater at oil spill sites is currently unknown. Virtually any aquifer has enough natural As to cause unsafe concentrations in drinking water if bioavailable organic carbon is introduced (Ziegler et al., 2017b). From 2010-2016, 1300 oil pipeline spills were reported in the U.S., totaling 9 million gallons of released petroleum (U.S. Department of Transportation, 2016). Since 2008, the rail transport of oil has increased more than 5100%, leading to more frequent, though smaller magnitude spills. Given the modeling results of this study, which suggest that naturally occurring As can have a longer and spatially greater impact on water quality at oil spill sites than contaminants derived from the oil, it is critical to investigate the vulnerability of drinking water aquifers in the U.S. and the potential threats to human health.

Last, little is known about the combined toxicological effects of a simultaneous exposure to benzene and As. Many studies have looked at these toxicological effects of exposure to benzene (Dean, 1985; Snyder et al., 1993; Smith et al., 2007) and As (Hughes, 2002; Leonard and Lauwerys, 1980; Pinto and Nelson, 1976; Ratnaike, 2003) individually. However, investigations into the toxicological effects of combined As and benzene exposure is warranted, as this study suggests the two can co-occur in petroleum-contaminated aquifers for centuries. Such a study would provide crucial knowledge into the human health risks at oil spill sites.

References

Anawar, H.M., Akai, J. and Sakugawa, H. (2004) Mobilization of arsenic from subsurface sediments by effect of bicarbonate ions in groundwater. Chemosphere 54, 753-762.

Appelo, C., Van der Weiden, M., Tournassat, C. and Charlet, L. (2002) Surface complexation of ferrous iron and carbonate on ferrihydrite and the mobilization of arsenic. Environmental Science & Technology 36, 3096-3103.

Baedecker, M.J. (1992) Authigenic mineral formation in aquifer rich in organic material, in: Kharaka, Y.K., Maest, A.S. (Eds.), Water-Rock Interaction-7. AA Balkeme, Rotterdam, pp. 257-261.

Baedecker, M.J., Cozzarelli, I.M., Eganhouse, R.P., Siegel, D.E. and Bennett, P.C. (1993) Crude oil in a shallow sand and gravel aquifer-III. Biogeochemical reactions and mass balance modeling in anoxic groundwater. Applied Geochemistry 8, 569-586.

Bekins, B.A., Cozzarelli, I.M. and Curtis, G.P. (2005) A simple method of calculating growth rates of petroleum hydrocarbon plumes. Ground Water 43, 817-826.

Bennett, P.C., Siegel, D.E., Baedecker, M.J. and Hult, M.F. (1993) Crude oil in a shallow sand and gravel aquifer—I. Hydrogeology and inorganic geochemistry. Applied Geochemistry 8, 529-549.

Bhattacharya, P., Claesson, M., Bundschuh, J., Sracek, O., Fagerberg, J., Jacks, G., Martin, R.A., Storniolo, A.d.R. and Thir, J.M. (2006) Distribution and mobility of arsenic in the Río Dulce alluvial aquifers in Santiago del Estero Province, Argentina. Science of The Total Environment 358, 97-120.

Bhowmick, S., Pramanik, S., Singh, P., Mondal, P., Chatterjee, D. and Nriagu, J. (2018) Arsenic in groundwater of West Bengal, India: A review of human health risks and assessment of possible intervention options. Science of The Total Environment 612, 148-169.

Charlet, L., Chakraborty, S., Appelo, C., Roman-Ross, G., Nath, B., Ansari, A., Lanson, M., Chatterjee, D. and Mallik, S.B. (2007) Chemodynamics of an arsenic “hotspot” in a West Bengal aquifer: a field and reactive transport modeling study. Applied Geochemistry 22, 1273-1292.

Cozzarelli, I.M., Baedecker, M.J., Eganhouse, R.P. and Goerlitz, D.F. (1994) The geochemical evolution of low-molecular-weight organic acids derived from the degradation of petroleum contaminants in groundwater. Geochimica et Cosmochimica Acta 58, 863-877.

Cozzarelli, I.M., Bekins, B.A., Baedecker, M.J., Aiken, G.M., Eganhouse, R.P. and Tuccillo, M.E. (2001) Progression of natural attenuation processes at a crude-oil spill site: I. Geochemical evolution of the plume. Journal of Contaminant Hydrology 53, 369-385.

Cozzarelli, I.M., Bekins, B.A., Eganhouse, R.P., Warren, E. and Essaid, H.I. (2010) In situ measurements of volatile aromatic hydrocarbon biodegradation rates in groundwater. Journal of Contaminant Hydrology 111, 48-64.

Cozzarelli, I.M., Schreiber, M.E., Erickson, M.L. and Ziegler, B.A. (2016) Arsenic cycling in hydrocarbon plumes: secondary effects of natural attenuation. Groundwater 54, 35-45.

Dean, B. J. (1978) Genetic toxicology of benzene, toluene, xylenes and phenols. Mutation Research/Reviews in Genetic Toxicology, 47(2), 75-97.

Dillard, L.A., Essaid, H.I. and Herkelrath, W.N. (1997) Multiphase flow modeling of a crude-oil spill site with a bimodal permeability distribution. Water Resources Research 33, 1617-1632.

Dixit, S. and Hering, J.G. (2003) Comparison of arsenic(V) and arsenic(III) sorption onto iron oxide minerals: implications for arsenic mobility. Environmental Science & Technology 37, 4182-4189.

Dzombak, D.A. and Morel, F.M. (1990) Surface complexation modeling: hydrous ferric oxide. John Wiley & Sons.

Eganhouse, R.P., Baedecker, M.J., Cozzarelli, I.M., Aiken, G.M., Thorn, K.A. and Dorsey, T.F. (1993) Crude oil in a shallow sand and gravel aquifer-II. organic geochemistry. Applied Geochemistry 8, 551-567.

Eganhouse, R.P., Dorsey, T.F., Phinney, C.S. and Westcott, A.M. (1996) Processes affecting the fate of monoaromatic hydrocarbons in an aquifer contaminated by crude oil. Environmental Science & Technology 30, 3304-3312.

Erickson, M.L. and Barnes, R.J. (2005) Glacial sediment causing regional-scale elevated arsenic in drinking water. Ground Water 43, 796-805.

Essaid, H.I., Bekins, B.A., Godsy, E.M., Warren, E., Baedecker, M.J. and Cozzarelli, I.M. (1995) Simulation of aerobic and anaerobic biodegradation processes at a crude oil spill site. Water Resources Research 31, 3309-3327.

Essaid, H.I., Bekins, B.A., Herkelrath, W.N. and Delin, G.N. (2011) Crude oil at the Bemidji site: 25 years of monitoring, modeling, and understanding. Ground Water 49, 706-726.

Essaid, H.I., Cozzarelli, I.M., Eganhouse, R.P., Herkelrath, W.N., Bekins, B.A. and Delin, G.N. (2003) Inverse modeling of BTEX dissolution and biodegradation at the Bemidji, MN crude-oil spill site. Journal of Contaminant Hydrology 67, 269-299.

Flanagan, S.V., Johnston, R.B. and Zheng, Y. (2012) Arsenic in tube well water in Bangladesh: health and economic impacts and implications for arsenic mitigation. Bulletin of the World Health Organization 90, 839-846.

Harbaugh, A.W. (2005) MODFLOW-2005, the US Geological Survey modular ground-water model: the ground-water flow process. US Department of the Interior, US Geological Survey Reston.

Harvey, C.F., Swartz, C.H., Badruzzaman, A., Keon-Blute, N., Yu, W., Ali, M.A., Jay, J., Beckie, R., Niedan, V. and Brabander, D. (2002) Arsenic mobility and groundwater extraction in Bangladesh. Science 298, 1602-1606.

Heron, G., Crouzet, C., Bourg, A.C. and Christensen, T.H. (1994) Speciation of Fe (II) and Fe (III) in contaminated aquifer sediments using chemical extraction techniques. Environmental Science & Technology 28, 1698-1705.

Hughes, M. F. (2002) Arsenic toxicity and potential mechanisms of action. Toxicology Letters, 133(1), 1-16.

Jung, H.B., Bostick, B.C. and Zheng, Y. (2012) Field, Experimental, and Modeling Study of Arsenic Partitioning across a Redox Transition in a Bangladesh Aquifer. Environmental Science & Technology 46, 1388-1395.

Jung, H.B., Charette, M.A. and Zheng, Y. (2009) Field, laboratory, and modeling study of reactive transport of groundwater arsenic in a coastal aquifer. Environmental Science & Technology 43, 5333-5338.

Knobeloch, L.M., Zierold, K.M. and Anderson, H.A. (2006) Association of arsenic-contaminated drinking-water with prevalence of skin cancer in Wisconsin's Fox River Valley. Journal of Health, Population and Nutrition, 206-213.

Kocar, B.D. and Fendorf, S. (2009) Thermodynamic Constraints on Reductive Reactions Influencing the Biogeochemistry of Arsenic in Soils and Sediments. Environmental Science & Technology 43, 4871-4877.

Leonard, A. and Lauwerys, R. R. (1980) Carcinogenicity, teratogenicity and mutagenicity of arsenic. Mutation Research/Reviews in Genetic Toxicology, 75(1), 49-62.

Lindberg, A.-L., Goessler, W., Gurzau, E., Koppova, K., Rudnai, P., Kumar, R., Fletcher, T., Leonardi, G., Slotova, K. and Gheorghiu, E. (2006) Arsenic exposure in Hungary, Romania and Slovakia. Journal of Environmental Monitoring 8, 203-208.

Lovley, D.R., Baedecker, M.J., Lonergan, D.J., Cozzarelli, I.M., Phillips, E.J. and Siegel, D.I. (1989) Oxidation of aromatic contaminants coupled to microbial iron reduction. Nature 339, 297-300.

Luo, Z.D., Zhang, Y.M., Ma, L., Zhang, G.Y., He, X., Wilson, R., Byrd, D.M., Griffiths, J.G., Lai, S., He, L., Grumski, K. and Lamm, S.H. (1997) Chronic arsenicism and cancer in Inner Mongolia — consequences of well-water arsenic levels greater than 50 μg/l, in: Abernathy, C.O., Calderon, R.L., Chappell, W.R. (Eds.), Arsenic: Exposure and Health Effects. Springer Netherlands, Dordrecht, pp. 55-68.

Ma, H.Z., Xia, Y.J., Wu, K.G., Sun, T.Z. and Mumford, J.L. (1999) Human exposure to arsenic and health effects in Bayingnormen, Inner Mongolia, Arsenic Exposure and Health Effects III. Elsevier, pp. 127-131.

McArthur, J., Ravenscroft, P., Safiulla, S. and Thirlwall, M. (2001) Arsenic in groundwater: testing pollution mechanisms for sedimentary aquifers in Bangladesh. Water Resources Research 37, 109-117.

McArthur, J.M., Banerjee, D.M., Hudson-Edwards, K.A., Mishra, R., Purohit, R., Ravenscroft, P., Cronin, A., Howarth, R.J., Chatterjee, A., Talukder, T., Lowry, D., Houghton, S. and Chadha, D.K. (2004) Natural organic matter in sedimentary basins and its relation to arsenic in anoxic ground water: the example of West Bengal and its worldwide implications. Applied Geochemistry 19, 1255-1293.

Neumann, R.B., Ashfaque, K.N., Badruzzaman, A.B.M., Ashraf Ali, M., Shoemaker, J.K. and Harvey, C.F. (2010) Anthropogenic influences on groundwater arsenic concentrations in Bangladesh. Nature Geoscience 3, 46-52.

Neumann, R.B., Pracht, L.E., Polizzotto, M.L., Badruzzaman, A.B.M. and Ali, M.A. (2014) Biodegradable organic carbon in sediments of an arsenic-contaminated aquifer in Bangladesh. Environmental Science & Technology Letters 1, 221-225.

Ng, C.G.H., Bekins, B.A., Cozzarelli, I.M., Baedecker, M.J., Bennett, P.C., Amos, R.T. and Herkelrath, W.N. (2015) Reactive transport modeling of geochemical controls on secondary water quality impacts at a crude oil spill site near Bemidji, MN. Water Resources Research.

Ng, G.H.C., Bekins, B.A., Cozzarelli, I.M., Baedecker, M.J., Bennett, P.C. and Amos, R.T. (2014) A mass balance approach to investigating geochemical controls on secondary water quality impacts at a crude oil spill site near Bemidji, MN. Journal of Contaminant Hydrology 164, 1-15.

Nickson, R., McArthur, J., Burgess, W., Ahmed, K.M., Ravenscroft, P. and Rahmanñ, M. (1998) Arsenic poisoning of Bangladesh groundwater. Nature 395, 338-338.

Nordstrom, D.K. (2002) Worldwide occurrences of arsenic in ground water. Science 296, 2143-2145.

Parkhurst, D.L. and Appelo, C. (2013) Description of input and examples for PHREEQC version 3--A computer program for speciation, batch-reaction, one-dimensional transport, and inverse geochemical calculations.

Pinto, S. S. and Nelson, K. W. (1976). Arsenic toxicology and industrial exposure. Annual Review of Pharmacology and Toxicology, 16(1), 95-100.

Polizzotto, M.L., Kocar, B.D., Benner, S.G., Sampson, M. and Fendorf, S. (2008) Near-surface wetland sediments as a source of arsenic release to ground water in Asia. Nature 454, 505-508.

Postma, D., Larsen, F., Hue, N.T.M., Duc, M.T., Viet, P.H., Nhan, P.Q. and Jessen, S. (2007) Arsenic in groundwater of the Red River floodplain, Vietnam: controlling geochemical processes and reactive transport modeling. Geochimica et Cosmochimica Acta 71, 5054-5071.

Postma, D., Larsen, F., Thai, N.T., Trang, P.T.K., Jakobsen, R., Nhan, P.Q., Long, T.V., Viet, P.H. and Murray, A.S. (2012) Groundwater arsenic concentrations in Vietnam controlled by sediment age. Nature Geoscience 5, 656.

Postma, D., Mai, N.T.H., Lan, V.M., Trang, P.T.K., Sø, H.U., Nhan, P.Q., Larsen, F., Viet, P.H. and Jakobsen, R. (2017) Fate of Arsenic during Red River Water Infiltration into Aquifers beneath Hanoi, Vietnam. Environmental Science & Technology 51, 838-845.

Prommer, H., Barry, D.A. and Zheng, C. (2003) MODFLOW/MT3DMS-based reactive multicomponent transport modeling. Ground Water 41, 247-257.

Radloff, K., Zheng, Y., Michael, H., Stute, M., Bostick, B., Mihajlov, I., Bounds, M., Huq, M., Choudhury, I. and Rahman, M. (2011) Arsenic migration to deep groundwater in Bangladesh influenced by adsorption and water demand. Nature geoscience 4, 793.

Ratnaike, R. N. (2003) Acute and chronic arsenic toxicity. Postgraduate Medical Journal, 79(933), 391-396.

Ravenscroft, P., Brammer, H. and Richards, K. (2009) Arsenic pollution: a global synthesis. John Wiley & Sons.

Rawson, J., Siade, A., Sun, J., Neidhardt, H., Berg, M. and Prommer, H. (2017) Quantifying Reactive Transport Processes Governing Arsenic Mobility after Injection of Reactive Organic Carbon into a Bengal Delta Aquifer. Environmental Science & Technology 51, 8471-8480.

Root, T.L., Gotkowitz, M.B., Bahr, J.M. and Attig, J.W. (2010) Arsenic geochemistry and hydrostratigraphy in midwestern U.S. glacial deposits. Ground Water 48, 903-912.

Rotiroti, M., Jakobsen, R., Fumagalli, L. and Bonomi, T. (2015) Arsenic release and attenuation in a multilayer aquifer in the Po Plain (northern Italy): Reactive transport modeling. Applied Geochemistry 63, 599-609.

Smedley, P. and Kinniburgh, D. (2002) A review of the source, behaviour and distribution of arsenic in natural waters. Applied Geochemistry 17, 517-568.

Smith, A.H., Lingas, E.O. and Rahman, M. (2000) Contamination of drinking-water by arsenic in Bangladesh: a public health emergency. Bulletin of the World Health Organization 78, 1093-1103.

Smith, M. T., Jones, R. M., Smith, A. H. (2007) Benzene exposure and risk of non-Hodgkin lymphoma. Cancer Epidemiology and Prevention Biomarkers, 16(3), 385-391.

Snyder, R., Witz, G., Goldstein, B. D. (1993) The toxicology of benzene. Environmental health perspectives, 100, 293.

Sø, H.U., Postma, D., Vi, M.L., Pham, T.K.T., Kazmierczak, J., Dao, V.N., Pi, K., Koch, C.B., Pham, H.V. and Jakobsen, R. (2018) Arsenic in Holocene aquifers of the Red River floodplain, Vietnam: Effects of sediment-water interactions, sediment burial age and groundwater residence time. Geochimica et Cosmochimica Acta 225, 192-209.

Stuckey, J.W., Schaefer, M.V., Benner, S.G. and Fendorf, S. (2015) Reactivity and speciation of mineral-associated arsenic in seasonal and permanent wetlands of the Mekong Delta. Geochimica et Cosmochimica Acta 171, 143-155.

Stuckey, J.W., Sparks, D.L. and Fendorf, S. (2016) Chapter Two - Delineating the Convergence of Biogeochemical Factors Responsible for Arsenic Release to Groundwater in South and Southeast Asia, in: Sparks, D.L. (Ed.), Advances in Agronomy. Academic Press, pp. 43-74.

Stute, M., Zheng, Y., Schlosser, P., Horneman, A., Dhar, R., Datta, S., Hoque, M., Seddique, A., Shamsudduha, M. and Ahmed, K. (2007) Hydrological control of As concentrations in Bangladesh groundwater. Water Resources Research 43.

Tuccillo, M.E., Cozzarelli, I.M. and Herman, J.S. (1999) Iron reduction in the sediments of a hydrocarbon-contaminated aquifer. Applied Geochemistry 14, 655-667.

U.S. Department of Transportation. Pipeline Incident 20 Year Trend. Pipeline and Hazardous Materials Safety Administration.

van Geen, A., Zheng, Y., Goodbred, S., Horneman, A., Aziz, Z., Cheng, Z., Stute, M., Mailloux, B., Weinman, B., Hoque, M.A., Seddique, A.A., Hossain, M.S., Chowdhury, S.H. and Ahmed, K.M. (2008) Flushing History as a Hydrogeological Control on the Regional Distribution of Arsenic in Shallow Groundwater of the Bengal Basin. Environmental Science & Technology 42, 2283-2288.

Varsányi, I. and Kovács, L.Ó. (2006) Arsenic, iron and organic matter in sediments and groundwater in the Pannonian Basin, Hungary. Applied Geochemistry 21, 949-963.

Whaley-Martin, K., Mailloux, B., van Geen, A., Bostick, B., Ahmed, K., Choudhury, I. and Slater, G. (2017) Human and livestock waste as a reduced carbon source contributing to the release of arsenic to shallow Bangladesh groundwater. Science of the Total Environment 595, 63-71.

Zachara, J.M., Kukkadapu, R.K., Gassman, P.L., Dohnalkova, A., Fredrickson, J.K. and Anderson, T. (2004) Biogeochemical transformation of Fe minerals in a petroleum-contaminated aquifer. Geochimica et Cosmochimica Acta 68, 1791-1805.

Zheng, C. and Bennett, G.D. (2002) Applied contaminant transport modeling. Wiley-Interscience New York.

Zheng, C. and Wang, P.P. (1999) MT3DMS: A modular three-dimensional transport model for simulation of advection, dispersion, and chemical reactions of contaminants in ground water systems. SERDP-99-1, U.S. Army Engineer Research and Development Center, Vicksburg, Mississippi.

Ziegler, B.A., Schreiber, M.E. and Cozzarelli, I.M. (2017a) The role of alluvial aquifer sediments in attenuating a dissolved arsenic plume. Journal of Contaminant Hydrology 204, 90-101.

Ziegler, B.A., Schreiber, M.E., Cozzarelli, I.M. and Ng, G.-H.C. (2017b) A mass balance approach to investigate arsenic cycling in a petroleum plume. Environmental Pollution 231, 1351-1361.

CHAPTER 5. DISSERTATION SUMMARY AND FUTURE RESEARCH

Arsenic in groundwater used for drinking water is a global human health concern. The desorption of As due to Fe-reduction coupled with biodegradation of organic matter is thought to be the primary mechanism releasing As to groundwater worldwide. To date, the majority of research on As mobilization during Fe-reduction has focused on how natural organic matter can trigger the As release. This dissertation demonstrates that organic carbon originating from human activity can also trigger As mobilization from aquifer sediments to groundwater and suggests that the occurrence of elevated As in groundwater may be more widespread than previously thought. An aquifer that experiences inputs of organic carbon from an oil spill, biofuel release, landfill, leaky septic systems, leaking underground storage tanks, or any source of biodegradable organic carbon is vulnerable to unsafe levels of As. Although known human-contaminated sites are often monitored and remediated, As is not commonly monitored at organic-contaminated sites, and thus can go unnoticed in groundwater

In Chapter 2, I examined the ability of aquifer sediments of a petroleum-contaminated aquifer to naturally attenuate a plume of As. Highlights from this study include:

- As concentrations in sediment were controlled predominantly by As sorption to Fe(III). This relationship was also observed in 1993, suggesting that As will be coupled to Fe as the plume ages.
- Arsenic and Fe were depleted near the oil due to extensive Fe-reduction and As mobilization. Arsenic and Fe were elevated in sediment at the plume's leading edge due to suboxic conditions precipitating an "iron curtain", which then sorbed dissolved As.
- Arsenic sequestration via sorption to Fe(III) is reversible and As can be remobilized into groundwater.

In Chapter 3, I reported results from a mass balance analysis for the distribution of As and Fe in the aquifer. Highlights from this study include:

- The majority of Fe (99.9%) and As (99.7%) masses are associated with aquifer sediments, despite elevated concentrations in groundwater.
- The distribution of As mass is inversely related in space between sediment and groundwater (i.e., where As is elevated in groundwater, concentrations are low in sediment, and vice versa).
- Only 0.02 mg/kg of As in sediment is needed to cause groundwater concentrations exceeding the drinking water standard.
- EPA Method 3051A for analyzing As has too high of a detection limit to identify sediments that could cause unsafe concentrations of As in groundwater.

In Chapter 4, I presented results from a reactive transport model that simulated As cycling in the petroleum plume for a 400-year period after the oil spill. Highlights from this study include:

- Arsenic in groundwater is attenuated predominantly be the formation of As(III) surface complexes with $Fe(OH)_3$ at the plume fringes.
- After 200 years, the leading edge of the As plume stabilizes approximately 300 m from the oil spill location,
- It takes 400 years for As to be attenuated to concentrations <10 μg/L
- Non-volatile dissolved organic carbon must be fully biodegraded before As can be fully attenuated.

- Over the lifespan of the hydrocarbon plume, more groundwater is expected to be contaminated by As than benzene.

Although this dissertation advances the knowledge of the occurrence of secondary contaminants in groundwater at oil spill sites, several opportunities remain to develop an even broader picture of naturally occurring contaminants mobilized due to human-sourced organic carbon. First, I note in Chapter 3 that the detection limit for As in aquifer sediments using EPA method 3051A is far too high to identify aquifers vulnerable to unsafe levels of As in drinking water. While lowering the detection limit by a factor of 22 is unlikely, a collaborative effort of geochemists and analytical chemists to either alter the chemical extraction method, analytical method, or develop a new procedure to quantify sediment concentrations of trace elements with a lower detection limit would be a valuable contribution to the regulatory community. Another method, laser ablation inductively coupled plasma mass spectrometry typically have lower detection limits, though analyses are cost and time intensive, and the detection limit is still not low enough to detect concentrations that could cause unsafe As in drinking water. Thus, more method development in this area is warranted.

Another important line of research is investigating how different types of aquifers respond to oil spills with respect to As mobilization. In the case of the Bemidji site, the alluvial aquifer has naturally high concentrations of Fe in sediment, which modeling results from Chapter 4 indicate are crucial to limiting As transport. The sensitivity analysis for the model shows that lower concentrations of Fe could allow for further transport of As in groundwater. It would be valuable to study aquifers of varying Fe concentrations to evaluate if As cycling responds differently after an influx of bioavailable organic carbon. Our sensitivity analysis also showed that competitive sorption of HCO_3^- is an important reaction for accurately simulating As cycling.

Given that much of the southwestern U.S. has elevated As in groundwater and is comprised of carbonate aquifers, a field investigation of As cycling in a carbonate aquifer would provide further information regarding the role of competitive sorption of HCO_3^-. With these additional field investigations, we can begin to make meaningful predictive assessments regarding how a variety of aquifer types might respond to influxes of organic carbon.

Similar to the importance of investigating different aquifer types, it is also important to consider that aquifers will respond differently to different sources of organic matter. For example, more biodegradable forms of organic carbon would likely cause more rapid mobilization of As into groundwater, leading to higher concentrations of As over a shorter period of time. This phenomenon has been observed in experimental petroleum/ethanol plumes, where the presence of the more biodegradable ethanol in combination with petroleum caused a faster release of As and a higher maximum concentration than petroleum alone (see Ziegler et al., 2015 for details). Although other human sources of organic matter can likely cause As mobilization, the rate of release and concentrations of As in groundwater are likely controlled by the biodegradability of the organic carbon source. Thus, further investigation is necessary to assess aquifer vulnerability to As mobilization when different forms of organic carbon are introduced into aquifers.

Last, this dissertation focused entirely on As cycling. Other trace elements that have human health implications naturally occur in aquifer sediments, many of them in association with Fe-oxides. Thus, it is possible that other trace elements are mobilized into groundwater at sites impacted by organic carbon. In the aforementioned experimental petroleum/ethanol plumes, cobalt, nickel and chromium were also observed to be released from aquifer sediments into groundwater due to organic carbon oxidation coupled with Fe-reduction. Other toxic elements,

including selenium, molybdenum, and cadmium can also sorb to Fe-oxides and may be released into groundwater if they naturally exist in sediment. Thus, to get a more holistic picture of secondary water quality contaminants in aquifers impacted by organic carbon, a comprehensive investigation of all trace elements is warranted.

APPENDIX A. SUPPLEMENTARY INFORMATION FOR CHAPTER 2

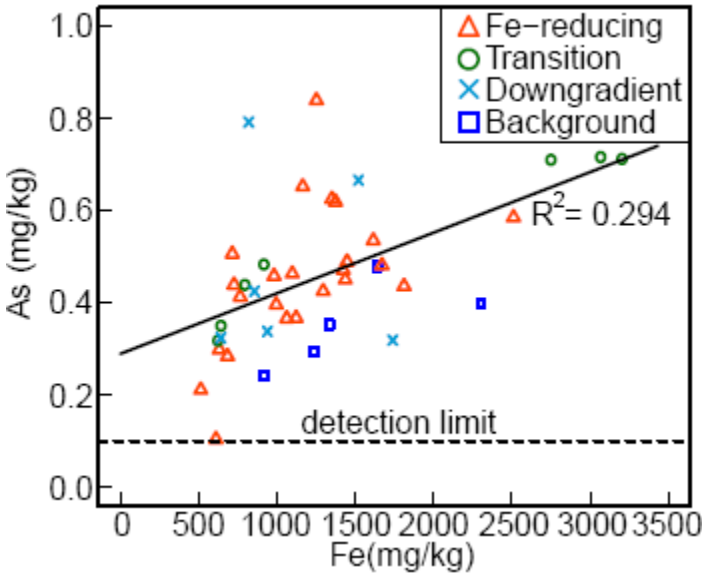

Figure A.1. Bivariate plot of HCl-extractable Fe (mg/kg) and As (mg/kg). Sediments were collected in 2013-2014. See Figure 1 for location of sediment cores.

Table A.1. Hydraulic conductivity estimates for sediment samples using the Hazen (Hazen, 1911) and Kozeny-Carman (Carman, 1937; Carman, 1956; Kozeny, 1927) methods.

Core sample	elevation (m AMSL)	d_{10} (mm)	d_{60} (mm)	K, Hazen (cm/s)	K, Kozeny-Carman (cm/s)	Facies
R4-20	423.55	0.28	1.24	9.50×10^{-2}	7.82×10^{-2}	Sand
R4-40	423.35	0.29	1.165	1.06×10^{-1}	9.27×10^{-2}	Sand
R4-60	423.15	0.28	1.105	9.98×10^{-2}	8.80×10^{-2}	Sand
R4-80	422.95	0.105	0.19	1.79×10^{-2}	2.35×10^{-2}	Silt
R4-110	422.65	0.085	0.175	1.14×10^{-2}	1.42×10^{-2}	Silt
R4-130	422.45	0.17	0.275	4.81×10^{-2}	6.61×10^{-2}	Sand
T2-16	423.22	0.12	0.215	2.34×10^{-2}	3.09×10^{-2}	Sand
T2-20	423.14	0.13	0.225	2.77×10^{-2}	3.71×10^{-2}	Sand
T2-32	423.06	0.155	0.275	3.92×10^{-2}	5.20×10^{-2}	Sand
T2-40	422.94	0.175	0.28	5.10×10^{-2}	7.05×10^{-2}	Sand
T2-55	422.83	0.07	1.125	3.10×10^{-3}	1.42×10^{-3}	Silt
T2-64	422.7	0.06	0.865	2.37×10^{-3}	1.11×10^{-3}	Silt
T2-74	422.58	0.045	0.775	1.25×10^{-3}	5.68×10^{-4}	Silt

Note: Core R4 and T2 were collected 102.6 m and 130.5 m downgradient from the center of the oil body, respectively.

Table A.2. Chemical extraction results of aquifer sediments in different redox zones

Sample	year	Distance from oil body (m)	Elevation (m AMSL)	near total As (mg/kg)	near total Fe (mg/kg)	sorbed As (mg/kg)	HCl-extractable As (mg/kg)	HCl-extractable Fe(III) (mg/kg)	HCl-extractable Fe(II) (mg/kg)
Background									
B-32	2013	-195.0	423.69	4.8	14421	2.4	0.399	2224.5	78.5
B-55			423.46	2.6	11008	2.3	0.353	1259.6	75.0
B-90			423.11	1.4	7750	1.1	0.242	775.0	138.3
B-120			422.81	2.4	13601	1.9	0.294	1102.8	130.4
B-148			422.53	1.8	11781	1.5	0.479	1610.0	29.7
mean				2.6	11712	1.8	0.353	1394.4	90.4
Methanogenic									
M1-1	2011	5.6	n.a.	0.7	3135	<0.9	--	--	--
M1-2			n.a.	0.6	3257	<0.9	--	--	--
M1-3			n.a.	0.8	4948	<0.9	--	--	--
M1-4			n.a.	0.9	4434	<0.9	--	--	--
M1-5			n.a.	0.9	4814	<0.9	--	--	--
mean				0.8	4118	<0.9	--	--	--
M2-40	2012	21.1	422.79	<0.4	7221	<0.9	--	--	--
M2-80			422.39	<0.4	3576	<0.9	--	--	--
M2-95			422.24	<0.4	4308	<0.9	--	--	--
M2-105			422.14	<0.4	4134	<0.9	--	--	--
M2-130			421.89	<0.4	5779	<0.9	--	--	--
M2-145			421.74	<0.4	5715	<0.9	--	--	--
mean				n.a.	5122	<0.9	--	--	--

Fe-reducing

R1-00	1993	86.0	423.60	2.3	4391	--	--	--	--
R1-10			423.49	1.7	5637	--	--	--	--
R1-38			423.23	1.5	4211	--	--	--	--
R1-53			423.08	1.4	4444	--	--	--	--
R1-68			422.93	1.1	9352	--	--	--	--
R1-90			422.70	7.2	4553	--	--	--	--
R1-98			422.63	1.3	9138	--	--	--	--
R1-113			422.48	1.3	4612	--	--	--	--
R1-138			422.23	1.3	12646	--	--	--	--
R1-143			422.18	1.0	5002	--	--	--	--
R1-158			422.03	1.0	4013	--	--	--	--
R1-173			421.88	1.5	6549	--	--	--	--
R1-190			421.70	2.8	3593	--	--	--	--
mean				1.5	6069	--	--	--	--
R2-30	2014	86.2	423.70	1.4	3112	--	0.298	525.3	105.7
R2-50			423.50	2.0	8867	--	0.439	384.0	341.6
R2-60			423.40	1.6	3803	--	0.506	398.7	315.8
R2-90			423.10	0.7	4195	--	0.284	270.8	413.2
R2-120			422.80	1.4	3923	--	0.652	169.4	994.7
R2-150			422.50	1.9	5170	--	0.458	140.0	840.8
mean				1.5	4845	--	0.439	314.7	502.0
R3-20	2014	93.8	423.37	1.6	4789	--	0.489	1376.6	70.7
R3-40			423.17	2.5	5829	--	0.450	1375.3	60.8
R3-80			422.77	1.6	3582	--	0.413	693.5	70.9
R3-120			422.37	1.0	4025	--	0.839	1000.7	250.9
R3-140			422.17	0.6	2820	--	0.463	754.9	342.5
R3-160			421.97	0.8	2468	--	0.366	665.0	397.0
R3-180			421.77	--	--	--	0.481	1075.6	594.9
R3-195			421.62	--	--	--	0.367	502.5	619.3
mean				1.4	3919	--	0.483	930.5	300.9

R4-20	2013	102.6	423.55	3.8	9728	1.6	0.535	943.7	670.9
R4-40			423.35	2.8	8328	2.6	0.619	666.9	706.7
R4-60			423.15	2.2	9638	1.5	0.585	740.7	1769.2
R4-80			422.95	1.8	5974	1.7	0.425	814.2	480.3
R4-110			422.65	1.9	5457	1.5	0.625	842.2	508.2
R4-130			422.45	0.9	3970	0.9	0.211	287.1	226.3
mean				2.2	7182	1.6	0.500	715.8	726.9
R5-20	2014	104.1	423.6296	3.9	8431	--	0.436	1623.7	187.0
R5-30			423.5296	3.4	6671	--	0.471	854.0	569.3
R5-110			422.7296	0.7	4362	--	0.396	322.2	672.9
R5-120			422.6296	0.4	2763	--	0.104	137.9	472.3
mean				2.1	5557	--	0.352	734.4	475.4
R6-00	2012	117.7	423.67	1.4	5674	1.3	--	--	
R6-03			423.64	0.8	5553	<0.9	--	--	
R6-35			423.32	5.2	12345	2.7	--	--	
R6-38			423.29	5.0	12312	2.7	--	--	
R6-70			422.97	3.1	9001	3.0	--	--	
R6-77			422.90	2.6	9554	2.3	--	--	
R6-107			422.64	2.6	8172	2.5	--	--	
mean				3.0	8944	2.4	--	--	
R7-15	2011	118.0	423.28	2.9	17701	1.9	--	--	
R7-30			423.13	2.8	14652	2.8	--	--	
R7-40			423.03	2.6	14340	2.4	--	--	
R7-52			422.91	3.1	14221	1.8	--	--	
R7-61			422.82	2.0	10097	1.4	--	--	
R7-70			422.73	1.5	5792	1.4	--	--	
R7-82			422.61	3.8	14489	1.9	--	--	
R7-91			422.52	1.9	7858	1.6	--	--	
R7-101			422.42	1.9	6910	1.6	--	--	
R7-113			422.30	1.3	6695	1.3	--	--	
R7-122			422.21	2.0	7686	1.5	--	--	

R7-137			422.06	5.8	23849	5.1	--	--	
R7-153			421.90	2.4	8808	2.1	--	--	
mean				2.6	11777	2.0	--	--	
Transition									
T1-15	1993	102.1	423.25	3.131	6781	--	--	--	
T1-30			423.10	1.855	11123	--	--	--	
T1-68			422.72	8.221	14714	--	--	--	
T1-93			422.47	40.627	69733	--	--	--	
T1-98			422.42	<0.685	6009	--	--	--	
T1-111			422.29	1.105	5106	--	--	--	
mean				9.2	18911	--	--	--	
T2-16	2013	130.5	423.22	1.6	5729	1.2	0.439	794.4	145.872
T2-20			423.14	1.6	6430	1.2	0.483	916.1	151.147
T2-32			423.06	1.2	4904	1.2	0.318	623.0	154.412
T2-40			422.94	1.2	5042	0.9	0.350	642.0	148.664
*T2-55**			422.83	11.3	21704	6.0	0.712	3202.4	11.174
*T2-64**			422.70	10.4	20467	4.0	0.716	3065.9	220.099
*T2-74**			422.58	7.0	16868	3.8	0.710	2748.8	16.510
mean				4.9	11592	2.6	0.533	1713.2	121.1
*mean***				1.4	5526	1.1	0.398	743.9	150.0
T3-15	1993	132	423.05	1.1	6795	--	--	--	--
T3-30			422.90	0.9	4413	--	--	--	--
T3-45			422.75	1.0	4635	--	--	--	--
T3-65			422.55	0.6	3261	--	--	--	--
T3-75			422.45	1.3	3999	--	--	--	--
T3-90			422.30	<0.4	3970	--	--	--	--
T3-105			422.15	1.4	6533	--	--	--	--
T3-120			422.00	2.0	6116	--	--	--	--
T3-130			421.90	1.4	5379	--	--	--	--
T3-145			421.75	1.0	5759	--	--	--	--
T3-160			421.60	1.3	5106	--	--	--	--

T3-175			421.45	<0.4	3304	--	--	--	--
T3-190			421.30	0.9	4474	--	--	--	--
T3-205			421.15	0.6	4288	--	--	--	--
T3-220			421.00	0.9	4210	--	--	--	--
T3-235			420.85	0.9	4581	--	--	--	--
T3-250			420.70	1.5	7368	--	--	--	--
T3-265			420.55	2.7	8629	--	--	--	--
mean				1.1	5766	--	--	--	--
Downgradient									
D-30	2013	212.2	422.81	1.9	8800	0.9	0.338	899.2	39.8
D-60			422.51	1.7	8020	1.3	0.319	1731.8	<7.0
D-90			422.21	2.2	7190	1.2	0.425	839.2	16.4
D-120			421.91	1.1	4778	1.0	0.324	623.9	18.1
D-150			421.61	1.8	8282	1.0	0.666	1493.7	26.1
*D-168**			421.43	2.8	11323	1.4	0.792	812.1	7.2
mean				1.9	8065	1.1	0.477	1066.6	21.5
*mean***				1.7	7414	1.1	0.414	1117.6	25.1

*Silt and clay comprised large fraction of sample
**mean excluding the silt and clay-rich samples
n.a. = not analyzed

APPENDIX B. SUPPLEMENTARY INFORMATION FOR CHAPTER 3

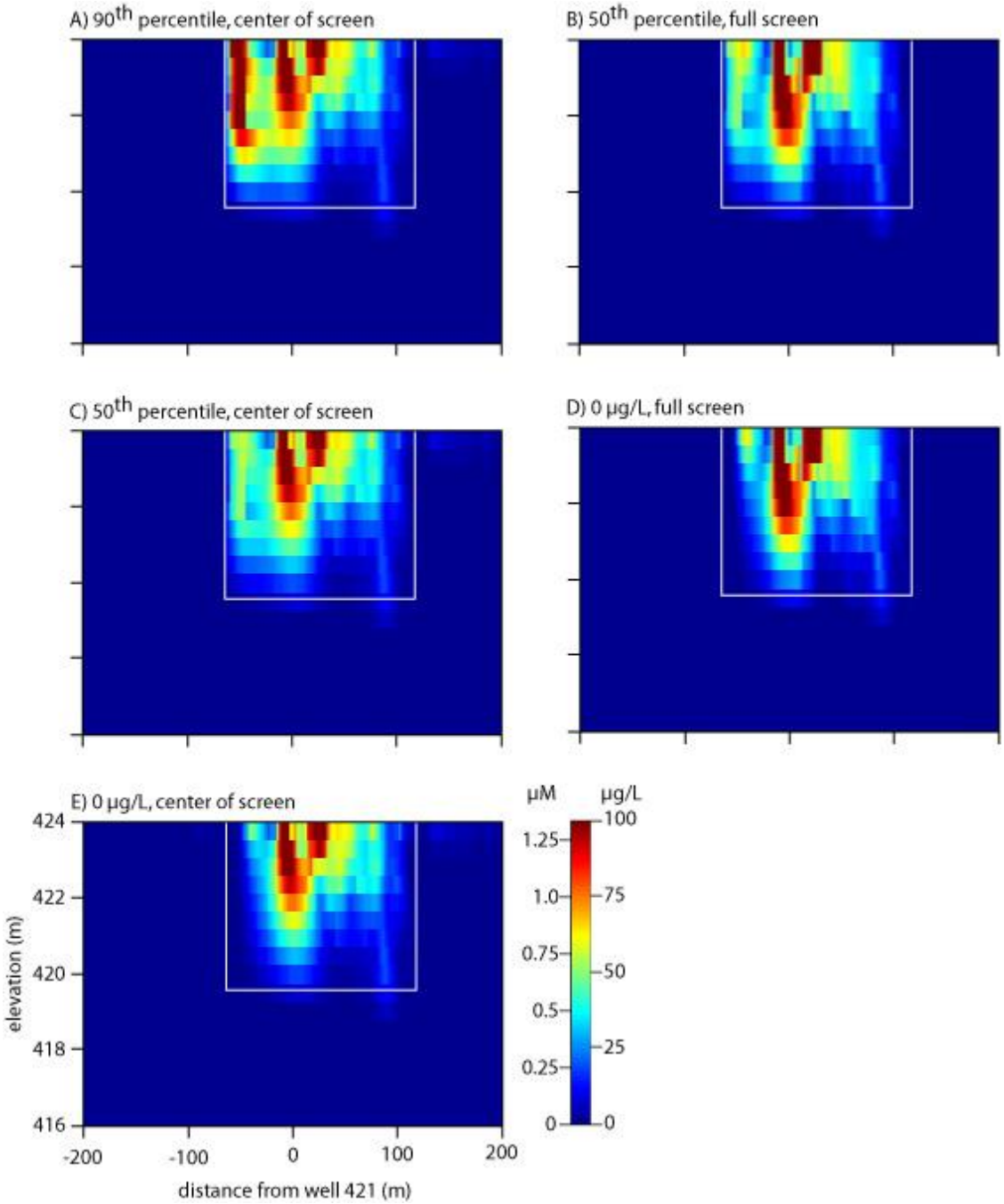

Figure B.1. Kriged dissolved As concentrations applying the 90th (A), 50th (B and C), and 0th (D and E) percentiles at the upper and lower corners of the left boundary of the domain. Measured concentrations were applied to the center of the screen (A, C, and E) and to the full length of the screen (B and D). The white rectangle denotes the domain boundary.

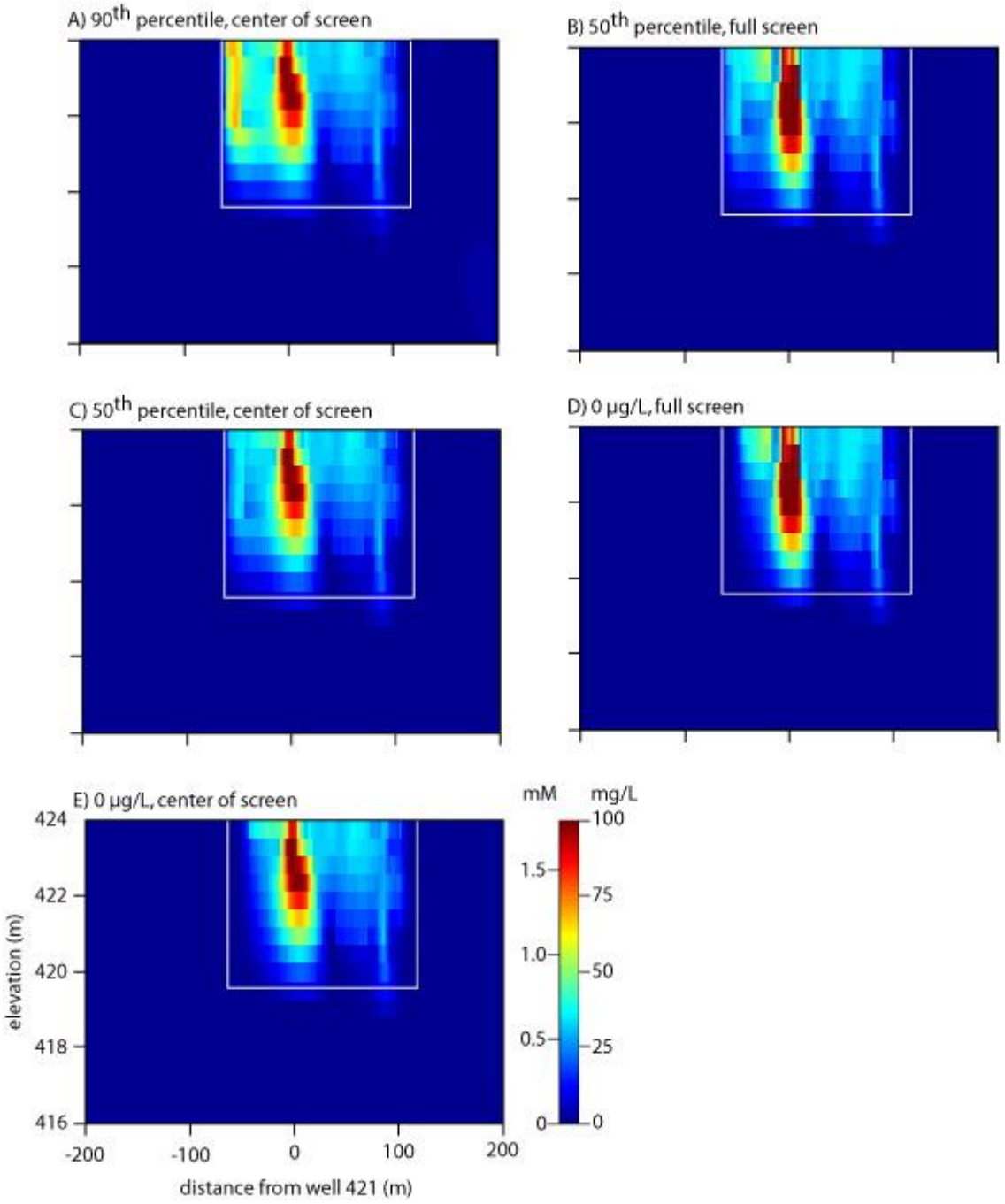

Figure B.2. Kriged dissolved Fe concentrations applying the 90th (A), 50th (B and C), and 0th (D and E) percentiles at the upper and lower corners of the left boundary of the domain. Measured concentrations were applied to the center of the screen (A, C, and E) and to the full length of the screen (B and D). The white rectangle denotes the domain boundary.

Table B.1. Scenarios for calculating dissolved Fe and As in domain

Scenario	percentile	As (µg/L)	Fe (mg/L)	Measured values were applied to:
1	90	113	71	full screen length
2	90	113	71	center of screen
3	50	55	34	full screen length
4	50	55	34	center of screen
5	0	0	0	full screen length
6	0	0	0	center of screen

Table B.2. Fe(II) and total Fe (Fe(T)) using Ferrozine method and ICP-OES for select wells

well	Fe(II) mg/L; Ferrozine	Fe(T) mg/L; Ferrozine	Fe(T) mg/L; ICP-OES
310B	3.1	3.1	2.7
310E	<0.2	<0.2	<0.1
311	11.7	11.7	11.9
530A	24.5	24.5	22.7
530B	33.1	33.1	31.2
530C	4.26	5.28	5.54
530D	26.7	27.2	28.7
9315A	24.8	24.8	26.6
9315B	27.3	27.3	28.3
9315C	30.1	30.1	33.1
9315D	27.9	27.9	28.1
1101A	22.5	22.5	23.3
1101B	0.232	0.232	<0.1
1101C	<0.2	<0.2	<0.1
1101D	<0.2	<0.2	<0.1

Table B.3. Comparison of scenarios for calculating dissolved mass

scenario	dissolved As mass (kg/m)	percent of domain total	dissolved Fe mass (kg/m)	percent of domain total
1	0.0112	0.34	8.77	0.057
2	0.0110	0.33	8.68	0.057
3	0.0107	0.32	8.09	0.053
4	0.00953	0.29	7.78	0.051
5	0.00915	0.28	7.45	0.049
6	0.00825	0.25	6.94	0.045